Rapid Identification and Classification of Food-relevant Spoilage Microorganisms by Raman- and IR-microspectroscopy

DISSERTATION

to obtain the degree of Doctor of Science

submitted by Daniel Klein (M. Sc.)

submitted to the School of Science and Technology
of the University of Siegen
Siegen 2023

Supervisor and first appraiser

Prof. Dr. Peter-Michael Kaul

Hochschule Bonn-Rhein-Sieg University of Applied Sciences

Second appraiser

Prof. Dr. Carsten Engelhard

University of Siegen

Date of the oral examination

23.08.2023

printed on non-ageing wood free and acid-free paper, no use of metal or plastic

Per aspera ad astra

I hereby declare in lieu of an oath that I have drawn up the present work without any undue assistance by third parties and without using any aids other than the ones specified. The data and concepts taken, either directly or indirectly, from any other sources have been marked, indicating the source.

The work has not been submitted to any other examining authority neither in Germany nor abroad and neither in the same nor in any similar form.

Use of the services of any PhD mediation institute or of any similar organisation has not been made.

Schwalmtal,

Daniel Klein

Abstract

Microorganisms not only contribute to the spoilage of food but can also cause illnesses through consumption. Consumer concerns and doubts about the shelf life of the products and the resulting enormous amounts of food waste have led to a demand for a rapid, robust, and non-destructive method for the detection of microorganisms, especially in the food sector. Therefore, a rapid and simple sampling method for the Raman- and infrared (IR)-microspectroscopic study of microorganisms associated with spoilage processes was developed. For subsequent evaluation pre-processing routines, as well as chemometric models for classification of spoilage microorganisms were developed.

The microbiological samples are taken using a disinfectable sampling stamp and measured by microspectroscopy without the usual pre-treatments such as purification separation, washing, and centrifugation. The resulting complex multivariate data sets were pre-processed, reduced by principal component analysis, and classified by discriminant analysis. Classification of independent unlabeled test data showed that microorganisms could be classified at genus, species, and strain levels with an accuracy of 96.5 % (Raman) and 94.5 % (IR), respectively, despite large biological differences and novel sampling strategies.

As bacteria are exposed to constantly changing conditions and their adaptation mechanisms may make them inaccessible to conventional measurement methods, the methods and models developed were investigated for their suitability for microorganisms exposed to stress.

Compared to normal growth conditions, spectral changes in lipids, polysaccharides, nucleic acids, and proteins were observed in microorganisms exposed to stress. Models were developed to discriminate microorganisms, independent of the involvement of various stress factors and storage times. Classification of the investigated bacteria yielded accuracies of 97.6 % (Raman) and 96.6 % (IR), respectively, and a robust and meaningful model was developed to discriminate different microorganisms at the genus, species, and strain levels.

The obtained results are very promising and show that the methods and models developed for the discrimination of microorganisms as well as the investigation of stress factors on microorganisms by means of Raman- and IR-microspectroscopy have the potential to be used, for example, in the food sector for the rapid determination of surface contamination.

Zusammenfassung

Mikroorganismen tragen nicht nur zum Verderb von Lebensmitteln bei sondern können durch deren Verzehr auch Krankheiten auslösen. Die Verunsicherung der Konsumenten sowie die Skepsis am Mindesthaltbarkeitsdatum der Produkte und die daraus resultierenden enormen Mengen an Lebensmittelabfällen sorgen für den Wunsch nach einer schnellen, robusten und zerstörungsfreien Methode zum Nachweis von Bakterien, insbesondere im Lebensmittelsektor. Daher wurde eine schnelle und einfache Probenahmemethode für die Raman- und Infrarot (IR)-Mikrospektroskopische Untersuchung von Mikroorganismen, die mit Verderbsprozessen in Verbindung stehen, konzipiert. Zur anschließenden Auswertung wurden pre-processing Routinen sowie chemometrische Modelle zur Klassifizierung der Verderbserreger entwickelt.

Mit einem desinfizierbaren Probenahmestempel werden die zu untersuchenden mikrobiologischen Proben, ohne die üblichen Vorbehandlungen wie Separation, Reinigung und Zentrifugation, entnommen und mikrospektroskopisch vermessen. Die resultierenden komplexen multivariaten Datensätze wurden durch eine Hauptkomponentenanalyse reduziert und mittels Diskriminanzanalyse klassifiziert. Die Klassifizierung unabhängiger ungelabelter Testdaten zeigt, dass Mikroorganismen trotz großer biologischer Unterschiede und neuartiger Probenahmestrategien mit einer Genauigkeit von 96,5 % (Raman) bzw. 94,5 % (IR) auf Gattungs-, Arten- und Stammebene klassifiziert werden können.

Da Bakterien sich ständig wechselnden Bedingungen ausgesetzt sind und durch ihre Anpassungen so für herkömmliche Messmethoden möglicherweise nicht mehr zugänglich sind, wurden die entwickelten Methoden und Modelle auf ihre Eignung für Stress ausgesetzten Mikroorganismen untersucht.

Im Vergleich zu normalen Wachstumsbedingungen wurden bei unter Stress stehenden Mikroorganismen spektrale Veränderungen in Lipiden, Polysacchariden, Nukleinsäuren und Proteinen beobachtet. Es wurden Modelle entwickelt, um die untersuchten Mikroorganismen unabhängig von der Beteiligung verschiedener Stressfaktoren und Lagerzeiten zu unterscheiden. Die Klassifizierung ergab Genauigkeiten von 97,6 % (Raman) bzw. 96,6 % (Infrarot) und es wurde ein robustes und aussagekräftiges Modell zur Unterscheidung verschiedener Mikroorganismen auf Gattungs-, Arten- und Stammebene entwickelt.

Die erzielten Ergebnisse sind sehr vielversprechend und zeigen, dass die entwickelten Methoden und Modelle zur Unterscheidung von Mikroorganismen sowie zur Untersuchung von Stressfaktoren auf Mikroorganismen mittels Raman- und IR-Mikrospektroskopie das Potenzial haben, beispielsweise im Lebensmittelbereich zur schnellen Bestimmung von Oberflächenkontaminationen eingesetzt zu werden.

Graphical Abstract

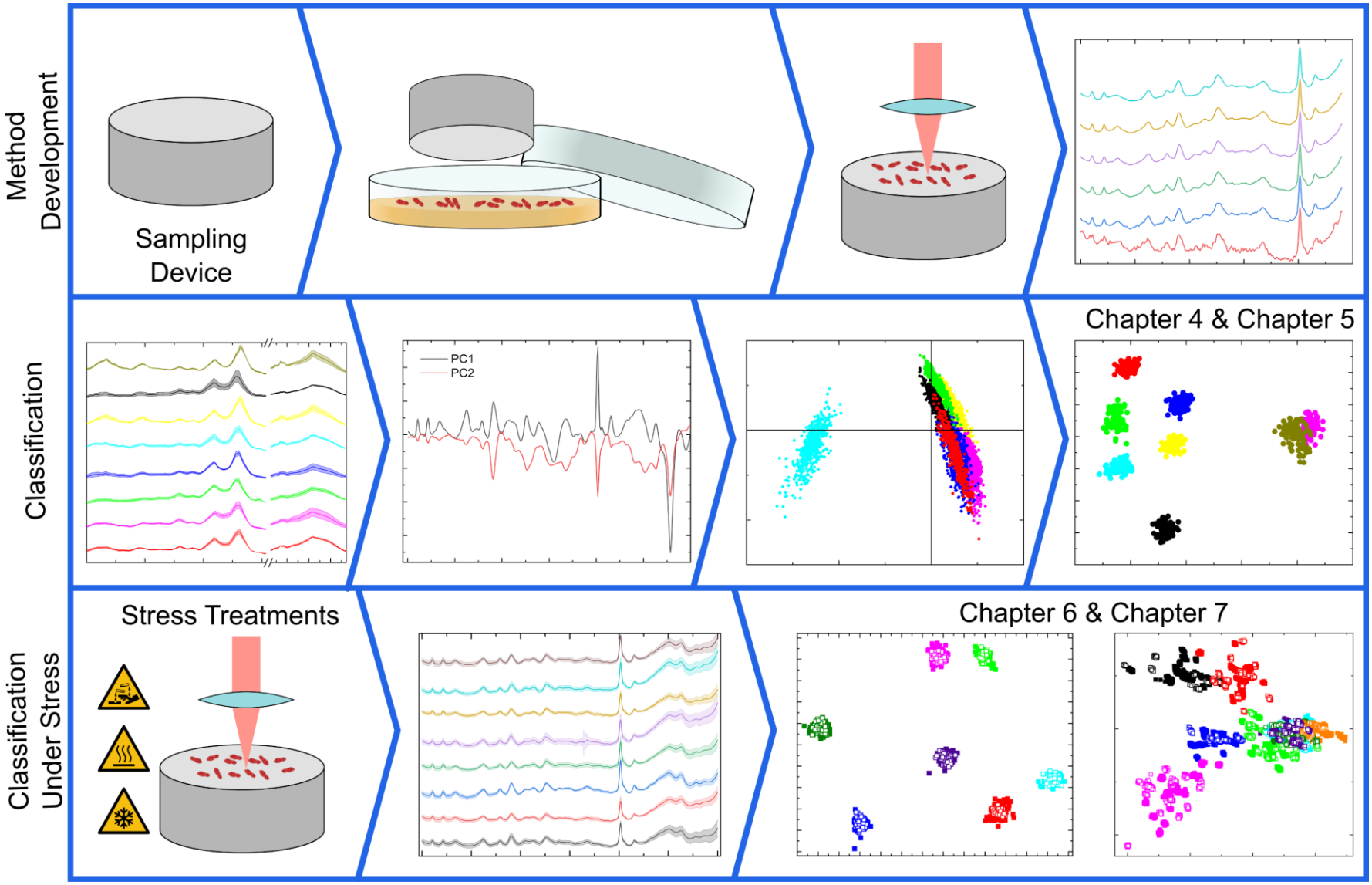

Table of Contents

Chapter 1

Introduction
&
Scope of the Thesis

Based on:

Klein, D., Breuch, R., von der Mark, S., Wickleder, C., Kaul, P., Detection of Spoilage Associated Bacteria using Raman-microspectroscopy Combined with Multivariate Statistical Analysis. Talanta 196 (2019), 325–328. https://doi.org/10.1016/j.talanta.2018.12.094.

Klein, D., Breuch, R., Reinmüller, J., Engelhard, C., Kaul, P., Rapid Detection and Discrimination of Food-related Bacteria using IR-microspectroscopy in Combination with Multivariate Statistical Analysis, Talanta 232 (2021), 122424. https://doi.org/10.1016/j.talanta.2021.122424.

Klein, D.; Breuch, R.; Reinmüller, J.; Engelhard, C.; Kaul, P., Investigation and Rapid Discrimination of Food-Related Bacteria under Stress Treatments Using IR Microspectroscopy. Foods 10 (2021), 1850. https://doi.org/10.3390/foods10081850.

Klein, D.; Breuch, R.; Reinmüller, J.; Engelhard, C.; Kaul, P., Discrimination of Stressed and Non-Stressed Food-Related Bacteria Using Raman-Microspectroscopy. Foods 11 (2022), 1506. https://doi.org/10.3390/foods11101506.

1.1 Introduction

The fact that the world population and the global demand for meat will continuously grow, the increasing importance of resource conservation and environmental protection in our world has become very clear in recent decades [1–8]. One particularly important aspect of this field is food safety, which consists not only of producing and consuming safe food, but also of wasting less food. This may be achieved by a more accurate determination of shelf life, thus reducing not only organic waste, but also environmental stress and the pollution of the planet by plastics [1,8–10]. The importance of global resource conservation is particularly evident in the staggering amounts of approximately 931 million tons of food waste generated each year [11].

Currently, the shelf life of a product is estimated very conservatively, because the manufacturer is liable for the edibility of the product until this date if certain aspects, such as storage conditions, are respected [12–16]. This conservative estimation of the shelf life is based on a very labor-, cost-, and time-intensive determination of the initial bacterial load of the product, which is typically executed by standard colony-counting methods [17–20]. Other methods such as sensory-mechanical studies, immunological, or genetic techniques did not prevail due to disadvantages in speed, complexity, and invasiveness on the way to an optimized determination of the initial bacterial load [17,18,21].

Considering 600 million annual cases of illness as well as 420,000 deaths world-wide caused by the consumption of contaminated food, the fear of the consumer of foodborne illnesses, the conservative estimation of the shelf life date and consumers' misunderstanding of the shelf life date of products contribute to the unnecessary disposal of products that would still be edible [9,22–24]. The immense importance of the expiry dates printed on products and their interpretation by consumers is demonstrated by the fact that half of the economic losses along the supply chain occur in households with meat products being a large proportion of these losses [2,11].

Based on these figures and the rapidly increasing number of scientific articles on food safety and on the determination of bacteria by Raman- or infrared (IR)-spectroscopy, the need for a fast and robust method for the determination of contaminations becomes obvious [4,10,25]. Attention must also be paid to the development of methods capable of determining bacterial contaminations in real

world samples, as bacteria are subject to constant variations in their growth conditions, both in nature and in the supply chain [26–29]. They have developed the ability to constantly adapt to conditions or even change to a viable but non-culturable state, making them inaccessible to conventional determination methods [18,26,30].

1.2 Scope of the Thesis

This thesis is dedicated to the development of a rapid and reliable spectroscopic detection and classification method for microorganisms that are significantly involved in the spoilage process of food, especially meat products. Besides the development of a basic methodology for sampling, analysis, and evaluation (Chapter 4 and Chapter 5), special emphasis is put on exceeding the limits of the development of a classical laboratory model by specifically considering extrinsic factors (Chapter 6 and Chapter 7) on the sample.

The objectives of Chapter 4 and Chapter 5 are to find a time-saving, cost-effective, and suitable sample preparation of microbiological samples and a suitable measurement method using Raman- and IR-microspectroscopy with subsequent data preparation, evaluation, and classification. For this purpose, a rapid and simple sampling procedure was developed using a disinfectable stainless steel stamp, with which samples of a surface, so-called surface blots, can be produced, e.g. from the surface of the culture medium. Furthermore, the investigations aimed at optimizing the required analysis time so that no loss of relevant spectral information occurs. For the complex multivariate data set, a manageable data set now had to be created by reasonable chemometric data processing using spectral data preprocessing and a PCA (principal component analysis) for data reduction. By means of a CDA (canonical discriminant analysis), a robust and reliable model for differentiation of food safety and especially meat spoilage relevant bacteria from genera to species level was created.

In summary, these two chapters present the development of a complete, rapid, and nondestructive analytical method for spoilage microorganisms that allows classification down to the species level using Raman and IR microspectroscopy.

However, as the methods and models developed may not adequately capture real-world samples that are not subject to ideal laboratory conditions, the aim is to expand the data set to ensure that the resulting models are not only based on

spectra generated under ideal conditions, but also include microorganisms under high stress.

For this purpose, in addition to the standard reference treatment, the microorganisms were subjected to controlled lifetime stress conditions (incubation under acidic and alkaline conditions, incubation at different temperatures and incubation under 2-propanol influence) and sampling stress conditions (cold sampling, heat sampling, and desiccation). Subsequently, the microbiological samples were measured by Raman- (Chapter 6) and IR- (Chapter 7) microspectroscopy. Moreover, one objective is to establish a careful preprocessing routine, and not only split the datasets into independent training and testing datasets, but also generate them from independent samples. The models presented are therefore based on balanced data sets and take into account different growth states as well as a variety of stress factors that have affected the microorganisms.

Finally, in Chapter 8, a summarizing conclusion is given with regard to the results of the thesis as well as future perspectives.

Chapter 2

Fundamentals

Based on:

Klein, D., Breuch, R., von der Mark, S., Wickleder, C., Kaul, P., Detection of Spoilage Associated Bacteria using Raman-microspectroscopy Combined with Multivariate Statistical Analysis. Talanta 196 (2019), 325–328. https://doi.org/10.1016/j.talanta.2018.12.094.

Klein, D., Breuch, R., Reinmüller, J., Engelhard, C., Kaul, P., Rapid Detection and Discrimination of Food-related Bacteria using IR-microspectroscopy in Combination with Multivariate Statistical Analysis, Talanta 232 (2021), 122424. https://doi.org/10.1016/j.talanta.2021.122424.

Klein, D.; Breuch, R.; Reinmüller, J.; Engelhard, C.; Kaul, P., Investigation and Rapid Discrimination of Food-Related Bacteria under Stress Treatments Using IR Microspectroscopy. Foods 10 (2021), 1850. https://doi.org/10.3390/foods10081850.

Klein, D.; Breuch, R.; Reinmüller, J.; Engelhard, C.; Kaul, P., Discrimination of Stressed and Non-Stressed Food-Related Bacteria Using Raman-Microspectroscopy. Foods 11 (2022), 1506. https://doi.org/10.3390/foods11101506.

2.1 Infrared- & Raman-spectroscopy

Vibrational spectroscopy analyzes changes in molecular vibrations and rotations induced by interaction with electromagnetic radiation, allowing conclusions to be drawn about the change in state of the molecule and hence the identification and quantification, as well as the structural elucidation, of unknown chemical compounds [61,62].

IR-spectroscopy covers the infrared region of the electromagnetic spectrum, which is usually divided into three regions. Near-IR (14,000–4,000 cm^{-1}) can excite overtone or combination bands. Mid-infrared, about 4,000–400 cm^{-1}, can be used to study fundamental vibrations, and far-infrared (400–10 cm^{-1}) which is used for rotational spectroscopy [61,62]. IR spectroscopy is based on the absorption of energy of the electromagnetic radiation by a molecule in the IR range, which corresponds to the frequency of the vibrating bond or functional group [61,62]. To transfer the energy of the IR photon to the molecule, the molecular vibration must cause a change in the dipole moment of the molecule [61,62].

Raman-spectroscopy, unlike IR-spectroscopy, is not based on the absorption of energy of the electromagnetic radiation, but on scattering processes of monochromatic laser light by molecules [61,62]. A prerequisite for the Raman effect is a change in the polarizability of a molecule during vibration [61,62]. In contrast to Rayleigh scattering, Raman signals result from inelastic collisions between photons and molecules in the sample, where some energy is transferred either from the photon to the molecule (Stokes scattering) or from the molecule to the photon (Anti-Stokes scattering) [61,62]. In the first case, the molecule is excited from the ground state to a higher, virtual vibrational, state [61,62]. The transition from the virtual vibrational to the first excited state decreases the energy of the photon by the energy difference between the two vibrational states [61,62].

Although Raman scattering spectra and IR absorption spectra of a chemical compound often resemble each other, they provide complementary information due to different selection rules [63]. This fact is useful in the analysis of complex chemical matrices, as overlapping absorption bands from one method can often be resolved by the other. The combination of spectroscopy and microscopy allows both classical, robust, and nondestructive material identification and local assignment of a spectrum on a microscopic image [64,65]. Thus, in addition to the analysis of traces

and surface contamination at the macroscopic and microscopic level, respectively, qualitative and quantitative information can also be derived [65,66].

2.2 Bacteria

Bacteria are surrounded by a stable cell wall that protects them from external influences [31,32]. Other intracellular as well as extracellular structures include bacterial DNA, plasmids and ribosome embedded in the cytoplasm, flagella involved in motility, and fimbriae that help the bacterium adhere to surfaces [31,32].

The basis for classifying bacterial species is the composition of their cell wall, which divides them into Gram-positive and Gram-negative species [31]. Gram-positive bacteria have a thick cell wall composed of peptidoglycans, teichoic acid, lipoteichoic acid, and lipoglycans covering the cytoplasmic membrane. Gram-negative bacteria have only a thin layer of peptidoglycans surrounded by an inner and outer membrane composed of phospholipids, lipopolysaccharides, and proteins [31]. However, regardless of genus, species, or strain level, the general structure of bacteria is very similar, which is outlined in Table 2.1.

Table 2.1: General composition of bacteria in mass percentage [33].

Cell component	Amount [%]
RNA	5–15
DNA	2–4
Proteins	40–60
Lipids	10–15
Carbohydrates	10–20

Bacterial species responsible for food spoilage include Gram-negative non-spore-formers (e.g., *Pseudomonas* spp.), Gram-positive spore-formers (*Bacillus* spp.), Gram-positive rods (e.g., *Brochothrix* spp.), Gram-positive cocci (*Micrococcus* spp.), and Enterobacteriaceae (e.g., *Escherichia* spp.) [34–39].

2.3 Examination of Bacteria

Bacterial contaminations are usually investigated by traditional colony counting methods or biological techniques such as bioluminescence or various staining techniques [40–46]. However, as these methods are very time-consuming, rapid alternatives have been sought for many years, especially for test environments where rapid identification is required. Particular attention has been paid to

vibrational spectroscopy [47–51]. Research in this field started with the first characterizations of microorganisms by IR spectroscopy [52–54] and developed for example to single cell characterizations by Raman spectroscopy [55–57]. Nevertheless, most methods require classical cultivation and some washing and separation steps [58,59].

As different bacterial strains have different but very similar biochemical compositions, which are reflected in the spectra, it is possible to differentiate them with the help of the spectra. These differences in composition can mostly be found for proteins and nucleic acids in the range of 540 cm^{-1} to 1800 cm^{-1} and for C-H stretching vibrations of alkyl groups in the range of 3060 cm^{-1} to 2870 cm^{-1} and should be present in the spectrum of any bacterium, as these functional groups are abundant in most biological molecules [33,60]. The differences in the spectra are often so small that they can only be detected by chemometric data analysis. The cell composition of bacteria can be concluded from the assignment of the functional groups to the respective bands of the vibrational spectra.

2.4 Chemometric Methods

Chemometrics is the process of using mathematical and statistical methods to analyze and interpret chemical data [67]. In spectroscopy, the chemometric process often begins with the preprocessing of spectra, as the spectrum is often affected by interfering effects such as fluorescence, noise, or impurities, for example, masking biologically induced spectral changes in the sample [68,69].

To subsequently find patterns in data and associate them with specific objects, projection methods such as principal component analysis are often used [67,70]. These methods are often used solely to reduce dimensions, as high-dimensional datasets are problematic to handle and analyze due to their size [71]. The low-dimensional dataset is then further processed in such a way that the mathematical combination of different variables into new variables ideally allows the separation of object classes and the prediction of object properties [67,70].

2.4.1 Pre-processing

Preprocessing is one of the most important steps in chemometric model development. During preprocessing, interfering signal components are removed from the spectrum in order to increase the analyzability of the data. However, this

can also result in the data being altered in such a way that this alteration has a negative influence on the result [72,73].
Baseline correction reduces deviations from the baseline that do not contain spectral information but are due to impurities and fluorescence [74,75]. However, important signals can be distorted by changing the baseline of the spectrum, so information can be lost [74,75].

Smoothing is often required for Raman spectra of biological material because the signal-to-noise ratio is usually low due to low scattering intensity [74,75]. Removing the noise generated by the spectrometer can reveal bands present that would otherwise be detected as noise [74,75]. However, it should be noted that smoothing can remove signals in an undesirable manner [74,76].
Normalization is performed to address the problem of varying sample thickness and differences in successive measurements due to changing conditions [49,77]. Two spectra that have the same signal components but different maximum intensity values look the same after normalization [78].

2.4.2 Principal Component Analysis

Principal component analysis is a so-called unsupervised method, which means that, in contrast to supervised methods, the membership of objects to certain classes is unknown in advance [67,70]. The purpose of PCA is to reduce dimensions by computing linear latent variables from the original data matrix without losing essential information [67,70]. These latent variables are used to create a new coordinate system that uses only the dimensions with the highest information content [67,70].
The principal components (PC) are determined based on the maximum variance criterion, which means that each subsequent PC describes a maximum of the variance that is not modeled by the previous components [67]. This means that the latent variable that has the highest variance and best preserves the relative distance between objects, and thus the information about their similarity, is defined as the first principal component (PC1) [67].

2.4.3 Canonical Discriminant Analysis

Unlike PCA, which examines data without considering information about group membership (unsupervised), discriminant analysis is a method for estimating how accurately a sample can be assigned to a group (supervised) [70]. In general, discriminant analysis increases variance between groups while decreasing variance within groups and can be divided into two types, linear and quadratic [67,70]. In linear discriminant analysis (LDA), two classes are separated by a linear boundary, whereas in quadratic discriminant analysis (QDA), the shape of the separating boundary is nonlinear [67,70]. In QDA, the distance is calculated using the variance-covariance matrix of the sample rather than the pooled matrix as in LDA [67,78]. Therefore, for large data sets where the variances of the different classes are very different, it may be more appropriate to use QDA instead of the linear method [67,78].

Chapter 3

Summary of Materials and Methods

Based on:

Klein, D., Breuch, R., von der Mark, S., Wickleder, C., Kaul, P., Detection of Spoilage Associated Bacteria using Raman-microspectroscopy Combined with Multivariate Statistical Analysis. Talanta 196 (2019), 325–328. https://doi.org/10.1016/j.talanta.2018.12.094.

Klein, D., Breuch, R., Reinmüller, J., Engelhard, C., Kaul, P., Rapid Detection and Discrimination of Food-related Bacteria using IR-microspectroscopy in Combination with Multivariate Statistical Analysis, Talanta 232 (2021), 122424. https://doi.org/10.1016/j.talanta.2021.122424.

Klein, D.; Breuch, R.; Reinmüller, J.; Engelhard, C.; Kaul, P., Investigation and Rapid Discrimination of Food-Related Bacteria under Stress Treatments Using IR Microspectroscopy. Foods 10 (2021), 1850. https://doi.org/10.3390/foods10081850.

Klein, D.; Breuch, R.; Reinmüller, J.; Engelhard, C.; Kaul, P., Discrimination of Stressed and Non-Stressed Food-Related Bacteria Using Raman-Microspectroscopy. Foods 11 (2022), 1506. https://doi.org/10.3390/foods11101506.

3.1 Bacterial Cultures and Sample Preparation

In this chapter, a brief overview of the microorganisms used and the sample preparation is given. More detailed information is given in the relevant chapter in the Materials and Methods section.

For this study, the following food spoilage-relevant bacteria were cultivated on a nutrient agar (10 g/L meat peptone, 10 g/L meat extract, 5 g/L sodium chloride, and 18 g/L agar-agar (Merck KGaA, Darmstadt, Germany)): *Escherichia coli* (*E. coli*) K12 DSM 498 (German Collection of Microorganisms), TOP10, and HB101; *Micrococcus luteus* DSM 20030 *Brochothrix thermosphacta* DSM 20171 (*B. therm*); *Pseudomonas fluorescens* (*Ps. fluor*) DSM 4358 and DSM 50090; *Bacillus subtilis* DSM 10 (*B. sub*); *Bacillus coagulans* DSM 1 (*B. coag*); and *Bacillus thuringiensis israelensis* DSM 5724 (*B. tii*) (Leibniz Institut DSMZ – German Collection of Microorganisms and Cell Cultures, Braunschweig, Germany).

The samples were taken by a blotting technique with the sample carrier (Figure 3.1) directly from the agar plate without any sampling pre-treatments.

Figure 3.1: Sampling device and sample carrier for blotting technique [79].

Spectra of samples that were cultivated under lifetime stress conditions were recorded immediately after sampling. Otherwise, the samples were subjected to sampling stress and examined spectroscopically without further incubation time after the stress impact.

3.2 Sample Treatment

In this chapter, a brief summary of the sample treatments used is given. More detailed information is given in the corresponding chapter in the respective Materials and Methods section.

3.2.1 Reference Samples (Regular Treatment)

All microorganisms were grown (Binder BD 240, BINDER GmbH, Tuttlingen, Germany) in compliance with DSMZ criteria (Leibniz Institut DSMZ - German Collection of Microorganisms and Cell Cultures, Germany). In this investigation, these samples served as reference samples.

3.2.2 Lifetime Stress Conditions

Samples were grown at 25 °C or 45 °C or were subjected to pH stress. A pH 1 hydrochloric acid (HCl) (36 %, Alfa Aesar, USA; confirmed using pH indicator paper, Th. Geyer GmbH & Co. KG, Renningen, Germany) solution or a pH 13 sodium hydroxide solution (sodium hydroxide pellets, Merck, Darmstadt, Germany, confirmed using pH indicator paper, Th. Geyer GmbH & Co. KG, Renningen, Germany) was prepared for this. The agar plates were filled with 2 mL solution of hydrochloric acid or sodium hydroxide before inoculation. The bacteria were stressed with 2-propanol (99.9 %, Höfer Chemie GmbH, Kleinblittersdorf, Germany) in the same way that they were stressed with acidic and alkaline stress.

3.2.3 Sampling Stress Conditions

Microorganisms that were exposed to sampling stress conditions were sampled from regular treated samples. They were dipped in liquid nitrogen for 60 seconds before being measured. Heat-dried samples were dried for 60 minutes at 50 °C and measured instantly, whereas desiccated samples were dried for 60 minutes on silica gel.

3.3 Microspectroscopic Setup

3.3.1 Raman-microscope

The dispersive Raman-microscope employed is a Bruker Senterra R200L (Bruker Optics GmbH, Ettlingen, Germany) with a motorized XYZ-sample stage (Märzhäuser Wetzlar GmbH & Co. KG, Wetzlar, Germany). It is attached to an Olympus BX51 (Olympus K.K, Shinjuku, Tokyo, Japan) microscope. A schematic diagram of the setup is depicted in Figure 3.2.The detector is a 2014 x 256 pixel thermoelectrically cooled CCD (charge-coupled device) of the type Andor Du420-OE. A 50x OLYMPUS LM Plan FL N (Olympus K.K, Shinjuku, Tokyo, Japan) with a numerical aperture of 0.5 and a working distance of 10.6 mm was used to focus the samples. A 785 nm diode laser (AlGaAs) was used as excitation wavelength.

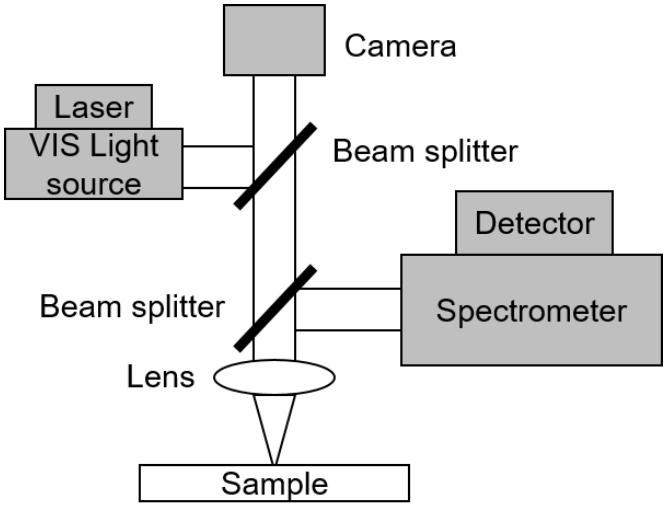

Figure 3.2: Schematic diagram of the setup of a Raman-microscope.

3.3.2 IR-microspcope

The Hyperion 3000 (Bruker Optics GmbH, Ettlingen, Germany) infrared microscope used does not have its own IR source, so it is coupled to a Vertex 70 (Bruker Optics GmbH, Ettlingen, Germany) Fourier-transform (FT)-IR spectrometer. A schematic diagram of the setup is depicted in Figure 3.3. It is equipped with a nitrogen cooled MCT (mercury cadmium telluride) detector and a 20x Cassegrain objective (Bruker Ser.910/1022346, working distance: 6 mm) with a numerical aperture of 0.6.

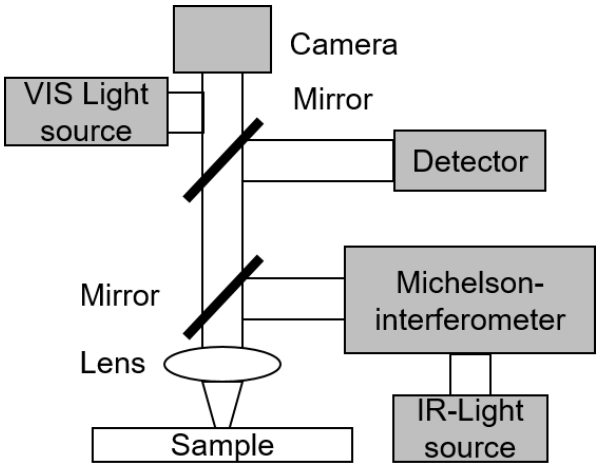

Figure 3.3: Schematic diagram of the setup of an IR-microscope.

3.4 Software

Data analytical methods were performed using OPUS 7.5 (Bruker Optics GmbH, Ettlingen, Germany), LabVIEW 2016 (National Instrument, Austin, Texas, USA) and OriginPro 2019b (OriginLab Corporation, Northampton, MA, USA). Preprocessing and data reduction was performed using OPUS, LabVIEW, and Origin. Classification using quadratic discriminant analysis was performed using OriginPro 2019b.

Chapter 4

Detection of Spoilage Associated Bacteria using Raman-microspectroscopy Combined with Multivariate Statistical Analysis

Based on:

Klein, D., Breuch, R., von der Mark, S., Wickleder, C., Kaul, P., Detection of Spoilage Associated Bacteria using Raman-microspectroscopy Combined with Multivariate Statistical Analysis. Talanta 196 (2019), 325–328. https://doi.org/10.1016/j.talanta.2018.12.094.

Supplemental Notice:

In Table 4.1, the percentage values and sums have been excluded in favor of better readability compared to the original publication. The original table can be found in the Supplementary Material (Chapter 4.5). Figures 4.3 and 4.4 have been optimized for better readability.
References have been moved into the sentence for consistency with the other chapters.

Authors' contribution Chapter 4:

Daniel Klein

Conceptualization, methodology, software, validation, formal analysis, investigation, data curation, visualization, writing—original draft, writing—review and editing

Rene Breuch

Software, Validation, writing—review and editing

Sune von der Mark

Investigation, writing—review and editing

Claudia Wickleder

Supervision, writing—review and editing

Peter Kaul

Supervision, writing—review and editing, project administration, funding acquisition

4.1 Introduction

Unsafe food can cause more than 200 different diseases which lead to 420,000 deaths due to food borne illnesses every year [24]. Although foodstuffs are subject to strict controls, food safety and the consumer's health protection are still of great importance. In Germany alone, more than one thousand cases of food borne illnesses lead to hospitalization every year in the last years and the EHEC O104:H4 outbreak in 2011 showed that dangerous epidemic food borne illnesses are not only a problem of the developing countries [80–82].

As a result of this fact and the large quantity of up to 115 kg wasted food per person every year due to the fear of food borne illnesses from spoiled or contaminated food the topic food waste reduction is of ecologic and economic importance [83].

Currently, the expiration date of fresh meat products is estimated very conservatively and because of this large amounts of food are disposed of, although the product would have been still suitable for consumption [16,40]. Today the initial bacterial load, which is essential to determine the shelf-life time of meat products, is subjected only in cost-, time- and labor-intensive sporadic tests, like the standard colony-counting methods and other sophisticated biological techniques such as bioluminescence or different staining techniques [35,40–46].

Consequentially there is a great demand on fast, non-destructive and cost-effective analysis methods to determine the initial bacterial load. This deficiency can be corrected by the fast, robust and non-destructive detection of bacteria by Raman-microspectroscopy.

The microbial flora of fresh and chilled meat during the spoilage process is mostly dominated by *Pseudomonas spp*., especially *Pseudomonas fluorescens (Ps. fluor.)*, *Brochothrix thermosphacta* (*B. therm.*) and *Enterobacteriaceae*, like *Escherichia coli* [35–39]. Additionally, *Micrococcus luteus* and Bacillus thuringiensis israelensis (*B. tii*) are often detected on spoiled meat or other foodstuffs for example [84–86].

Therefore, the objective of this study was to find a timesaving and suitable sample preparation of microbiological samples, rapid measurement parameters and a reasonable chemometric data processing for a rapid and non-destructive analysis of food safety and especially meat spoilage relevant bacteria. For this an adequate preprocessing method and chemometric evaluation to classify and distinguish between the measured bacteria was developed.

The differentiation of genera and strains is very important in application because for example *Pseudomonas spp.* is a genus of great diversity including for example food safety relevant pathogenic species [87].

4.2 Materials and Methods

4.2.1 Bacterial Cultures and Sample Preparation

Seven important spoilage related bacteria, namely Brochothrix thermosphacta DSM 20171, Escherichia coli HB101, Escherichia coli TOP10, Micrococcus luteus (M. luteus), Pseudomonas fluorescens DSM 4358, Pseudomonas fluorescens DSM 50090 and Bacillus thuringiensis israelensis DSM 5724 (Leibniz Institut DSMZ – German Collection of Microorganisms and Cell Cultures, Braunschweig, Germany) were cultivated and separately grown according to the DSMZ guidelines [88]. The nutrient agar consisted of 10 g/L meat peptone, 10 g/L meat extract, 5 g/L sodium chloride and 18 g/L agar-agar (Merck KGaA, Darmstadt, Germany).

The colonies were then harvested by a rapid blotting technique. To this end, a disinfected round stainless steel cylinder with a diameter of eight millimeter on the front face was pressed directly on the agar plates. Raman measurements were performed directly after the blotting from the agar plate. All training data points were generated on at least two independent blots per strain and at a different spot for each spectrum. The test data were generated on at least three different blots of two independent biological replicates of the samples.

4.2.2 Instrumentation

In this study a SENTERRA Raman-Microscope (Bruker Optics GmbH, Ettlingen, Germany) with a charge-coupled device (CCD) detector was used. The microbiological samples were placed on a motorized XYZ-sample stage and focused with a LMPlanFL N 50x objective lens (Olympus K.K, Shinjuku, Tokyo, Japan). The measurements were performed with a 785 nm diode laser. Controlling and data acquisition is carried out by the OPUS 7.5 Raman environment software.

All measurements were collected with an initial laser power of 100 mW and an integration time of nine seconds. The influence of the spectral quality with respect to the number of coadditions was tested between 4 and 150 coadditions. To further reduce the measurement time and to cover the most relevant bacterial Raman

features, the parameters were set to nine seconds integration time, four coadditions and a spectral range of 410–1790 cm^{-1} with a spectral resolution of 3 ~ 5 cm^{-1} was chosen.

4.2.3 Data Processing

During preprocessing all Raman spectra were cut to the range 600–1200 cm^{-1}, as this range shows the highest information content and the most distinct spectral information. In addition, all spectra were concave rubber band baseline corrected with eleven iterations and 64 baseline points, 13-point Savitzky-Golay smoothed and minimum-maximum-normalized.

For the subsequent chemometric analysis and to simplify the complex multivariate Raman data principal component analysis (PCA) and discriminant analysis were used. PCA is an unsupervised chemometric technique which does not need any previous information about the data set and transforms the given n-dimensional data in a projected space where the given variance of the data set is maximized in less than n-dimensions. The subsequent analysis was performed using Origin Pro 2017G (OriginLab Corporation, Northampton, Massachusetts, USA).

After data reduction by PCA, the complex spectral information of very similar microbiological spectra is made manageable for classification by canonical discriminant analysis (CDA). CDA is used to determine a linear combination of the variables which maximizes the relation of inter-group and intra-group variations [89,90].

4.3 Results and Discussion

At the beginning, the sampling and data acquisition was designed in such a way that it is as fast and uncomplicated as possible. For this purpose, a sample of *E. coli* was produced according to the described sampling technique without any pretreatments like matrix separation or washing and measured with different cumulative measuring times. For this the cumulative measuring time was varied by the amount of coadditions of each measurement and the integration time of nine seconds is kept constant (Figure 4.1).

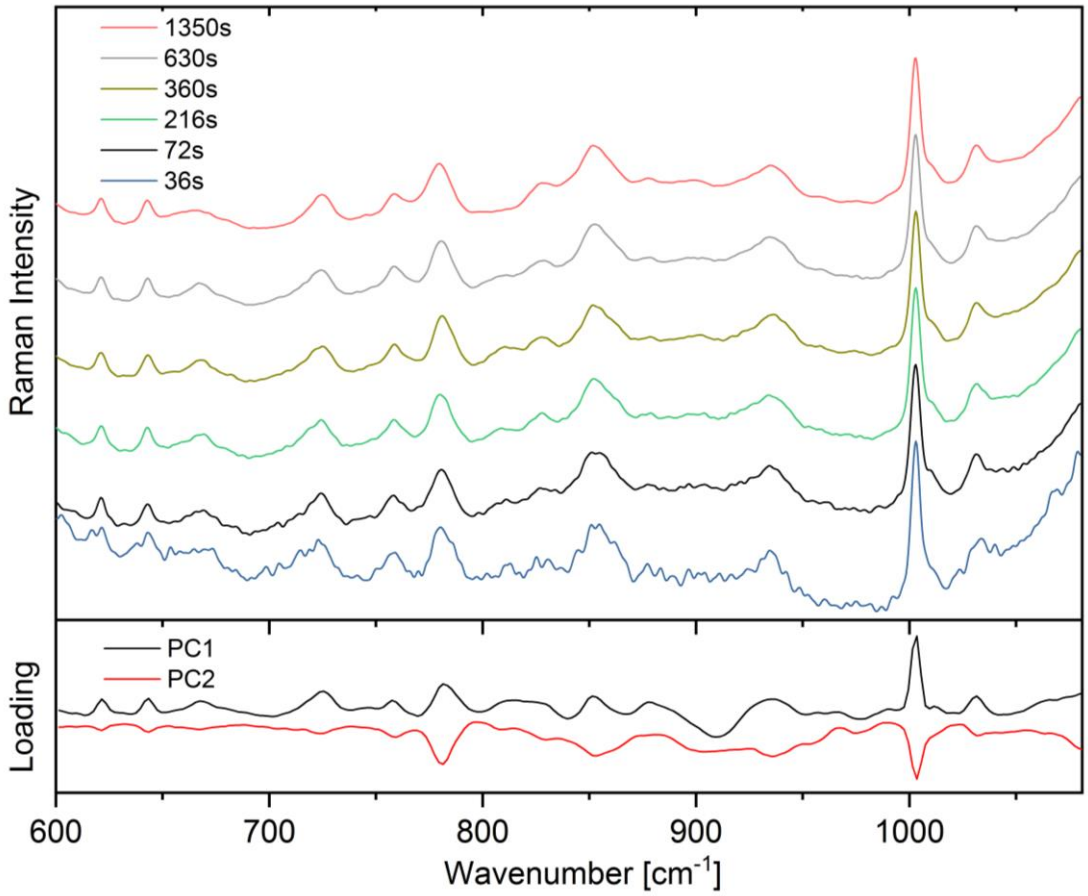

Figure 4.1: Raw Raman spectra of *E. coli* recorded with six different cumulative measurement times, each with nine seconds integration time but different amount of coadditions. Below the spectra the loadings for PC1 and PC2 from a PCA of a data set of 36s measuring time are displayed.

It can be seen that the signal to noise ratio improves considerably with increasing cumulative measuring time and that spectral characteristics display better visibility than in the rapidly recorded spectra, in which only a few characteristics are distinguishable from the noise.

In order to compare the information content of the different measurements with the information given in the spectra for 1350s the sums of least squares of the given spectra were calculated. The sums of least squares of the measurements with 630s to 72s are in a range between 1.7 and 3.0. This indicates no significant changes in information content.

However, the sum of least squares of the measurement with 36s (9s4coad) is 106, which indicates a significant deviation in comparison to the spectra shown before. This allows the conclusion that the information content of this spectrum is much lower or could be obscured by noise.

Finally, the shortest measurement time was used for this study in order to test the method presented below with the lowest information content, the noisiest spectra and thus the most rapid method.

In order to check whether the highly attenuated information content of the rapidly recorded spectra did not falsify the evaluation with regard to a possible separation on the basis of statistical noise a deeper look into the loadings of a PCA is needed. This comparison of the Raman spectra and the loadings of a PCA show that the data for the pending classification are based on spectral information (Figure 4.1).

To illustrate the variations within the spectra of one strain the mean Raman spectra with standard deviations of each wavenumber of 500 spectra for each strain are shown (Figure 4.2). In total 3500 spectra are presented with 500 spectra each of *Pseudomonas fluorescens* DSM 50090 and DSM 4358, *Micrococcus luteus*, *Escherichia coli* TOP10 and HB101, *Brochothrix thermosphacta* and *Bacillus thuringiensis subsp. israelensis* are shown.

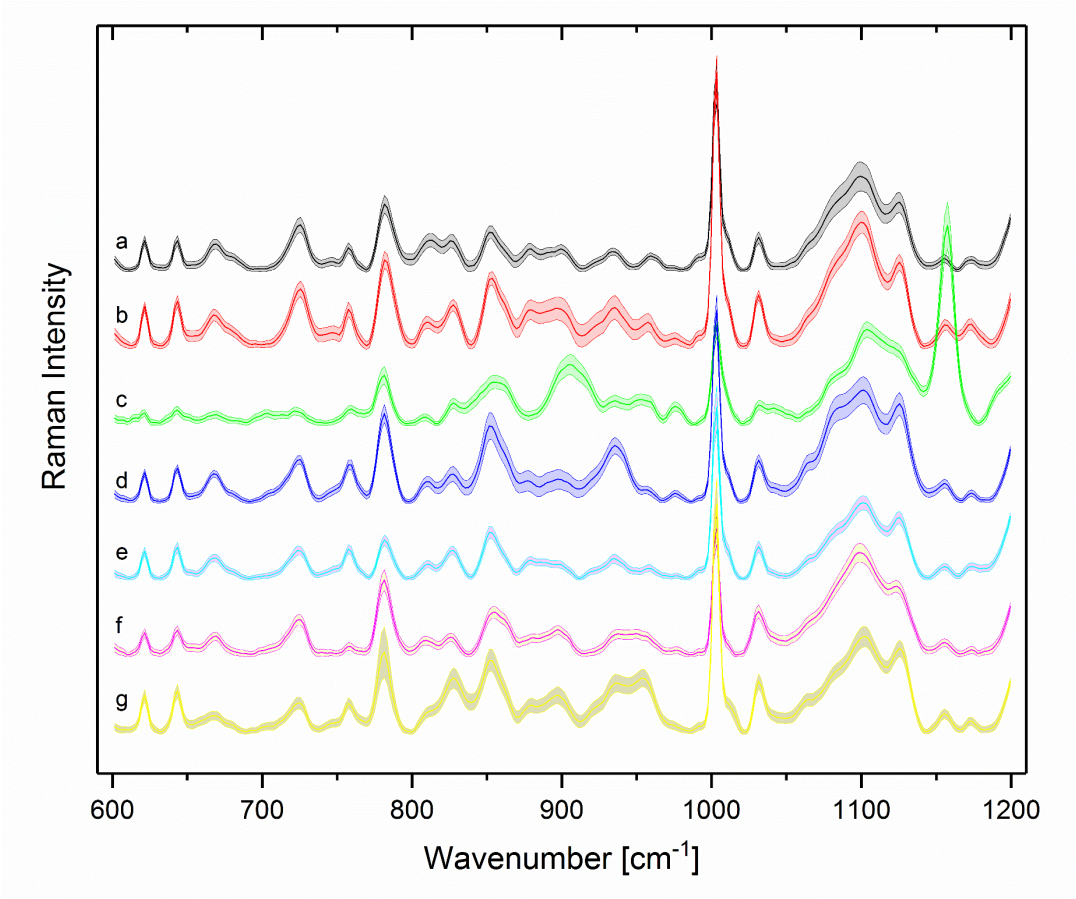

Figure 4.2: Mean Raman spectra and the standard deviations of 500 spectra of each sample of *Ps. fluo*rescens DSM 50090 (a), *Ps. fluo*rescens DSM 4358 (b), *Micrococcus luteus* (c), *E. coli* TOP10 (d), *E. coli* HB101 (e), *Brochothrix thermosphacta* (f) and *Bacillus thuringiensis subsp. israelensis* (g) after preprocessing.

Only very tiny visual differences in the spectral profile of the different microorganisms can be noticed. These variations result from the composition differences of the microbial cell for example the variation of proteins and lipids in the cell. An obvious difference is the ostentatious band of *Micrococcus luteus* which results from the carotenoid sarcinaxanthine at 1158 cm^{-1}, which is responsible for the yellowish color of *Micrococcus luteus* [91].

Multivariate statistics such as principal component analysis and discriminant analysis were used to analyze and classify the spectral data. For these multivariate statistical methods it is essential to operate with same size data sets within the classes, because not only PCA is sensitive to imbalanced data sets but also discriminant analysis is sorely affected in performance [92,93].

To validate the developed sampling, preprocessing and evaluation model with independent data, a test dataset was created that not only consists of at least three independent blots but also of two independent biological replicates of the chosen spoilage bacteria.

For the subsequent discriminant analysis the first seven principal components of the PCA, which represent 92.81 % of the variance of all training data, were used. As the equality test of covariance matrices of each bacterium of the training data showed that the covariance matrices are not equivalent between the bacteria, a quadratic discriminant function was used instead of a linear discriminant function.

The results of the trained CDA model using the first four canonical variables (CV) are depicted in Figure 4.3. This scatter matrix plot shows that all used spoilage related bacteria can be separated successfully.

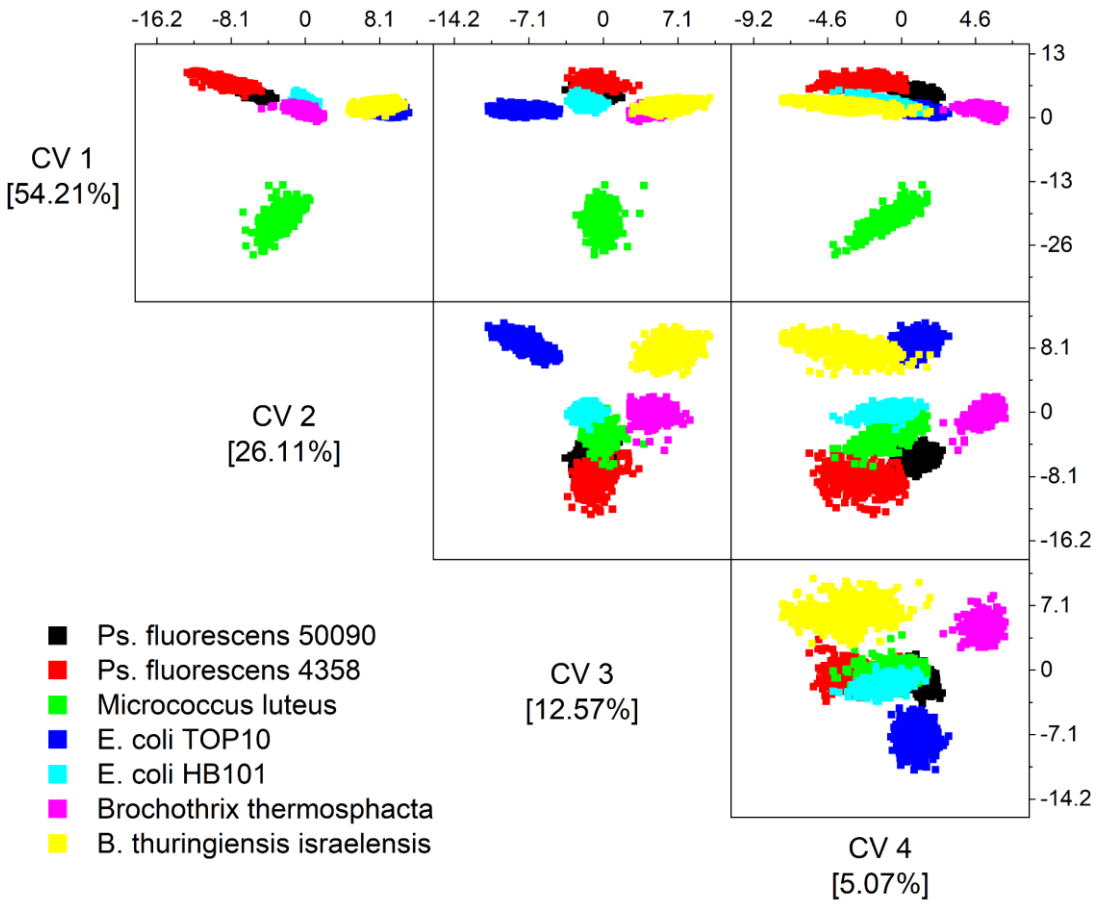

Figure 4.3: Scatter matrix plot of the score diagrams for the first four canonical variables of the first seven principal components derived the Raman spectra of the 3500 spectra of the training data set.

For independent testing of the generated model, the test data must be processed independent of the training data set. The spectra of the test data set were preprocessed in the same way as the training data and then converted to new scores in the space of the training data set (Figure 4.4) using the loadings obtained from the trained model.

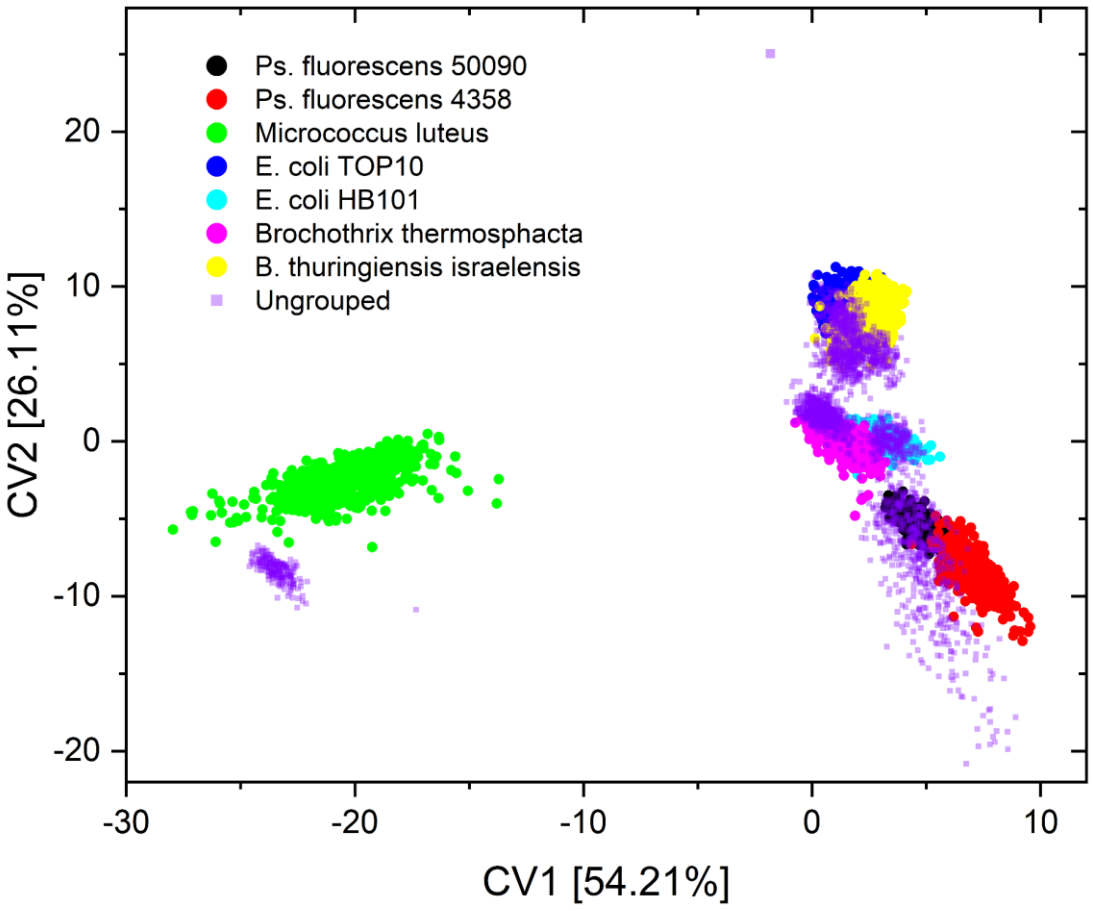

Figure 4.4: Score diagram based on the first two canonical variables of the first seven principal components derived of the training data set including the independent test data set of 2434 spectra.

The test data could have been classified with just an error rate of 3.5 %, which means that only 85 of 2434 spectra are not classified correctly (Table 4.1).

Table 4.1: Confusion matrix for the independent test data set 2434 spectra. The rows show the observed groups and the columns show the predicted groups. The values in the diagonal of the table reflect the correct classifications of observations into groups.

	Predicted class							
	B. therm	***B. tii***	***E. coli* HB101**	***M. luteus***	***Ps. fluor.* 4358**	***Ps. fluor.* 50090**	***E. coli* TOP10**	***Not classified***
B.therm	557	0	0	0	0	0	0	0
B. tii	0	294	0	0	0	0	0	0
E. coli HB101	0	0	228	0	48	0	0	0
M. luteus	0	0	0	199	0	0	0	0
Ps. fluor. 4358	2	1	1	0	509	32	0	1
E. coli TOP10	0	0	0	0	0	0	562	0

The results show that the presented sampling- and measuring technique with a single subsequent chemometric evaluation is able to differentiate between spoilage related microorganisms on genera and even on strain level in a fast, efficient, and easy way. Although all usual washing, centrifugation and singulation steps were omitted, qualitatively good spectra could be generated using the presented fast preparation and measurement method and thus a robust method for discriminating different bacteria on genera and strain level could be shown.

4.4 Conclusion

To summarize, the method of Raman-microspectroscopy with subsequent chemometric evaluation could successfully be used to rapidly and non-destructively analyze meat spoilage microorganisms out of fast but noisy spectra generated directly from rapid surface blots. The presented preprocessing method, the successive principle component analysis and canonical discriminant analysis showed that seven different spoilage related microorganisms could be separated and classified with only an error rate of 3.5 % at genera and strain level from fast generated and noisy spectra. The received results are very promising and this technology has the potential to be used for the rapid differentiation of microorganism and potentially to determine microbial contaminations in food safety issues.

4.5 Supplementary Material

Table 4.2: Confusion matrix for the independent test data set 2434 spectra. The rows show the observed groups and the columns show the predicted groups. The values in the diagonal of the table reflect the correct classifications of observations into groups.

	Predicted class								
	***B. therm*.**	***B. tii*** i	***E. coli* HB101**	***M. luteus***	***Ps. fluor*. 4358**	***Ps. fluor*. 50090**	***E. coli* TOP10**	***Not classified***	***Sum***
B. therm	557	0	0	0	0	0	0	0	557
	100%	0%	0%	0%	0%	0%	0%	0%	100.00%
B. tii	0	294	0	0	0	0	0	0	294
	0%	100%	0%	0%	0%	0%	0%	0%	100.00%
***E. coli* HB101**	0	0	228	0	48	0	0	0	276
	0%	0%	82.61%	0%	17.39%	0%	0%	0%	100.00%
M. luteus	0	0	0	199	0	0	0	0	199
	0%	0%	0%	100%	0%	0%	0%	0%	100.00%
***Ps. fluor*. 4358**	2	1	1	0	509	32	0	1	546
	0.37%	0.18%	0.18%	0%	93.22%	5.86%	0%	0.18%	100.00%
***E. coli* TOP10**	0	0	0	0	0	0	562	0	562
	0%	0%	0%	0%	0%	0%	100%	0%	100.00%

Chapter 5

Rapid Detection and Discrimination of Food-related Bacteria using IR-microspectroscopy in Combination with Multivariate Statistical Analysis

Based on:

Klein, D., Breuch, R., Reinmüller, J., Engelhard, C., Kaul, P., Rapid Detection and Discrimination of Food-related Bacteria using IR-microspectroscopy in Combination with Multivariate Statistical Analysis, Talanta 232 (2021), 122424. https://doi.org/10.1016/j.talanta.2021.122424.

Supplemental Notice:

In Table 5.2, the percentage values have been excluded in favor of better readability compared to the original publication. The original table can be found in the Supplementary Material (Chapter 5.5)

Authors' contribution Chapter 5:

Daniel Klein

Conceptualization, methodology, software, validation, formal analysis, investigation, data curation, visualization, writing—original draft, writing—review and editing

Rene Breuch

Software, Validation, writing—review and editing

Jessica Reinmüller

Investigation, writing—review and editing

Carsten Engelhard

Supervision, writing—review and editing

Peter Kaul

Supervision, writing—review and editing, project administration, funding acquisition

5.1 Introduction

Perishable foods and food products are not only nourishing for the consumer but may eventually become unsafe for the consumer due to microbial growth [94]. Microbial growth in unsafe foods can cause several diseases particularly affecting infants, young children, and the elderly. As a result, the World Health Organization estimates that 420,000 deaths can be attributed to foodborne diseases [24]. In contrast, because of fear of contracting a disease ad food safety guidelines approximately 3.5 billion kg per year of meat and poultry are disposed of along the supply chain and by the consumer only in the United States [95]. Therefore, food waste reduction is of great ecologic and economic importance [83,94] and the expiration date of a product is an almost omnipresent topic of discussion. The best-before date is usually estimated very conservatively and, therefore, many foods are disposed of although they would still have been consumable [16,96].

To ensure food safety, producers and suppliers have to implement effective microbial growth detection methods. Standard culture-based methods to detect bacterial contamination require several days to be completed. They are time-consuming and labor-intensive and, therefore, only provide backdated information, which, in turn, leads to problems in industry, especially in the food sector [19,94,97,98]. Thus, the food industry needs a rapid microbial testing process to reduce potential health hazards for consumer safety, economic risks and environmental burden [96,99,100]. Recently, methods such as molecular-based and immunological assays, polymerase chain reaction, fluorescence staining or the use of metabolic markers have come into focus to optimize the analysis time [44,45,97,98].

In addition, vibrational spectroscopy of biological samples, especially of microorganisms, has been in the focus of research for three decades [47–51]. Since then, the potential of infrared (IR)- [53,101,102] and Raman-spectroscopy [103–105] for the determination, typing and classification of microorganisms and especially pathogenic bacteria has been shown. More specifically, Davis *et al.* (2012) [53], Johler *et al.* (2016) [101] and Martak *et al.* (2019) [102] investigated the possibilities of typing and subtyping of pathogenic microorganisms by IR-spectroscopy in comparison to standard microbiological methods such as multilocus variable-number tandem repeat analysis (MLVA), pulsed-field gel electrophoresis (PFGE) and multilocus sequence typing (MLST),

where they found that IR-spectroscopy is a possibility for rapid detection of these pathogens, with comparable results to classical microbiological methods. Additionally, Grewal *et al.* showed the influence of using different spectral ranges of spectra for classification [106].

In the field of Raman-spectroscopy, Meisel *et al.* (2014) [103], Ho *et al.* (2019) [104] and Breuch *et al.* (2020) [105] focused on the classification of the most common pathogenic microorganisms and mostly pathogenic microorganisms related to meat spoilage using modern deep learning methods, support vector machines, and discrimination analysis. Furthermore, traditional microbiological techniques and other sophisticated analytical methods were adapted or coupled to spectroscopic methods for a better analysis of biological samples [45,107–113]. The development of reliable measurement methods, their standardization and the improvement of data evaluation including the data preprocessing appear to be important fields of research [68,114–116].

The most dominant microorganisms detected on fresh and chilled meat and other foodstuffs are Pseudomonas spp., especially *Pseudomonas fluorescens* (*Ps. fluor*) and *Enterobacteriaceae*, such as *Escherichia coli* (*E. coli*), *Micrococcus luteus* (*M. luteus*), *Bacillus thuringiensis israelensis* (*B. tii*), *Bacillus coagulans* (*B. coag*) and *Bacillus subtilis* (*B. sub*) [37,117–122].

As the need for rapid and non-destructive analysis of food-related microorganisms still exists, the aim of this study was the development of a fast, easy, and inexpensive way to sample food-related microorganisms and to build a robust and meaningful model to discriminate these microorganisms by IR-microspectroscopy down to strain level irrespective of their time after incubation.

5.2 Materials and Methods

5.2.1 Bacterial Cultures and Sample Preparation

For the preparation of the bacterial cultures, our previously published method, which is in accordance to the DSMZ guidelines, was used [88,123]. Eight important food-related bacteria (*Bacillus subtilis* DSM 10, *Bacillus coagulans* DSM 1, *Escherichia coli* K12 DSM 498, *Escherichia coli* HB101, *Micrococcus luteus* DSM 20030, *Pseudomonas fluorescens* DSM 4358, *Pseudomonas fluorescens* DSM 50090 and *Bacillus thuringiensis israelensis* DSM 5724 (Leibniz Institut DSMZ – German Collection of Microorganisms and Cell Cultures, Braunschweig, Germany)) were

cultivated on nutrient agar (10 g/L meat peptone, 10 g/L meat extract, 5 g/L sodium chloride and 18 g/L agar-agar (Merck KGaA,Darmstadt, Germany)).

Microorganisms were obtained directly with the sample carrier — a disinfected round stainless steel cylinder. For this, the cylinder was slightly pressed on the agar plate to blot microorganisms to the front face of the sample carrier. IR spectra were taken directly after the blotting from the surface of this cylinder without any drying processes [123].

After incubation the inoculated agar plates were sealed with Parafilm (Bemis Company, Inc., Neenah, United States) and stored at 4 °C.

To generate fully independent training and test data sets, all microorganisms were measured from three independent batches with different time periods after incubation to form three independent data sets (Table 5.1).

The sampling and data acquisition were designed to be as fast as possible. Sampling was performed without any pretreatments such as matrix separation, washing or singulation.

5.2.2 Instrumentation

In this study, a Hyperion 3000 IR-microscope coupled to a Vertex 70 spectrometer (Bruker Optics GmbH, Ettlingen, Germany) with a liquid nitrogen cooled Mercury/Cadmium/Telluride (MCT) detector was used. The microbiological samples were placed on a motorized XYZ-sample stage and focused with a 20x Cassegrain objective (Bruker Ser.910/1022346, numerical aperture: 0.6, working distance: 6 mm). Controlling and data acquisition is carried out by the OPUS 7.5 software.

All measurements were collected in reflectance mode with 20 scans per spectra. The spectral resolution was set to 4 cm^{-1}.

5.2.3 Data Handling

During preprocessing, all IR spectra were sum normalized and cut to the range 2815–3680 cm^{-1} within Origin Pro2019b and afterwards the first derivative was generated and a 13-point Savitzky-Golay filter was used within an own LabVIEW 2016 script. The three independent data sets of each microorganism (see Chapter “Bacterial Cultures and Sample Preparation”) were divided into two independent data sets, which form the training data set, and one independent data set, which represents the test data set.

The splitting for training and test data was carried out as described in Table 5.1.

Table 5.1: Data splitting scheme for the tested microorganisms. The time period after preparation according to the DSMZ guidelines is given in days.

Organism	Testdata Time period after inoculation [days]	Training Time period after inoculation [days]
Micrococcus luteus	7, 24	1
Bacillus coagulans	6, 8	12
Bacillus subtilis	8, 12	6
Bacillus thuringiensis israelensis	6, 12	8
Escherichia coli K12	6, 7	12
Escherichia coli HB101	6, 7	12
Pseudomonas fluorescens DSM 50090	7, 8	6
Pseudomonas fluorescens DSM 4358	6, 7	1

Complex spectral information of bacteria requires a closer look inside the variances of a data set. For this, the unsupervised chemometric technique, principal component analysis (PCA), was applied to the training data to focus on the variances and reduce the dimensionality of the data [124]. Afterwards, the test data set was converted into the same dimensional space by applying the descriptive statistics of the training data set and the eigenvectors also called loadings from the PCA of the training data set to the test data set (own LabVIEW 2016 script). The manageable data set was classified by a supervised classifier, called canonical discriminant analysis (CDA), which uses a linear combination of the input data variables to maximize the ratio of inter-group and intra-group variations of the different classes [89,90].

An overview of the data handling process is schematically shown in Figure 5.1.

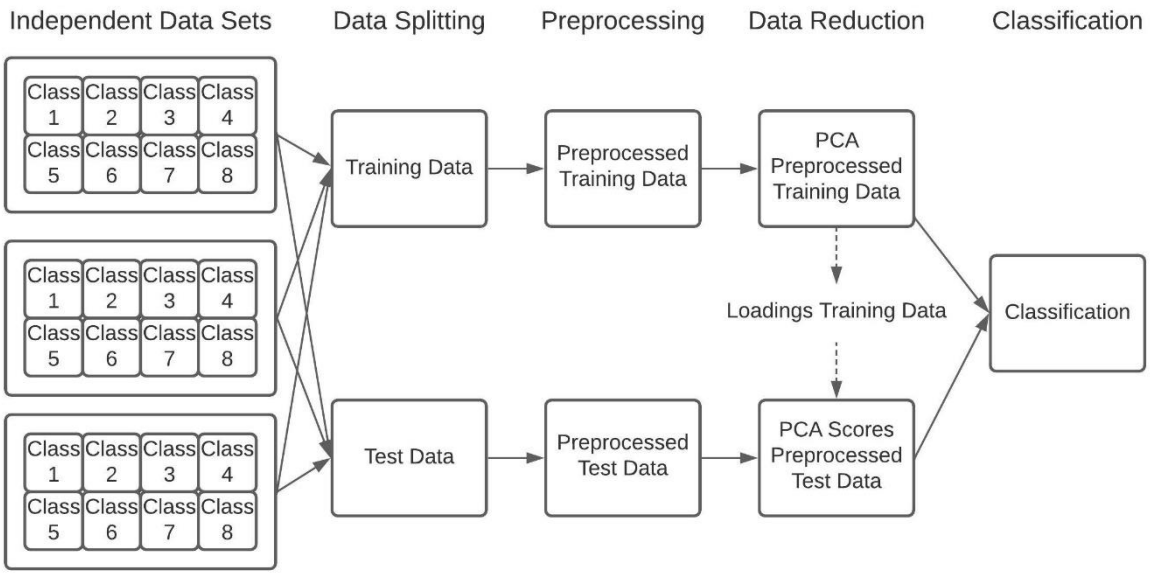

Figure 5.1: Schematic overview of the described data handling process.

The data handling was performed using Origin Pro 2019b (OriginLab Corporation, Northampton, Massachusetts, USA) and National Instruments LabVIEW 2016 (National Instrument, Austin, Texas, USA).

5.3 Results and Discussion

First, a spectral library of the tested food-related microorganisms on a stainless steel substrate was obtained in IR reflectance mode. With this, characteristic spectral features and signal variations among spectra from one microorganism could be monitored. In Figure 5.2, mean IR spectra (1000–3680 cm^{-1}, n = 150 acquisitions) and their standard deviations are depicted for each microorganism. In total 1,200 spectra with 150 spectra each of *B. subtilis* DSM 10, *B. coagulans* DSM 1, *E. coli* K12 DSM 498, *E. coli* HB101, *M. luteus* DSM 20030, *Ps. fluor* DSM 4358, *Ps. fluor* DSM 50090, and *B. thuringiensis israelensis* DSM 5724 are presented.

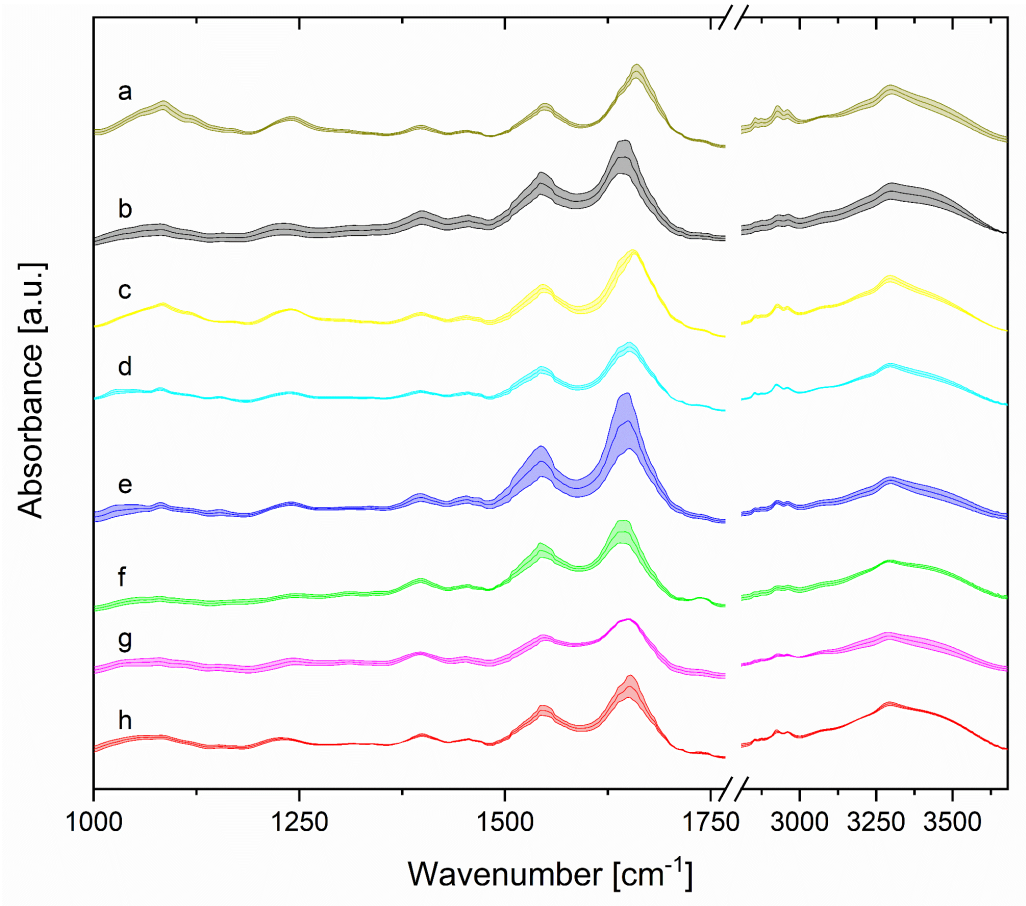

Figure 5.2: Stacked mean IR spectra of the normalized data of 150 spectra of each sample of *Ps. fluor* 4 and *Ps. fluor* 5 (a & c), *B. coag* (b), *E. coli* TOP10 and K12 (d & e), *B. tii* (f), *M. luteus* (g) and *B. sub* (h). Standard deviations are indicated by color-coded bands around the mean value.

As the fingerprint area was determined to be highly sensitive to sample age and thickness by means of the standard deviation from Figure 5.2, this area was excluded from further modelling and only the spectral range of specific –CH/–NH/–OH excitations from 2815 cm^{-1} to 3680 cm^{-1} was used for further evaluation (Figure 5.3).

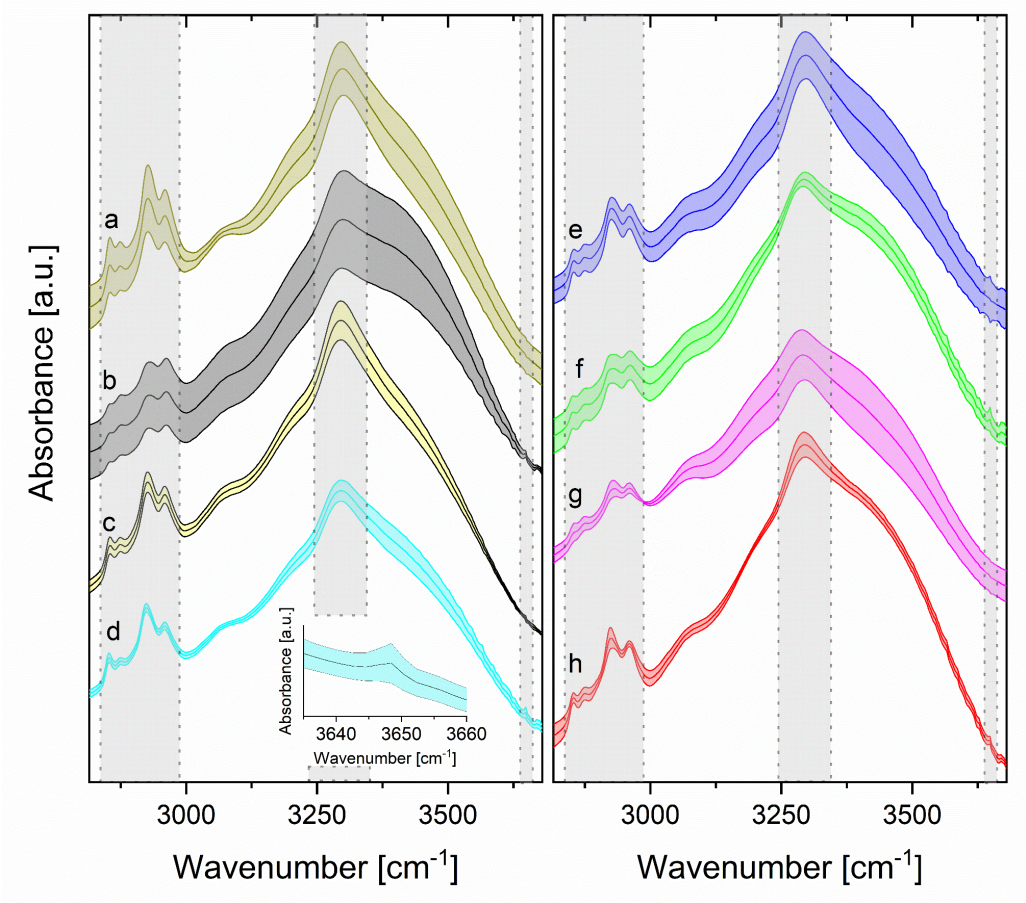

Figure 5.3: Stacked mean CH range of the IR spectra and the standard deviations of the normalized data of 150 spectra of each sample of *Ps. fluor* 4 and *Ps. fluor* 5 (a&c), *B. coag* (b), *E. coli* TOP10 and K12 (d&e), *B. tii* (f), *M. luteus* (g) and *B. sub* (h). In this graph, spectral ranges are highlighted in gray, which were identified by loading plot analysis to be important. Additionally, an inset graph exemplarily shows a zoom-in into the peak area highlighted at 3650 cm^{-1}.

A visual differentiation or even classification of the spectra is not only very time-consuming, but also nearly impossible due to only small differences. These small spectral differences of the different microorganisms result, for example, from the different composition of the proteins, nucleic acids, lipopolysaccharides or lipids of the cell [49]. To focus on these small differences the first derivative was used in the following data processing.

Here, the use of multivariate statistics is an efficient way to obtain a fast comparison among spectra based on their spectral differences. In this study, PCA was used for data reduction of the preprocessed spectra and CDA for classification.

Since PCA and discriminant analysis are affected in performance by unequally large (imbalanced) data sets the creation of balanced data sets for a chemometric evaluation is essential [92,93]. Therefore, each data set and each class needs the

same sample size. This prevents unintentional weighting within the model generation.

To ensure that the underlying model is based on spectral features and is not differentiated by noise or sample preparation, an analysis of the PCA loadings is useful (Figure 5.4).

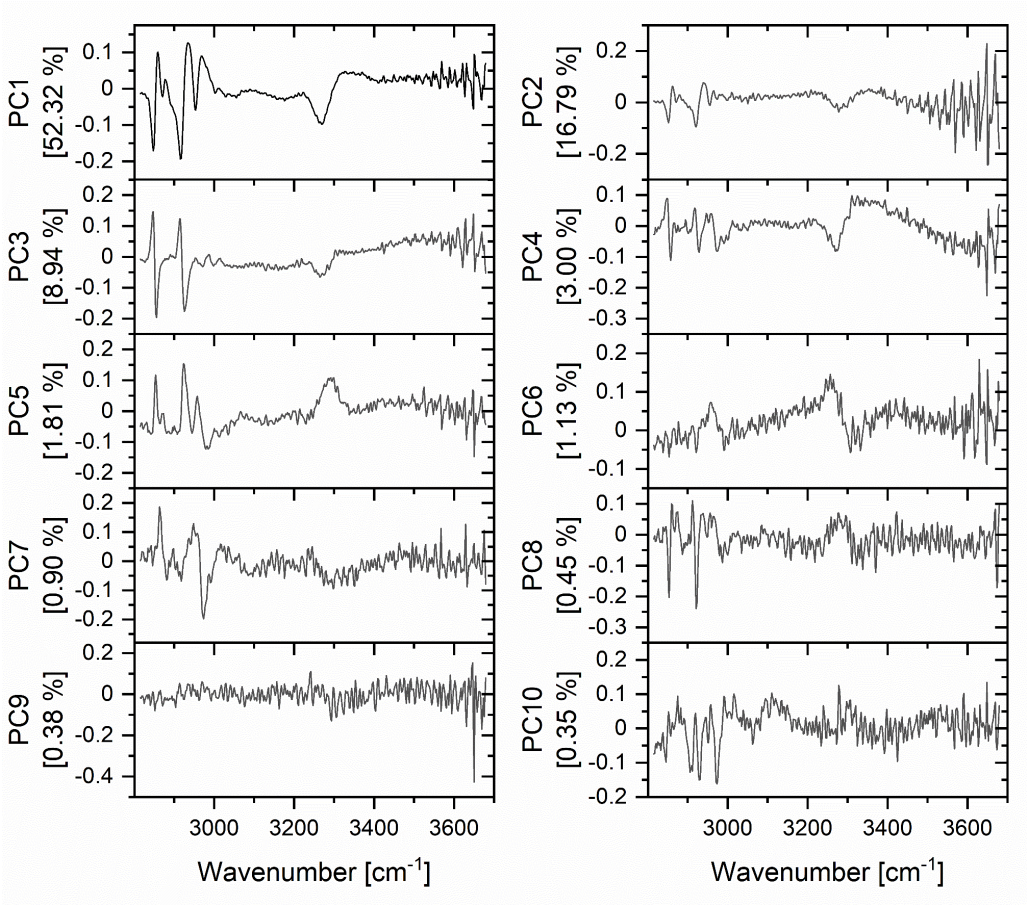

Figure 5.4: Loadings (PC1 – PC10) of the PCA of the training data set (consisting of spectra of all eight measured bacteria).

The comparison of the IR spectra with the characteristics of the loadings clearly shows that the highest loading values match to spectral features highlighted in gray in Figure 5.3.

The most of the variance can be found on the first three PCs, but it can be seen that important spectral information can be extracted even from the PCs, which represent just small variances.

Especially for PC8 and PC9 (Figure 5.4), the spectral feature at about 3650 cm^{-1} (free O–H stretching vibrations), which is shown in the inset in Figure 5.3, is striking. Additionally, the oscillations of C–H stretching vibrations corresponding to the fatty

and amino acids (2850–3000 cm^{-1}) and N–H stretching vibrations corresponding to the amide A in proteins (~3300 cm^{-1}) are highlighted [33,125,126].

As there was no significant equality of the covariance matrices of the training data classes a quadratic instead of a linear discriminant function had to be used [127–129].

For the subsequent discriminant analysis, the first ten principal components of the PCA, which represent 86.11 % of the total variance of the training data set, were used. The QDA classification was cross-validated without any misclassification. The first four canonical variables (CV) of the quadratic discriminant analysis (QDA) are depicted in Figure 5.5.

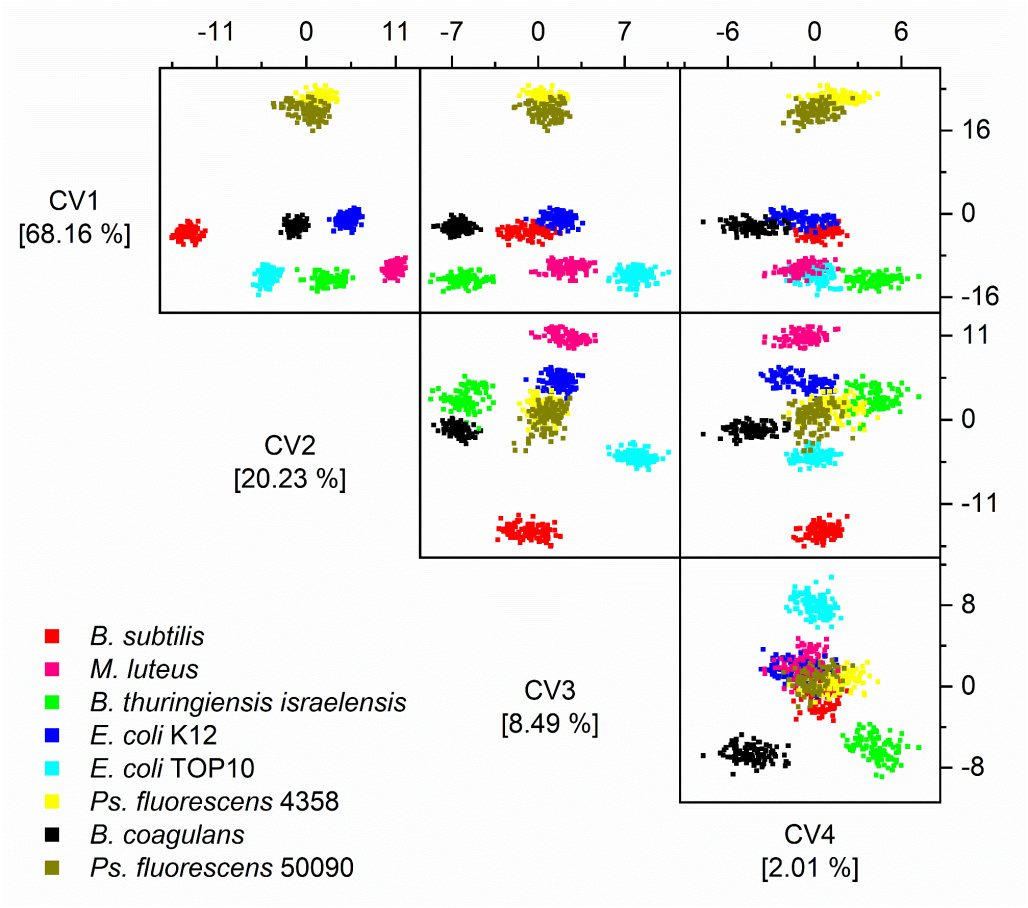

Figure 5.5: Scatter matrix plot of the training data set with canonical variables 1 to 4 of the QDA.

The first two canonical variables are sufficient to separate all classes on strain and species level except the *Pseudomonas fluorescens* strains. A visual separation of the two *Pseudomonas* strains seems to be difficult. But in general, a model could be created that separates the different genera of *Bacillus* from *Pseudomonas* and from *Micrococcus* and *E. coli*.

To validate the developed preprocessing and chemometric model for its robustness, data integrity and accuracy with independent data, a test data set of each class was subjected to the same preprocessing as the training data set. Then the new scores of the test data set were calculated by means of the loadings and descriptive statistics of the training data set. These were projected into the existing model of discriminant analysis for classification.

The test data of the corresponding classes have the same color code as the training data, only with unfilled squares (Figure 5.6). At a closer look at the combination of all four canonical variables, it can be seen that the test data is close to the training data.

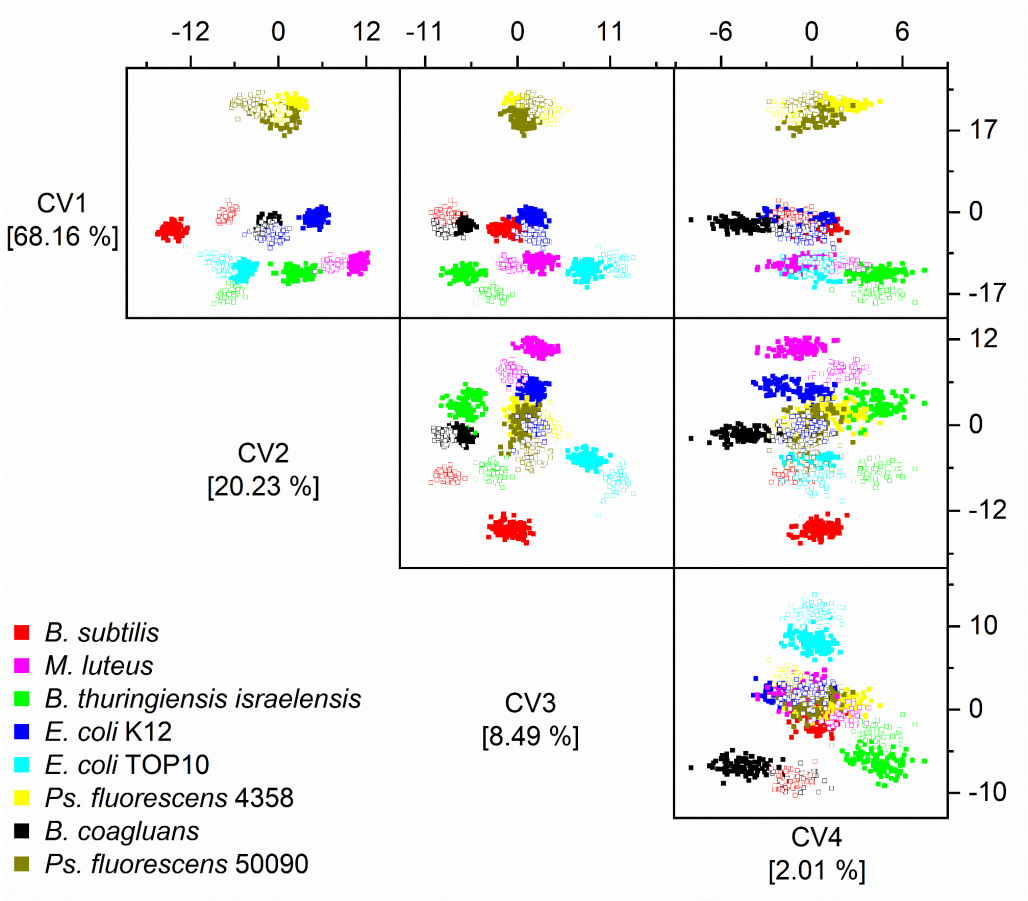

Figure 5.6: Scatter matrix plot of canonical variable 1 to 4 of the QDA including the independent test data set.

In conclusion of the CDA results, Table 5.2 shows the confusion matrix of the results of the independent test data of the CDA. The test data could be classified with an error rate of only 5.5 %. In contrast to the results of Rebuffo-Scheer *et al.* and Janbu *et al.*, who pointed out that IR-microspectroscopy leads to higher

misclassification rates than classical macroscopic FTIR measurements [130,131], our results are by no means inferior to macroscopic classification rates.

The error rate of 5.5 % is caused by a partial assignment of *M. luteus* to *B. thuringiensis israelensis*. Furthermore, a part of the *E. coli* K12 samples is assigned to *B. subtilis*.

Table 5.2: Confusion matrix for the independent test data set. The rows show the observed groups and the columns show the predicted groups. The values in the diagonal of the table reflect the correct classifications of observations into groups.

	Predicted class							
	B. tii	***Ps. fluor* 4358**	***B. coag***	***M. luteus***	***Ps. fluor* 50090**	***B. sub***	***E. coli* K12**	***E. coli* TOP10**
B. tii	50	0	0	0	0	0	0	0
Ps. fluor 4358	0	50	0	0	0	0	0	0
B. coag	0	0	50	0	0	0	0	0
M. luteus	10	0	0	40	0	0	0	0
Ps. fluor 50090	0	0	0	0	50	0	0	0
B. sub	0	0	0	0	0	50	0	0
E. coli K12	0	0	0	0	0	12	38	0
E. coli TOP10	0	0	0	0	0	0	0	50

In the last decades, many studies have been performed for the identification and/or differentiation of microorganisms of all kinds. The most significant differences compared to the present study were mostly the typical use of longer measurement times (typically between 128 and 256 scans per spectrum [47,52,54,106,131,132]) a very labor and time-consuming sample preparation often with different purification, dilution, and drying steps [47,52,54,101,106,133], and the use of the fingerprint and –CH/–NH/–OH excitations, which includes the deformation vibrations of DNA/RNA, amide I-III, lipids, fatty acids, and proteins [47,49,101,106,130].

Furthermore, the classification rates of various studies show that the identification and classification down to species level of, for example, *Salmonella*, *Staphylococcus aureus*, *Lactic acid bacteria* or *Listeria* is feasible by means of partial least squares discriminant analysis or artificial neural networks with an accuracy of 77–100 % [130,133–135].

Although all usual purification, dilution and drying steps were omitted, our results second these works and show that the analysis of the spectral range of specific –CH/–NH/–OH excitations, which include stretching vibrations from amide A, proteins, fatty and amino acids [33,125,126], from IR-microspectroscopic data coupled with the presented sampling and measuring technique is sufficient to differentiate between food-related microorganisms on genera, species and even on strain level efficiently, easily and rapidly, compared to traditional methods such as polyacrylamide gel electrophoresis and pulsed-field gel electrophoresis [47,101].
Thus, a robust method for discriminating different food-related bacteria irrespective of sample age on genera, species and strain level could be shown. Additionally, the presented chemometric model is resilient with respect to sampling, samples size, number of classes and accuracy, due to a balanced data set.

5.4 Conclusion

IR-microspectroscopy in combination with chemometric analysis was used successfully for the rapid and non-destructive analysis of food-related bacteria directly from rapid surface blots. A combination of data preprocessing, principal component analysis and canonical discriminant analysis showed that eight different microorganisms irrespective of their time after incubation could be separated and classified with 94.5 % accuracy at genera, species and strain level. In addition, it was observed that the spectral range of specific –CH/–NH/–OH excitations (2815–3680 cm^{-1}) of IR spectra forms a useful biochemical signature of the biological cell and thus a cross-sectional signal from amide A, proteins, fatty and amino acids. The received results are very promising and this technology has the potential to be used for the rapid differentiation of microorganism and potentially to determine microbial contaminations and even spoilage levels in food safety issues. This means that this scope of research has an immense potential to develop a reliable, flexible and fast way for microbiological analysis. For this, clearly, the next step will be the analysis of more complex sample types such as direct analysis of meat products and at different spoilage levels.

5.5 Supplementary Material

Table 5.3: Confusion matrix for the independent test data set. The rows show the observed groups and the columns show the predicted groups. The values in the diagonal of the table reflect the correct classifications of observations into groups.

	Predicted class							
	B. tii	***Ps. fluor* 4**	***B. coag***	***M. luteus***	***Ps. fluor* 5**	***B. sub***	***E. coli* K12**	***E. coli* TOP10**
B. tii	50	0	0	0	0	0	0	0
	100 %	0 %	0 %	0 %	0 %	0 %	0 %	0 %
***Ps. fluor* 4**	0	50	0	0	0	0	0	0
	0 %	100 %	0 %	0 %	0 %	0 %	0 %	0 %
B. coag	0	0	50	0	0	0	0	0
	0 %	0 %	100 %	0 %	0 %	0 %	0 %	0 %
M. luteus	10	0	0	40	0	0	0	0
	20 %	0 %	0 %	80 %	0 %	0 %	0 %	0 %
***Ps. fluor* 5**	0	0	0	0	50	0	0	0
	0 %	0 %	0 %	0 %	100 %	0 %	0 %	0 %
B. sub	0	0	0	0	0	50	0	0
	0 %	0 %	0 %	0 %	0 %	100 %	0 %	0 %
***E. coli* K12**	0	0	0	0	0	12	38	0
	0 %	0 %	0 %	0 %	0 %	24 %	76 %	0 %
***E. coli* TOP10**	0	0	0	0	0	0	0	50
	0 %	0 %	0 %	0 %	0 %	0 %	0 %	100 %

Chapter 6

Discrimination of Stressed and Non-Stressed Food-related Bacteria Using Raman-microspectroscopy

Based on:

Klein, D.; Breuch, R.; Reinmüller, J.; Engelhard, C.; Kaul, P. Discrimination of Stressed and Non-Stressed Food-Related Bacteria Using Raman-Microspectroscopy. Foods 11 (2022), 1506. https://doi.org/10.3390/foods11101506.

Supplemental Notice:

For better readability, Figures 6.2 and 6.4 - 6.6 have been optimized for better readability.

Authors' contribution Chapter 6:

Daniel Klein

Conceptualization, methodology, software, validation, formal analysis, investigation, data curation, visualization, writing—original draft, writing—review and editing

Rene Breuch

Software, Validation, writing—review and editing

Jessica Reinmüller

Investigation, writing—review and editing

Carsten Engelhard

Supervision, writing—review and editing

Peter Kaul

Supervision, writing—review and editing, project administration, funding acquisition

6.1 Introduction

The increasing demand for food, as well as the ever-increasing population of the planet makes the food sector an essential industry [3,4,6,136]. Due to the massive amount of 931 million tons of food waste, as well as the 600 million cases of food-borne illnesses occurring annually and the associated consumer fear, the research area of food safety is of particular interest [11,23,24]. In particular, bacterial detection is a critical concern in the food sector; for example, for determining shelf life dates [137,138]. Therefore, methods that identify the contamination of products at an early stage are of major importance [137,138].

However, the typical methods for detecting and determining bacteria, such as classical microbiological determination and immunological or genetic approaches are exceedingly expensive, difficult, and time-consuming due to the need of cultivation times, DNA extractions and well trained employees [20,26,94,138–141]. Another problem with these approaches is that they are standardized to laboratory conditions, resulting in the loss of real-world samples and the possibility of missing relevant information [26,27]. Because bacteria are typically exposed to a variety of external influences, both in the environment and directly on the samples to be examined, detection and determination methods must incorporate these external influences in order to account for rapid reactions of the microorganisms caused by external stress in their calculations [27–29,142]. This is especially essential because bacteria can not only adjust their metabolic activity in response to changing environments, but they can also change to a viable but non-culturable state, leaving them inaccessible to traditional determination methods [18,26,30,142]. Therefore, it is necessary to study the stress response of microorganisms and to consider it in the databases and classification models for quality control or shelf-life data determination [141,143].

These reactions can be studied by rapid and non-destructive vibrational spectroscopy on a microscopic level by coupling Raman- or IR-spectrometers with a microscopic system, as these couplings are able to study samples in the range of a few micrometers [4,33,144,145].

While Raman-spectroscopy is based on the scattering of monochromatic light and the shift in polarizability, infrared (IR) -spectroscopy is based on the absorption of polychromatic infrared light and the resulting change in dipole moment [33,49,145–148]. Certainly, IR-active vibrational modes often exhibit weak

Raman signals and vice versa and so both methods provide complementary information about the molecular composition of microorganisms that thus contribute to classification [18,52,61,137].

IR-spectroscopy is more susceptible to interference due to the materials used, the disturbance by water and the strong influence of sample thickness, as well as external influences, but it is still easier to handle [18,49,149]. Raman-spectroscopy offers high flexibility of excitation wavelengths and sample properties and a higher spatial resolution, often at a higher cost [18,146,147,150]. A more detailed explanation of Raman- and IR-spectroscopy and their ability to differentiate microorganisms can be found in the literature [18,33,49,54,62,145,151].

The suitability of Raman-spectroscopy for the identification of bacteria at the genus, species, and strain level has already been demonstrated [103,105,123,152]. Since many factors and parameters have an influence on the sample and the resulting spectrum, the exact consideration of the influencing factors is an important approach [51]. The use of Raman-spectroscopy to study the effect of stress factors on bacteria has typically been limited to specific factors or individual microorganisms. Most Raman-spectroscopic studies on how bacteria respond to stress stimuli have used *Escherichia coli* (*E. coli*) as an example. Studies on *E. coli* include the effect of different antibiotics [21,153–155], as well as the effect of storage time and sample preparation such as centrifugation [156], the influence of CO2 [157], the effect of alcohols [21,158,159], and the effect of temperature and different growth media [160]. In addition, investigations on the different stages of the lifecycle of *E. coli*, *Vibrio vulnificus*, *Pseudomonas aeruginosa*, and *Staphylococcus aureus* [140]; the metabolic monitoring of *Metschnikowia sp*. under different temperatures and C:N ratios [161]; and the effect of UV radiation on *E. coli*, *Serratia marcescens*, and *Micrococcus luteus* (*M. luteus*) [162] have been conducted. Furthermore, the influence of transportation and storage on *E. coli*, *Klebsiella terrigena*, *Listeria innocua, Pseudomonas stutzeri, Staphylococcus cohnii*, and *Staphylococcus warneri* [143]; the spore composition of *Lysinibacillus boronitolerans* in different broth media [163]; and the impact of NaCl, MgSO4, and acetate on *Synechocystis* PCC6803 [164] have been investigated. However, to the best knowledge of the authors the investigation of different stress factors and storage times on diverse food relevant microorganisms has not been reported so far in the peer-reviewed literature.

As a result, this study's goal was to extend the standard models for various defined stress factors on microorganisms that are significant in the food sector (*Bacillus subtilis*; three *E. coli* strains; *M. luteus*; *Brochothrix thermosphacta*; two *Pseudomonas fluorescens* strains; and *Bacillus thuringiensis israelensis*) in order to validate the impact of the stress variables on the quality and reliability of the classification model. In the same context, the spectral variations of different microorganisms caused by stress influence can be noticed, as can attempts to standardize Raman research on biological material in terms of sample preparation and pre-processing.

6.2 Materials and Methods

6.2.1 Bacterial Cultures and Sample Preparation

For this study, the food spoilage-relevant bacteria were cultivated on a nutrient agar with the composition of 18 g/L agar-agar, 10 g/L meat extract, 10 g/L meat peptone and 5 g/L sodium chloride (Merck KGaA, Darmstadt, Germany). The bacteria were as follows:

*Escherichia col*i K12 DSM 498, TOP10, and HB101; *Micrococcus luteus* DSM 20030 *Brochothrix thermosphacta* DSM 20171 (*B. therm*); *Pseudomonas fluorescens* (*Ps. fluor*) DSM 4358 and DSM 50090; *Bacillus subtilis* DSM 10 (*B. sub*); and *Bacillus thuringiensis israelensis* DSM 5724 (*B. tii*).

The microbial samples to be examined were taken directly from the medium by means of a swab through a stainless steel cylinder without further sample preparation [123,165]. Raman spectra of samples that were cultivated under lifetime stress conditions were recorded immediately after sampling. Otherwise, the samples were subjected to sampling stress and examined spectroscopically without further incubation time after the stress impact.

6.2.2 Sample Treatment

In addition to the regular reference treatment, the microorganisms were exposed to acidic and alkaline incubation, incubation at lower temperature and incubation under 2-propanol influence, which are summarized as lifetime stress conditions. Furthermore, they were subjected to different sampling conditions (heat sampling, cold sampling, and desiccation).

All microorganisms were incubated in a Binder BD 240 (BINDER GmbH, Tuttlingen, Germany) incubator.

6.2.2.1 Lifetime Stress Conditions

All samples were cultivated according to DSMZ (Leibniz Institut DSMZ, German Collection of Microorganisms and Cell Cultures, Germany) guidelines, except for those that were stressed by incubation at 25 °C. No further sample preparation, like the drying steps of the sample were performed after sampling.
In addition to the reference samples and the samples that were cultivated at 25 °C, the microorganisms were exposed to pH stress. For this, a hydrochloric acid (HCl) solution with pH 1 (36 %, Alfa Aesar, USA; confirmed using pH indicator paper, Th. Geyer GmbH & Co. KG, Renningen, Germany) was prepared, as well as a sodium hydroxide solution (sodium hydroxide pellets, Merck, Darmstadt, Germany) with pH 13. The agar plates were thoroughly covered with a 2 mL solution of hydrochloric acid or sodium hydroxide and the inoculation was performed on the covered agar plates.
Analogously to the acidic and alkaline stress incubation, the bacteria were stressed with 2-propanol (99.9 %, Höfer Chemie GmbH, Kleinblittersdorf, Germany).

6.2.2.2 Sampling Stress Conditions

Microorganisms that were exposed to sampling stress conditions were sampled from regular treated samples. For cold sampling they were covered with liquid nitrogen for 60 s and instantly measured. The heat-dried samples were dried for 60 min at 50 °C and instantaneously measured, whereas the desiccated samples were dried for 60 min over silica gel and instantly measured.

6.2.3 Instrumentation

A SENTERRA Raman-Microscope (Bruker Optics GmbH, Ettlingen, Germany) with a 785 nm diode laser and a charge-coupled device (CCD) detector was employed in this investigation. The microbiological samples were placed on a motorized XYZ-sample stage (Märzhäuser Wetzlar GmbH & Co. KG, Wetzlar, Germany) and focused with a 50× LMPlanFL N objective lens (Olympus K.K, Shinjuku, Tokyo, Japan). The OPUS 7.5 Raman environment software was used for data acquisition and control.

All measurements were performed with a 100 mW initial laser power, an integration time of eight seconds, and ten co-additions. A spectral range of 410–1790 cm^{-1} with a spectral resolution of 3–5 cm^{-1} was chosen to shorten the measuring time.

6.2.4 Data Handling and Statistical Analysis

Raman spectra were truncated to the range of 600–1200 cm^{-1} to cover the most relevant bacterial Raman characteristics and sum normalized (OriginPro 2019b, OriginLab Corporation, Northampton, MA, USA).

Independent training and test data sets were built so that one of three independent data sets of each stress condition could be used as a test data set (Figure 6.1). Table 6.3 (Chapter 6.5) contains detailed information on the exact splitting pattern and the time duration during which bacteria were exposed to lifetime stress conditions.

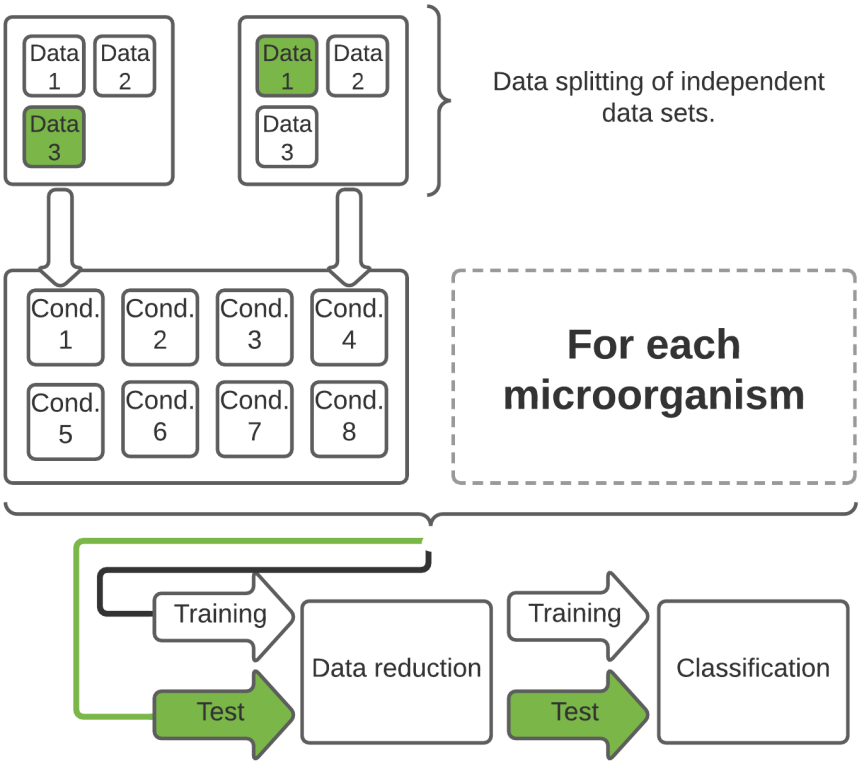

Figure 6.1: The data splitting, reduction and classification are depicted in this diagram. The corresponding information about the measured microorganisms, stress conditions, and storage times can be found in the training and test data set.

Using LabVIEW 2016 and OriginPro 2019b, a principal component analysis (PCA), an unsupervised chemometric technique was executed to the training data set to reduce the data set's dimensionality [124]. The test data sets were converted to the

dimensional space of the training data set by applying the training data set's descriptive statistics and the loadings of the performed PCA to the test data set.
A canonical discriminant analysis (CDA), which uses a linear combination of the data variables to maximize the ratio of between-group and within-group variations of the distinct classes was used in OriginPro 2019b for classification [89,90].

6.3 Results and Discussion

Figure 6.2 illustrates the mean Raman spectra of bacteria under regular cultivation conditions versus bacteria under different stress conditions, along with their standard deviations.

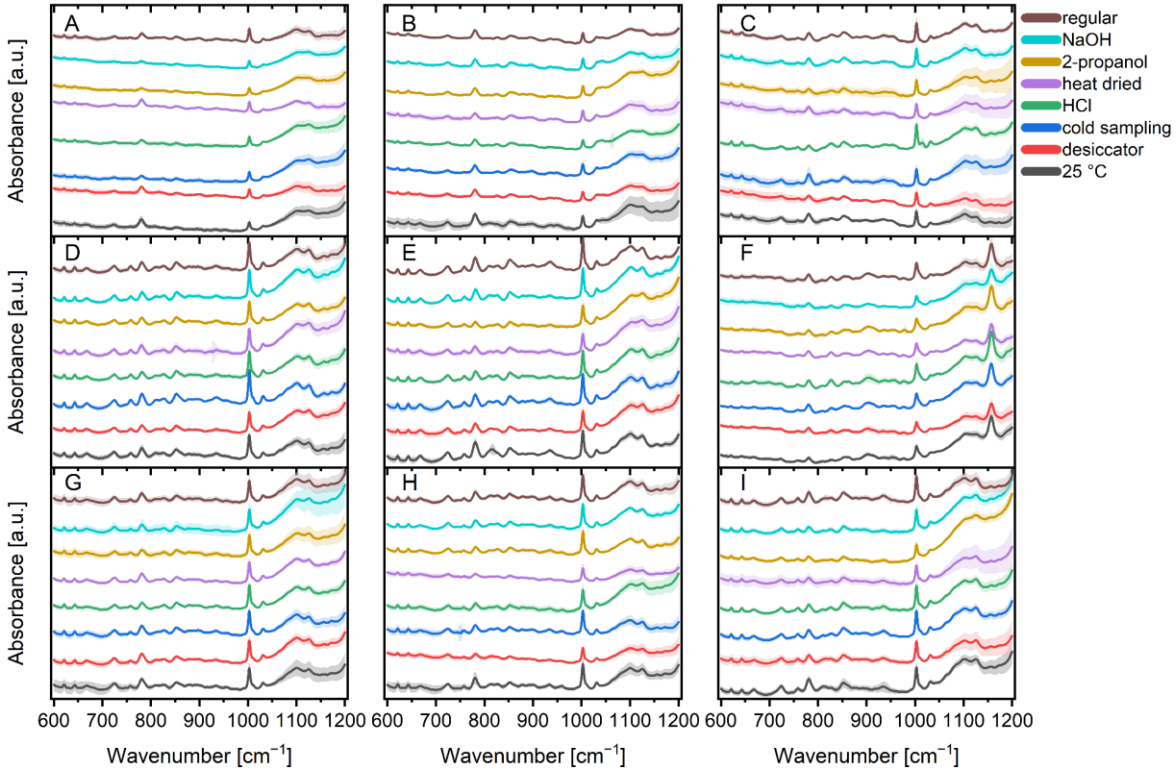

Figure 6.2: Stacked mean Raman spectra of the normalized data of in total 5,450 spectra subdivided into seven stress conditions and regular treatment of *B. sub* (A), *B. therm* (B), *B. tii* (C), *E. coli* K12 (D), *E. coli* HB101 (E), *M. luteus* (F), *Ps. fluor* 4358 (G), *Ps. fluor* 50090 (H) and *E. coli* TOP10 (I). Pale colored bands around the mean value represent the standard deviations.

A closer look at the spectra reveals a few variations between the microorganisms. For example, the region between 650 cm^{-1} and 900 cm^{-1} (proteins, polysaccharides, nucleic acids) [139,145,160,166] which is distinctive for specific bacteria, shows not only differences between Bacilli and *E. coli*, but also variances between Bacilli. For example, the vibration in the cytochrome and DNA [153,160] region around 750 cm^{-1} varies slightly between Bacilli, while the vibration in the

region around 890 cm^{-1} (protein, polysaccharide) [139,153] is more pronounced in Bacilli and the vibration in the guanine/DNA region around 665 cm^{-1} [139,153] is less pronounced in the other microorganisms measured. Aside from the obvious difference due to the sarcinaxanthine carotenoid peak at 1157 cm^{-1} [91,167], *M. luteus*, *M. luteus* and *B. therm* also have a band at 1047 cm^{-1} which can be assigned to carbohydrates [153,168] that the other species do not have.

Apart from the differences between the individual microorganisms, there are a few differences between the various stressors of the individual microbial species. The detection of a peak at 1016 cm^{-1} for HCl stressed *B. tii* is by far the most noticeable change. This peak is not found in any other stress factor and can be linked to the symmetric ring breathing vibration of calcium dipicolinic acid during bacterial spore germination [169–172]. *M. luteus* bacteria cultured at 25 °C possess less exposed tyrosine (828 cm^{-1}) [139] than those incubated at other temperatures. Incubation with 2-propanol and sodium hydroxide reveals additional impact on DNA/RNA occurrence in *B. sub* as the peaks for the nucleic acids (810 cm^{-1}) [168,173] and bases (665 cm^{-1}, 722 cm^{-1}, 783 cm^{-1}, 828 cm^{-1}) [139] are substantially less pronounced. Nucleic acids and tyrosine (810 cm^{-1}; 828 cm^{-1}) [139,168,173] are also impacted in 25 °C incubated *E. coli* K12 as instead of two peaks, there is only one peak with considerably higher intensity. *E. coli* TOP10 exhibits spectral changes in DNA/RNA and carbohydrates (1100–1130 cm^{-1}) [174,175] after incubation with 2-propanol, as well as changed peak ratios for nucleic acids and tyrosine (810 cm^{-1}/828 cm^{-1}) [139,168,173] ranges after incubation at 25 °C. Such alterations are also found for HCl stressed *Ps. fluor* 50090 and NaOH stressed *Ps. fluor* 4358 in the range of 1100–1130 cm^{-1} (DNA/RNA and carbohydrates) [174,175]. In addition to the increased intensity, there is a shift in favor of carbohydrates [175]. This change can also be seen in HCl and 2-propanol stressed *B. therm*. Furthermore, *B. therm* incubated at 25 °C exhibits more pronounced peaks at 667 cm^{-1} and 810 cm^{-1} (guanine und nucleic acids) [139,168,173] compared to the other parameters.

As spectral variations between specific bacteria and stress conditions are founded on the differences in cell proteins, nucleic acids, lipopolysaccharides, and lipids, visual discrimination of the complete 5450 spectra (Figure 6.2) is nearly unachievable [26] and chemometric techniques can help with classification.

To achieve optimal model development and avoid overfitting (performance plot: Figure 6.7 Chapter 6.5), 30 PCs were selected for discriminant analysis model building.

Because there was no substantial equality in the covariance matrices of the training data classes, a quadratic discriminant function was chosen rather than a linear discriminant function [21,156,176].

The classification and cross-validation errors for the training data were 0.78 % and 1.5 %, respectively. To assess the robustness, accuracy, and reproducibility of the constructed classification model, independent test data sets were added to the model.

Figure 6.3 depicts canonical variables (CV) 1 and 2 of the quadratic discriminant analysis (QDA) of training (solid squares) and test data (unfilled squares).

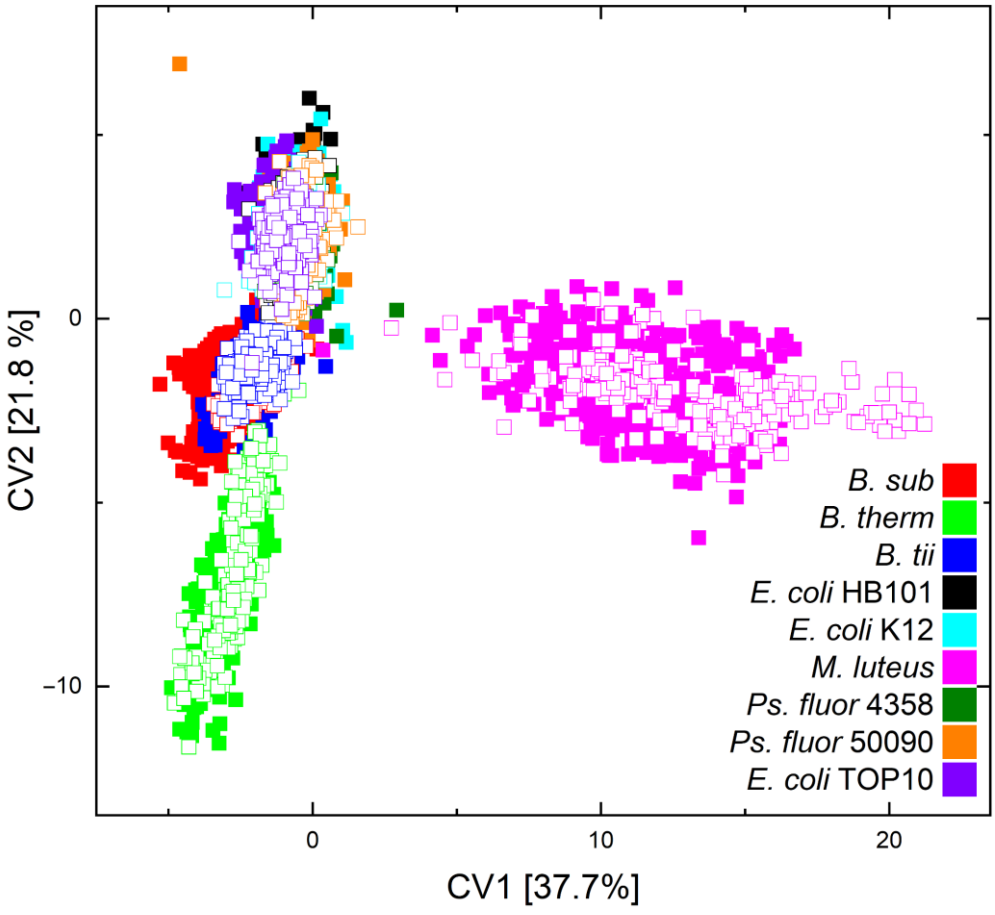

Figure 6.3: Scatter plot of canonical variable 1 vs. 2 of the QDA of all training data (solid squares) and the independent test data (unfilled squares) of all microorganisms and sampling or lifetime conditions.

The group centroids of the training data for CV1 vs. CV2 are given in Figure 6.4.

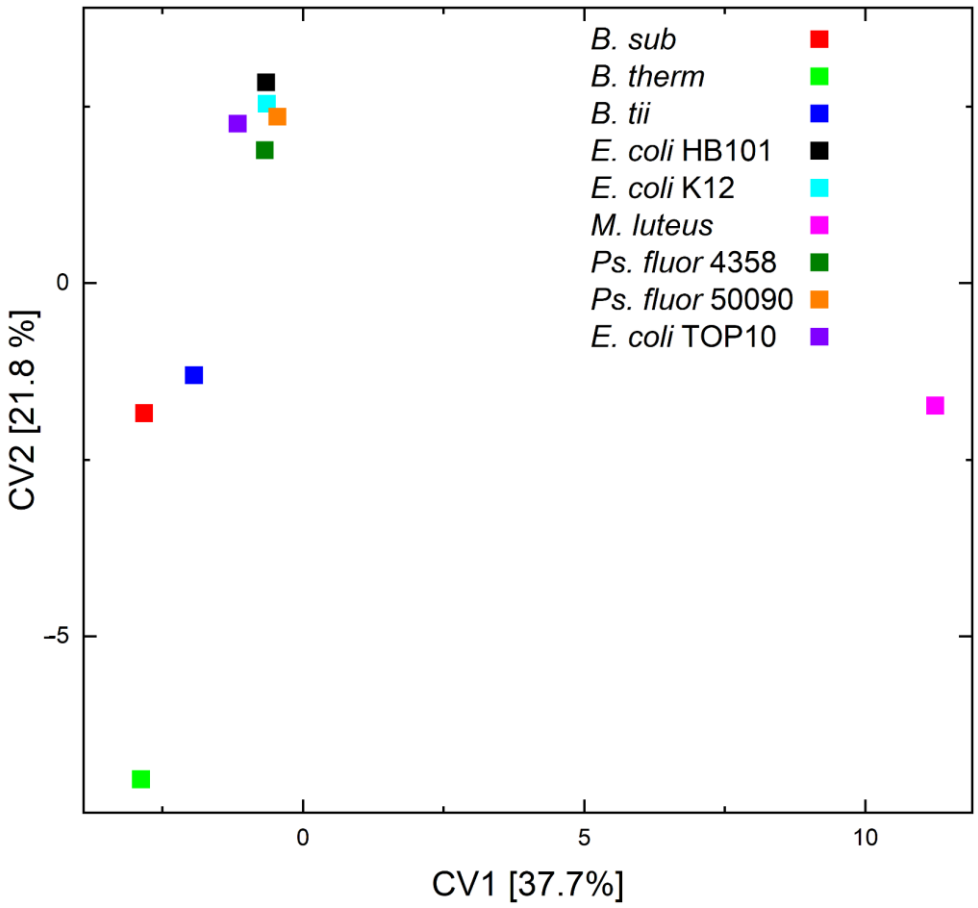

Figure 6.4: Scatter plots of canonical variable 1 vs. 2 of the QDA of the group centroids of the training data.

The above-mentioned spectral differences are also reflected in the graphical depiction of the discriminant analysis. The reported differences clearly differentiate the point clouds of *M. luteus* and *B. therm* from the other point clouds. However, due to the magnitude of the point clouds, further visual distinction is difficult in the plot. The plot of the group centroids, on the other hand, indicates that *M. luteus* is well separated from the other groups by its obvious extra features and *B. therm* is separated from the other bacteria, although the Bacilli cluster together overall. The separation of *E. coli* and *Ps. fluor*escens between or among themselves does not appear to be achievable.

However, in general, the independent test data are found in the space of the training data, and so the assignment of these data is achievable.

Figure 6.5 and Figure 6.6 depict the group centroids in the eight dimensions of the discriminant analysis in order to analyze the separation of the two remaining bacilli, particularly the separation of *E. coli* and *Ps. fluor*escens.

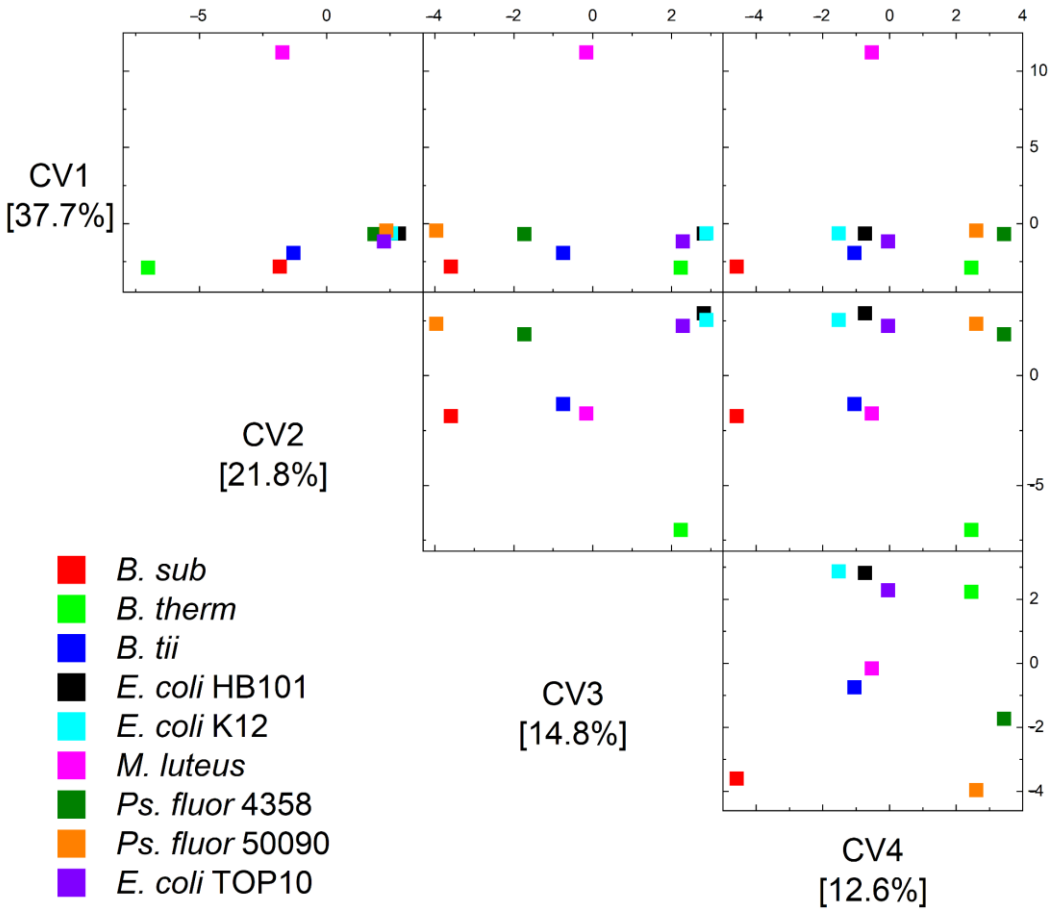

Figure 6.5: Scatter matrix plot of canonical variable 1-4 of the QDA of the group centroids of the training data of all nine microorganisms and their eight sampling and lifetime conditions.

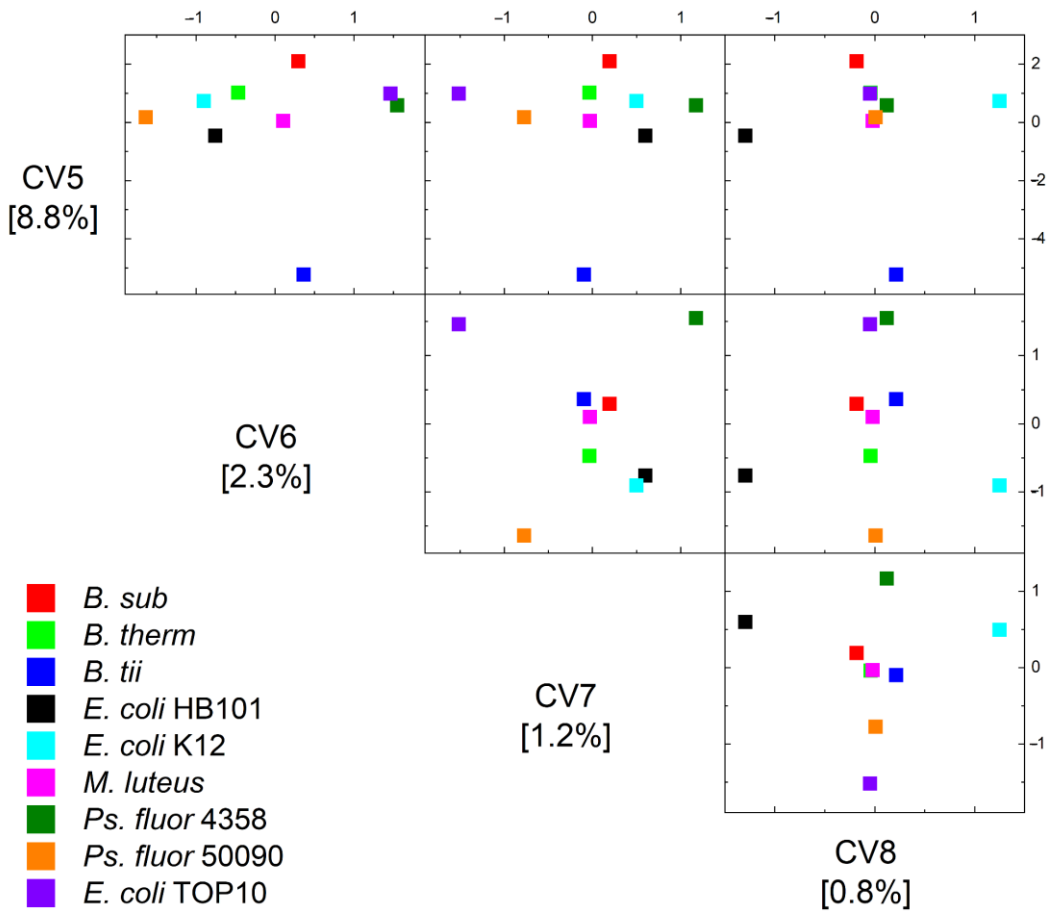

Figure 6.6: Scatter matrix plot of canonical variable 5-8 of the QDA of the group centroids of the training data of all nine microorganisms and their eight sampling and lifetime conditions.

This demonstrates that all Bacilli are separated in the first three dimensions, but Pseudomonads and *E. coli* require more dimensions in order to be completely separated. The clear distinction of *E. coli* germs in particular is only achievable in the eighth dimension.

The classification results of the independent test data are provided in a confusion matrix (Table 6.1) which gives the number of spectra categorized to the correct (diagonal) or incorrect predicted class.

Table 6.1: Confusion matrix for the independent test data set: Rows represent the observed groups and columns represent the expected groups. The values in the table's diagonal correspond to the correct grouping of observations.

	Predicted class								
Class	***B. sub***	***B. therm***	***B. tii***	***E. coli*. HB101**	***E. coli* K12**	***M. luteus***	***Ps. fluor* 4358**	***Ps. fluor* 50090**	***E. coli* TOP10**
B. sub	**199**	0	1	0	0	0	0	0	0
B. therm	0	**204**	1	0	0	0	0	0	0
B. tii	0	0	**199**	0	0	0	0	0	1
E. coli HB101	0	0	0	**138**	62	0	0	0	5
E. coli K12	0	0	0	24	**139**	0	0	0	42
M. luteus	0	0	0	0	0	**210**	0	0	0
Ps. fluor 4358	0	0	0	7	0	0	**197**	6	0
Ps. fluor 50090	0	0	0	0	0	0	29	**181**	0
E. coli TOP10	0	0	0	3	51	0	0	0	**151**

The test data categorization and, as a result, the creation of a robust and applicable model was successful. The independent test data classification error rate was 12.5 % and was distributed throughout all classes except *M. luteus*.

Table 6.2 offers a detailed assessment of the classification errors on the sub-class level because the overall dataset is made up of a significant number of sub-datasets per microorganism.

Table 6.2: Examination of the classification mistakes in the independent test data set at the sub-dataset level. The figures represent the overall number of misclassified spectra in the relevant sub-dataset.

Error Distribution	*B. tii*	*E. coli* HB101	*E. coli* K12	*Ps. fluor* 4358	*Ps. fluor* 50090	*E. coli* TOP10
B. sub—cold sampling	1					
B. therm—25 °C	1					
B. tii—heat dried						1
E. coli HB101—desiccator			4			
E. coli HB101—cold sampling			1			3
E. coli HB101—HCl			22			1
E. coli HB101—heat dried			1			
E. coli HB101—2-propanol			10			1
E. coli HB101—NaOH			18			
E. coli HB101—regular			6			
E. coli K12—desiccator						5
E. coli K12—HCl		3				9
E. coli K12—heat dried		1				20
E. coli K12—2-propanol		4				1
E. coli K12—NaOH		16				7
Ps. fluor 4358—desiccator		7			6	
Ps. fluor 50090—25 °C				3		
Ps. fluor 50090—HCl				22		
Ps. fluor 50090—heat dried				4		
E. coli TOP10—25 °C		2	15			
E. coli TOP10—desiccator			12			
E. coli TOP10—heat dried			1			
E. coli TOP10—2-propanol			1			
E. coli TOP10—regular		1	22			

The improper assignment of *E. coli* K12 to TOP10 and HB101 and vice versa, as well as the incorrect classification of *Ps. fluor*escens 50090 to *Ps. fluor*escens 4358 and vice versa, accounted for most of the errors.

The graphical representation of the classification results already indicated the problem of separation for *Ps. fluor*escens, but especially for *E. coli* separation. The accumulation of 187 misclassifications in the area of *E. coli* out of a total of 232 misclassifications shows that the developed model has good separating power but has weaknesses for separating *E. coli* strains. The modification of the model in

such a way that the model for the differentiation of genera, species, and strain level is retained and the differentiation of *E. coli* remains at the species level leads to a false classification rate of only 2.4 %.

In comparison to other studies concerning the determination of microorganisms, as well as the influence of stress factors on microorganisms by Raman-spectroscopy which partly point to a stricter standardization of the methods [115,156,177] and mainly employ complex and time-consuming sample preparation [154,160,162,178], the presented results show that a reconsideration of the common practice would be helpful, particularly with regard to real-world samples. Because the relevant literature focuses on the analysis of stress factors on specific microorganisms [21,153–156,158–160] or individual stress factors on a few microorganisms [140,162], it was possible to confirm the results observed in this study, namely that the areas influenced by stress factors in microorganisms are primarily found in proteins, lipids, nucleic acids, and polysaccharides [21,154,159,160,162,178]. The combination of numerous stress factors with the traditional reference samples in a model also demonstrated that the classification of unknown samples is not inferior to the classification rates of earlier studies [103,159,179].

In summary, despite the various spectral changes in the range of proteins, lipids, nucleic acids and polysaccharides due to the eight different stress factors applied (lifetime and sampling conditions) to nine different microorganisms, a robust and reliable classification model for food-relevant microorganisms down to strain level could be developed.

6.4 Conclusions

Stress causes alterations in the Raman spectral characteristics of food-relevant microorganisms. Regardless of cultivation conditions, sampling and storage time, a method using simple sample preparation, rapid measurement by Raman-microspectroscopy, and chemometrics was developed for the rapid and non-destructive analysis of food-relevant bacteria. A robust and reliable model was created using a canonical discriminant analysis to discriminate nine different microorganisms at genus down to strain level, despite their storage time and sampling of lifetime condition, with about 12 % misclassification for independent test data accuracy. The modification of the model for the differentiation on

genera, species and strains was retained and the differentiation of *E. coli* remained at the species level, leading to an overall accuracy of 97.6 %.

Compared to reference microorganisms that were cultivated under specified standards, stressed microorganisms showed alterations in the spectral range of lipids, nucleic acids, polysaccharides, and proteins.

The results approve the potential of Raman-microspectroscopy for the discrimination of bacteria and interpretation of microbial stress responses. Additionally, they indicate that sample preparation and standardization should be reconsidered, and existing standardized databases should also contain stress conditions.

6.5 Supplementary Material

Table 6.3: Scheme for data splitting for trained and tested microorganisms. Each data set's storage time is specified in days. Test data are highlighted in green.

	25 °C			Desiccator			Cold sampling			HCl			Heat dried			2-propanol			NaOH			Regular		
Data set	**1**	**2**	**3**	**1**	**2**	**3**	**1**	**2**	**3**	**1**	**2**	**3**	**1**	**2**	**3**	**1**	**2**	**3**	**1**	**2**	**3**	**1**	**2**	**3**
B. sub	1	2	3	8	9	10	8	12	14	3	9	14	7	9	10	1	9	15	1	6	7	4	6	8
B. therm	4	9	1	9	15	1	3	7	20	9	10	14	8	14	16	10	11	15	2	7	8	5	7	15
B. tii	1	9	1	8	9	10	11	12	3	7	8	9	7	9	10	2	8	15	6	7	8	5	6	8
E. coli K12	4	9	1	9	15	1	3	7	20	6	9	14	8	14	16	2	9	15	2	7	8	21	5	12
E. coli HB101	11	9	1	9	10	1	3	15	7	6	8	14	8	9	11	2	9	16	3	6	7	21	1	7
M. luteus	8	2	13	18	10	16	3	11	15	3	9	14	8	9	11	1	9	15	1	6	7	21	18	7
Ps. fluor 4358	1	8	1	9	15	1	3	16	20	6	8	14	8	14	16	2	9	15	6	6	7	12	5	18
Ps. fluor 50090	8	4	1	9	15	1	3	11	23	6	9	14	8	14	16	1	8	16	6	6	7	5	21	12
E. coli TOP10	1	9	1	15	15	1	16	20	7	8	9	14	17	14	16	2	8	15	2	7	8	1	5	12

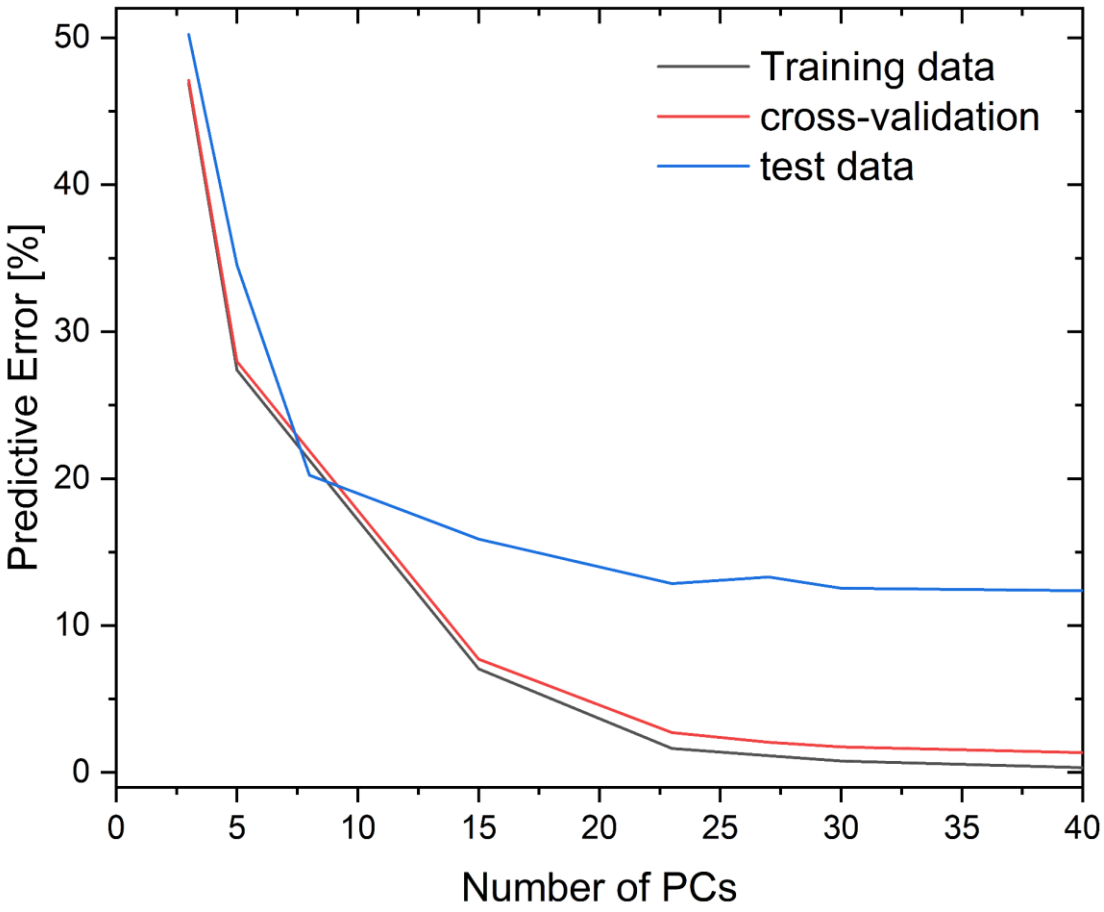

Figure 6.7: Check for overfitting by plotting the error rate of the training data, the cross-validation and the test data against the number of PCs used for classification.

Chapter 7

Investigation and Rapid Discrimination of Food-related Bacteria Under Stress Treatments Using IR-microspectroscopy

Based on:

Klein, D.; Breuch, R.; Reinmüller, J.; Engelhard, C.; Kaul, P., Investigation and Rapid Discrimination of Food-Related Bacteria under Stress Treatments Using IR Microspectroscopy. Foods 10 (2021), 1850. https://doi.org/10.3390/foods10081850.

Supplemental Notice:

Figures 7.2 - 7.5 and 7.7 - 7.9 were optimized for better readability.

Authors' contribution Chapter 7:

Daniel Klein

Conceptualization, methodology, software, validation, formal analysis, investigation, data curation, visualization, writing—original draft, writing—review and editing

Rene Breuch

Software, Validation, writing—review and editing

Jessica Reinmüller

Investigation, formal analysis, writing—review and editing

Carsten Engelhard

Supervision, writing—review and editing

Peter Kaul

Supervision, writing—review and editing, project administration, funding acquisition

7.1 Introduction

Because meat and meat products are highly appreciated by consumers for their nutritional value and taste, the global supply of meat is expected to continue to increase in the coming years [4]. However, meat is highly prone to microbial spoilage and, therefore, a rapid and easy identification of contamination is a major concern in food safety [4,137]. This will help to ensure measures to minimize health hazards and thus prevent foodborne illness and unnecessary food waste along the supply chain [137].

However, as bacteria are subject to constant fluctuations in their growth conditions both in nature and along the supply chain, they have developed capabilities to constantly adapt to conditions or even change to a state of viability but non-cultivable [30,142,180]. This makes sublethally damaged cells difficult to detect with classical laboratory culture techniques [137]. Additionally, standard methods such as classical microbiology, sensory-mechanical studies and immunological or genetic techniques have disadvantages in speed, complexity, and invasiveness [4,17,18,21,94]. However, these viable but non-culturable microorganisms can be revived within the supply chain and thus not only affect the product's usability, but may also be a health hazard [18,49,137,181].

Therefore, especially infrared (IR)-spectroscopy has been successfully used to detect and identify microorganisms [49,52,105,165]. In the recent years many studies dealt with the IR-spectroscopic evaluation of specific effects of stress conditions on microorganisms such as the protein misfolding [182], the phase behavior of cell membranes of *Escherichia coli* (*E. coli*) during desiccation, rehydration and growth recovery [183,184] or the sonication injury on *Listeria monocytogenes* [185]. Moreover, IR-spectroscopy was used to study the influence of nanoparticles on *E. coli* [186,187] and the effects of heavy metals on *Brevundimonas sp., Gordonia sp.* and *Microbacterium oxydans* using the analysis of variance, hierarchical cluster analysis, principal component analysis (PCA) and soft independent modelling of class analogies (SIMCA) [188,189]. Additionally, the influence of heat on *Lactococcus lactis, Salmonella enterica* and *Listeria monocytogenes* was evaluated by the analysis of the IR-peak area of amide I and amide II bands and the extent of injury was predicted by the analysis of the wavenumber area of 900–1300 cm^{-1} by SIMCA and partial least squares regression analysis (PLSR) [190,191]. Furthermore, the response of *E. coli,*

Campylobacter jejuni and *Pseudomonas aeruginosa* exposed to cold-[58,192], chemical- [58] and pH-stressors [58,178,193] was studied by DNA microarrays and Fourier-transform (FT)-IR analysis coupled to PCA, discriminant function analysis and PLSR.

While interesting findings have been reported, IR-microspectroscopy in combination with PCA and canonical discriminant analysis has not been used so far to combine different stress conditions on numerous food-related microorganisms at different times after incubation in one chemometric model.

The food industry is particularly interested in the most dominant microorganisms detected on fresh and chilled meat and other food products: *Pseudomonas spp.*, especially *Pseudomonas fluorescens* (*Ps. fluor*) and *Enterobacteriaceae*, such as *E. coli, Micrococcus luteus* (*M. luteus*), *Bacillus thuringiensis israelensis* (*B. tii*), *Bacillus coagulans* (*B. coag*), *Bacillus subtilis* (*B. sub*) and *Brochothrix thermosphacta* (*B. therm*) [37,117–122,194].

Therefore, the aim of this study was the development of a rapid and non-destructive analysis method for food-related microorganisms. The influences of numerous stress conditioned microorganisms as well as regularly treated microorganisms over various aging stages on agar plates were analyzed with IR-spectroscopy to build up an extensive data set. Chemometric models were developed to discriminate the influence of stress and also to discriminate the selected microorganisms independent of their stress conditions within one model down to the strain level.

7.2 Materials and Methods

7.2.1 Bacterial Cultures and Sample Preparation

The following nine microorganisms were cultivated on nutrient agar (10 g/L meat peptone, 10 g/L meat extract, 5 g/L sodium chloride and 18 g/L agar-agar (Merck KGaA, Germany)) and prepared according to our previously published method [88,123,165]: *Bacillus subtilis* DSM 10, *Bacillus coagulans* DSM 1, *Escherichia coli* K12 DSM 498, *Escherichia coli* TOP10, *Micrococcus luteus* DSM 20030, *Brochothrix thermosphacta* DSM 20171, *Pseudomonas fluorescens* DSM 4358, *Pseudomonas fluorescens* DSM 50090 and *Bacillus thuringiensis israelensis* DSM 5724.

As described in our previously published methods [123,165], the samples were taken by a blotting technique with the sample carrier (stainless steel cylinder)

directly from the agar plate without any sampling pre-treatments (e.g. centrifugation, washing, drying). IR spectra were recorded directly (lifetime conditions) after sampling or directly after the stress impact (sampling condition) without any incubation period after sampling. Detailed information can be found in Chapter 7.2.2. The spectral data set of each microorganism, consisting of four independent data sets for each stress condition, were divided into independent training and test data sets. Further information can be found in the Chapter “Data Handling and Visualization”.

7.2.2 Sample Treatment

In order to expose the microorganisms to different influences, they were subjected to lifetime conditions (incubation under acidic and alkaline conditions, incubation at different temperatures and incubation under 2-propanol influence) and sampling conditions (cold sampling, heat sampling and desiccation) in a controlled manner in addition to the regular reference treatment. Incubation was performed for all microorganisms in a Binder BD 240 (BINDER GmbH, Germany) incubator.

7.2.2.1 Reference Samples (Regular Treatment)

All microorganisms were cultivated in accordance to DSMZ (Leibniz Institut DSMZ – German Collection of Microorganisms and Cell Cultures, Germany) guidelines. These samples served as reference samples in this study.

7.2.2.2 Incubation Under Acidic Conditions

To expose microorganisms to acidic pH stress, a hydrochloric acid (HCl) solution (36 %, Alfa Aesar, USA) with pH 1 (verified by means of pH indicator paper, Th. Geyer GmbH & Co. KG, Germany) was prepared. The agar plates were completely covered with the hydrochloric acid solution (2 mL) and the inoculation took place onto the hydrochloric-acid covered agar plates. Afterwards the cultivation was performed in accordance to DSMZ guidelines.

7.2.2.3 Incubation Under Alkaline Conditions

Complementary to the incubation under acidic conditions, a sodium hydroxide solution (sodium hydroxide pellets, Merck, Germany) (pH 13 (verified by means of pH indicator paper)) was prepared to expose microorganisms to alkaline pH stress. Afterwards the cultivation was performed in accordance to DSMZ guidelines.

7.2.2.4 Incubation at Lower/Higher Temperatures

Microorganisms were incubated at a temperature of 25 °C and 45 °C.

7.2.2.5 Incubation with 2-propanol

Complementary to the incubation under acidic and alkaline stress, the microorganisms were stressed with 2-propanol (99.9 %, Höfer Chemie GmbH, Germany). Afterwards the cultivation was performed in accordance to DSMZ guidelines.

7.2.2.6 Cold Sampling

Microorganisms were sampled from regular treated samples, covered with liquid nitrogen for 60 seconds and instantly measured.

7.2.2.7 Heat-drying

Microorganisms were sampled from regular treated samples, dried at 50 °C for 60 minutes and instantly measured.

7.2.2.8 Desiccation

Microorganisms were sampled from regular treated samples, dried in a desiccator filled with silica gel for 60 minutes and instantly measured.

7.2.3 Instrumentation

The samples were examined in reflectance mode, 20 scans per spectrum, 4 cm^{-1} resolution and 20x magnification (Cassegrain objective (Bruker Ser.910/1022346, numerical aperture: 0.6, working distance: 6 mm) by means of a Hyperion 3000/Vertex 70 Fourier-transform-IR-microspectrometer (Bruker Optics GmbH, Germany) with Mercury/Cadmium/Telluride (MCT) detector. Instrument controlling and data acquisition was carried out by the OPUS 7.5 software.

Due to the microscopic component, the morphological properties of heterogeneous samples can be combined with spectral data and samples with a few hundred microorganisms can be determined [33,195]. This often results in no further sample preparation than a transfer of the sample to a sample carrier [131]. In addition, the required analysis time is reduced compared to classical IR-spectroscopy [33].

7.2.4 Data Handling and Visualization

IR spectra were subsequently sum normalized (OriginPro 2019b, OriginLab Corporation, USA), data reduced to the range of 915–1750 cm^{-1} and 2825–3680 cm^{-1} to exclude the characteristic CO_2 region and the lower fingerprint area, the first derivative was built and smoothed with a 13-point Savitzky-Golay filter (LabVIEW 2016; National Instruments, USA).

The splitting for training and test data was carried out so that one or two independent data sets each with 50 spectra for each stress condition and regular treatment was used as test data (Figure 7.1).

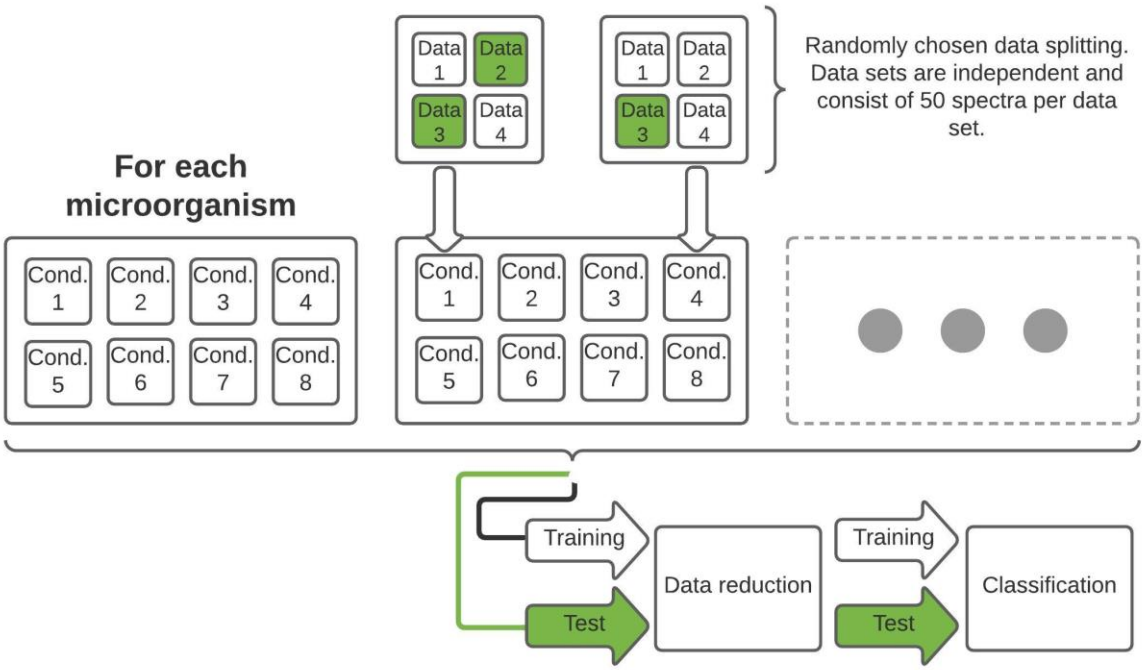

Figure 7.1: Schematic representation of the data set structure as well as the splitting process with subsequent data reduction and classification. The training and test data set contains the corresponding information of each measured microorganism and thus of each growth and sampling condition.

The splitting ratios of training and test data is depicted in Table 7.1. Detailed information about the exact splitting pattern, the time after incubation of the microorganisms at the time of measurement and thus how long the microorganisms were exposed to the lifetime stress conditions can be found in Table 7.4 (Chapter 7.5).

Since balanced training data sets are important, not only for data reduction by PCA, but also for robust, reliable and unweighted model development [92,93], the data

sets were split into training and test data in different ways for the reason that not all stress conditions could be measured for all bacteria (see Results and Discussion).

Table 7.1: Training and test data set sizes and data splitting ratio for the trained and tested microorganisms.

Class	Training data	Test data	Training data [%]
B. coag	1050	350	75.0
B. sub	1050	750	58.3
B. therm	1050	750	58.3
B. tii	1050	550	65.6
E. coli K12	1050	750	58.3
M. luteus	1050	750	58.3
Ps. fluor 4358	1050	550	65.6
Ps. fluor 50090	1050	550	65.6
E. coli TOP10	1050	750	58.3

For the following data evaluation, principal component analysis (PCA) was applied to the training data; the test data were converted into the vector space of the training data and the data were classified by a canonical discriminant analysis (CDA) by means of LabVIEW 2016 and OriginPro 2019b.

7.3 Results and Discussion

First, the microorganisms were exposed to the different bacterial stress conditions mentioned above and IR-microspectroscopic data was carefully acquired. Figure 7.2 shows the mean IR spectra including their standard deviations of bacteria under normal culture conditions versus bacteria under stress conditions. It is important to note that for *B. coag* no bacterial growth was detected at 25 °C and when 2-propanol was used. Also, *B. tii* and *Ps. fluor* did not grow at 45 °C. This suggests that these stress conditions lead a non-culturable state. As a result, these conditions are not shown in Figure 7.2 and cannot be used for further evaluation.

Because spectral differences between individual microorganisms and individual stress conditions are based on different composition in proteins, nucleic acids, lipopolysaccharides or lipids of the cell, visual discrimination of 15,200 spectra in total (Figure 7.2) is almost impossible [10]. The fine spectral differences are in the range of the P=O vibrations of phospholipids (1085 cm^{-1} & 1240 cm^{-1}) and the C–O–C vibrations in polysaccharides (900–1200 cm^{-1}) [33,49]. In addition, differences can be noted in the C=O, C-H and C–O–H vibrations of fatty acids and

proteins [33,49]. In the area of proteins, strong bands of amide I and amide II vibrations (1550–1675 cm^{-1}) can also be observed [33,49]. Furthermore, various C–H and N–H stretching vibrations from fatty acids and proteins can be identified in the range of 2850 cm^{-1} [33,49]. Here, chemometric approaches can aid in the classification and were carefully optimized as discussed below.

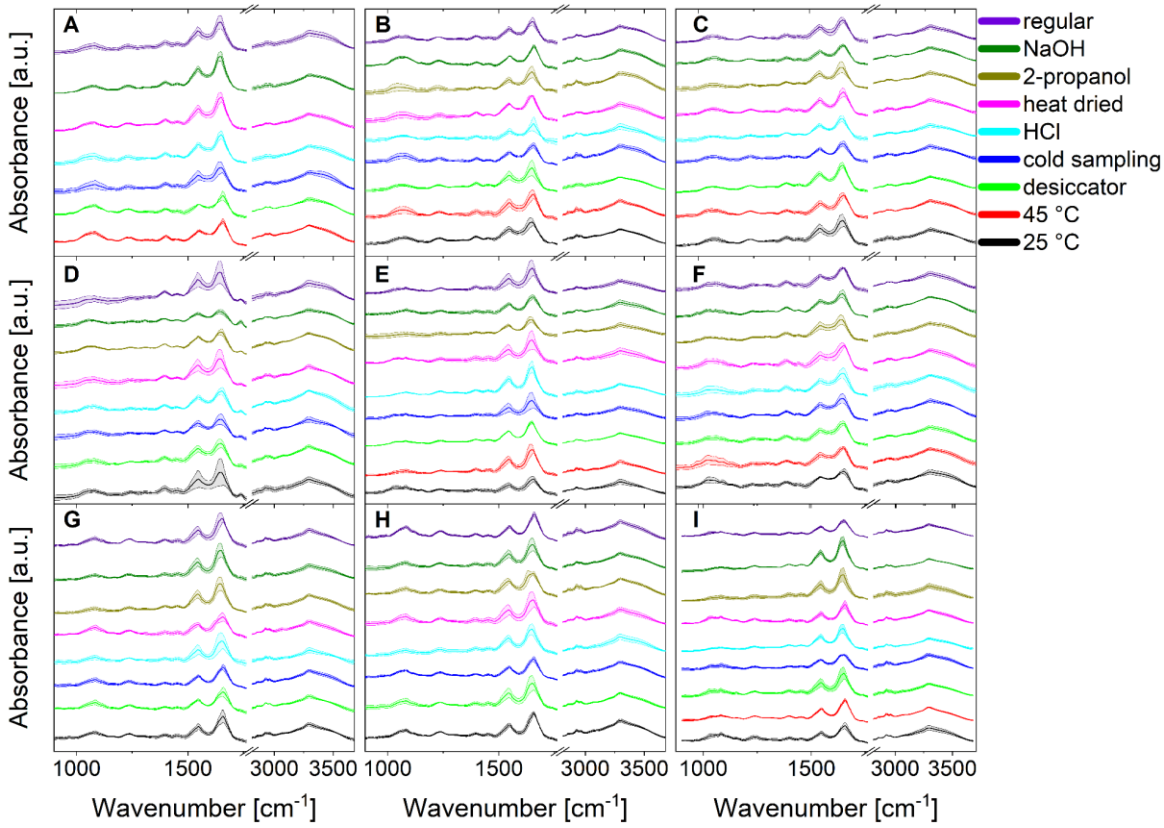

Figure 7.2: Stacked mean IR spectra of the normalized data of in total 15,200 spectra (200 spectra of each stress condition and regular treatment) of *B. coag* (A), *B. sub* (B), *B. therm* (C), *B. tii* (D), *E. coli* K12 (E), *M. luteus* (F), *Ps. fluor* 4358 (G), *Ps. fluor* 50090 (H) and *E. coli* TOP10 (I). Standard deviations are indicated by color coded bands around the mean value.

7.3.1 Bacteria Prediction Model

To ensure optimal model development and to avoid overfitting (performance plot: Figure 7.6; Chapter 7.5), the first 20 PCs (Figure 7.7 & Figure 7.8; Chapter 7.5) were used for model building using discriminant analysis.

As the covariance matrices of the training data classes had no significant equality, a quadratic instead of a linear discriminant function was chosen [127–129].

The error for classification and cross-validation of the training data was 0.01 %; one spectrum of *E. coli* K12 was assigned to *E. coli* TOP10. In order to test the developed model for the classification of food-related microorganisms for

robustness, accuracy and reproducibility, independent test data sets of the trained classes were added to the model.

The first two (left) and the first four (right) canonical variables (CV) of the quadratic discriminant analysis (QDA) of the training data (solid squares) and test data (unfilled squares) are depicted in Figure 7.3. On closer examination, it is noticeable that the test data are located exactly in the space of the training data.

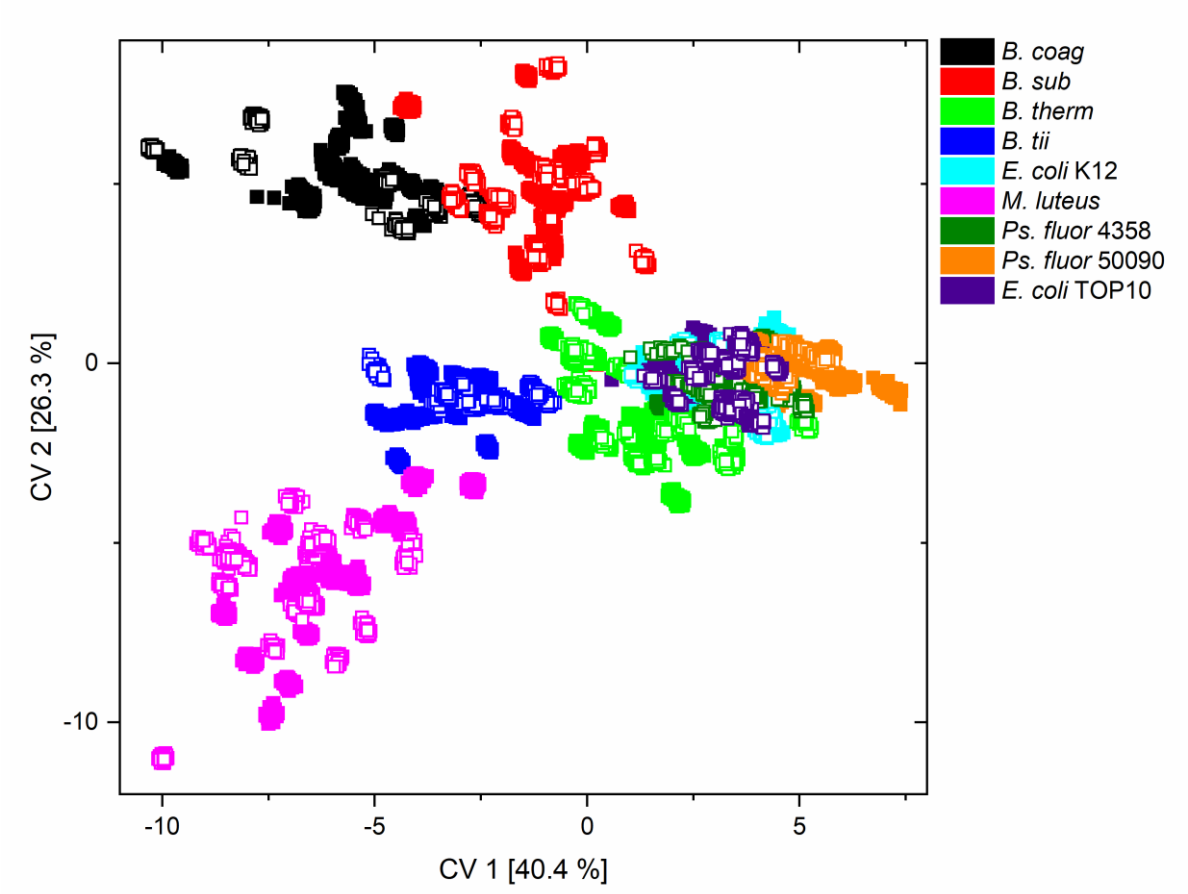

Figure 7.3: Scatter plot of canonical variable 1 and 2 of the QDA of the training data (solid squares) and the independent test data (unfilled squares) of all nine microorganisms and all nine conditions.

M. luteus and all *Bacillus spp*. (*B. coag, B. sub, B. therm, B. tii*) could be separated from each other by the first two canonical variables and *Pseudomonas fluorescens* from *E. coli* could be separated by the first four canonical variables (Figure 7.4).

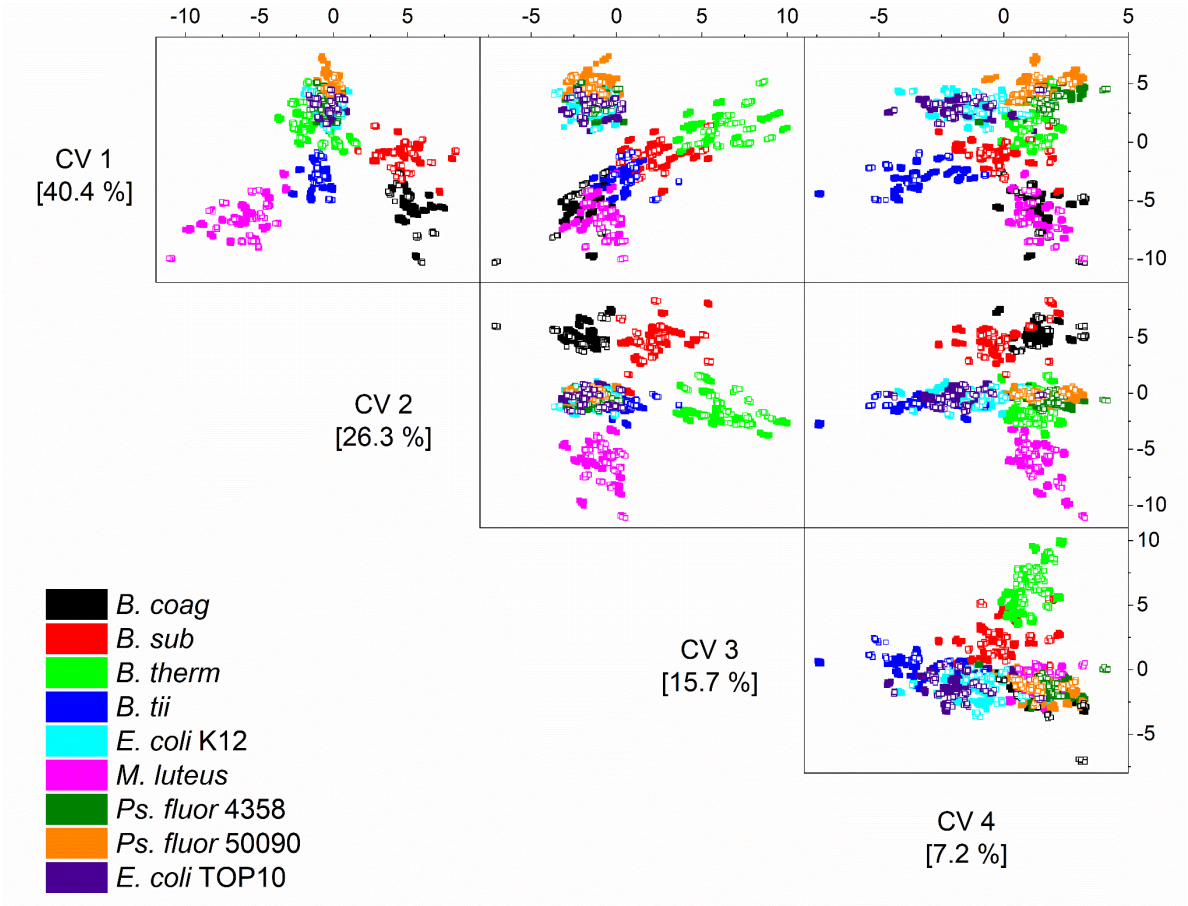

Figure 7.4: Scatter matrix plot of canonical variable 1 to 4 of the QDA of the training data (solid squares) and the independent test data (unfilled squares) of all nine microorganisms and all nine conditions.

In conclusion, the data of the classification of the independent test data are presented in a confusion matrix (Table 7.2), which gives the number of spectra which were classified to the correct (diagonal) or wrong predicted class.

Table 7.2: Confusion matrix for the independent test data set. All nine conditions were pooled as one class per microorganism. The rows show the observed groups and the columns the predicted groups. The values in the diagonal of the table reflect the correct classifications of observations into groups.

	Predicted class								
Class	***B. coag***	***B. sub***	***B. therm***	***B. tii***	***E. coli* K12**	***E. coli* TOP10**	***Ps. fluor* 4358**	***Ps. fluor* 50090**	***M. luteus***
B. coag	**349**	1	0	0	0	0	0	0	0
B. sub	0	**750**	0	0	0	0	0	0	0
B. therm	0	0	**750**	0	0	0	0	0	0
B. tii	0	0	0	**550**	0	0	0	0	0
E. coli K12	0	0	0	0	**601**	99	0	50	0
E. coli TOP10	0	0	0	0	10	**740**	0	0	0
Ps. fluor 4358	0	0	0	0	1	11	**514**	24	0
Ps. fluor 50090	0	0	0	0	0	0	0	**550**	0
M. luteus	0	0	0	0	0	0	0	0	**750**

It can be seen that the classification of the test data and thus the model development of a robust and meaningful model was successful. The error rate of the classification of the independent test data was only 3.4 % and can be found in the classes of *B. coag, E. coli* K12 and TOP10 and *Ps. fluorescens*.

Because the complete dataset consists of a large number of sub-datasets per microorganism, a detailed analysis of the classification errors on the sub-datasets is given in Table 7.3.

Table 7.3: Detailed analysis of the classification errors of the independent test data set on the sub-dataset level. The numbers are the total numbers of misclassified spectra in the specific sub-dataset.

Error distribution	***B. sub***	***E. coli* K12**	***E. coli* TOP10**	***Ps. fluor* 50090**
B. coag - HCl	1	--	--	--
E. coli K12 - heat dried	--	--	49	--
E. coli K12 - 2-propanol	--	--	--	50
E. coli K12 - regular	--	--	50	--
E. coli TOP10 - heat dried	--	1	--	--
E. coli TOP10 - regular	--	9	--	--
Ps. fluor 4358 - cold sampling	--	--	8	--
Ps. fluor 4358 - 2-propanol	--	--	3	24
Ps. fluor 4358 - NaOH	--	1	--	--

The detailed analysis of the error rate shows that a major part of the error was due to the misclassification of *E. coli* K12 to TOP10 and vice versa, and the assignment of *Ps. fluorescens* 4358 to *Ps. fluorescens* 50090. In addition, another part of the misclassification was due to the assignment of *E. coli* K12 to *Ps. fluorescens*.

These misclassifications were also indicated by the graphical representations (Figure 7.4) of the classification results, where it is at least visually apparent that the distinction between the respective *E. coli* and *Ps. fluorescens* strains as well as the separation between *E. coli* and *Ps. fluorescens* appears difficult. However, the detailed error analysis shows that the separation between the *Ps. fluorescens* strains was feasible, but the separation between the *E. coli* strains was more difficult.

In contrast to other approaches, the presented results for the general discrimination of food-related bacteria were carried out with 20 scans per sample as comparatively short measurement times [106,131,182,186,188–190] and in absence of further sample preparation steps [58,106,182,185,188,189,192]. Nonetheless, the results demonstrate a non-inferior classification even compared to macroscopic and microscopic studies, in which standardized work was performed in other approaches [130,131,133,134,165,190,192]. The novel aspect of this model in comparison to the literature are the inclusion of numerous stress conditions on microorganisms and the consideration of these stress conditions on numerous bacteria in one model since often only the influence of a few stress conditions on single or a few selected microorganisms were investigated [186,188–190,192].

7.3.2 Stress Condition Prediction Model

Since clusters within a class (microorganisms) were visible but do not seem to significantly influence the model for discrimination of food-related microorganisms, it was reasonable to investigate which general influence the stress conditions have on the bacteria or on the model. Therefore, we tested whether this type of model was also able to separate different stress conditions from each other.

All data were preprocessed as already described for the discrimination model. The model building for the discrimination of different stress conditions per microorganism was executed as in the previously described model. For this purpose, the fourth of the independent data sets for each stress condition was used as test data and the first three independent data sets were used as training data.

The summary of the quadratic discriminant analyses of each microorganism is depicted in Figure 7.5.

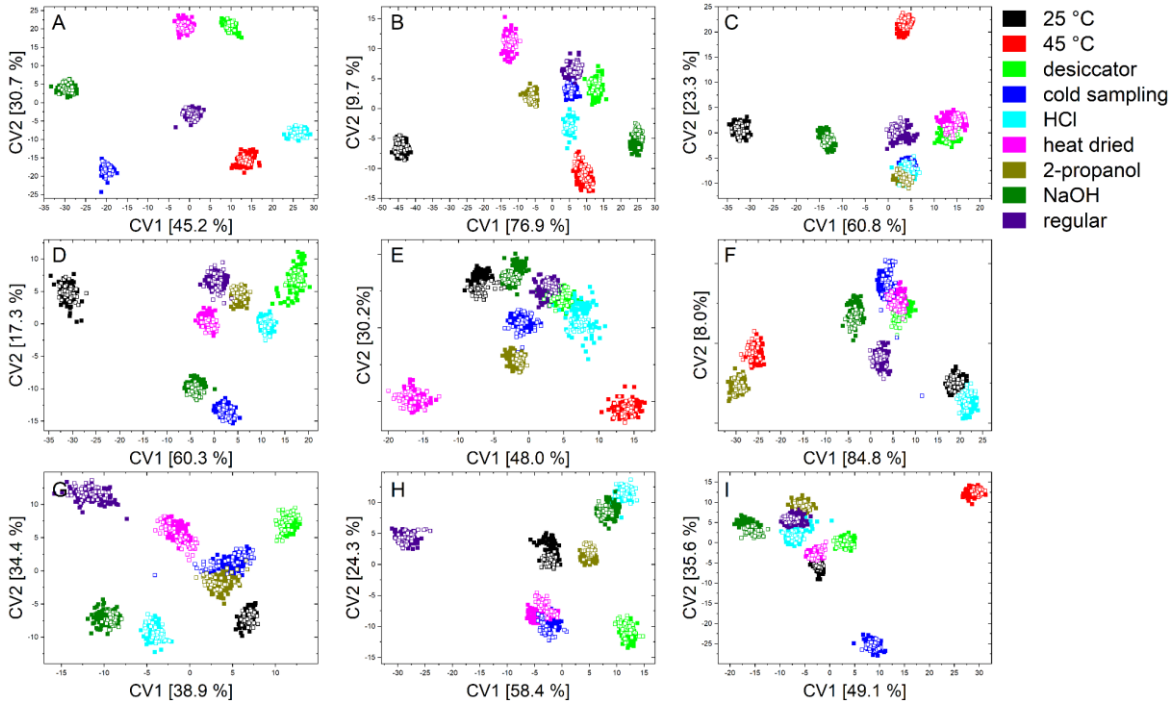

Figure 7.5: Scatter plots of canonical variable 1 and 2 of the QDA of the training data (solid squares) and the independent test data (unfilled squares) of *B. coag* (A), *B. sub* (B), *B. therm* (C), *B. tii* (D), *E. coli* K12 (E), *M. luteus* (F), *Ps. fluor* 4358 (G), *Ps. fluor* 50090 (H) and *E. coli* TOP10 (I) to discriminate all nine conditions.

The first two canonical variables clearly separate almost all stress conditions for each microorganism. Furthermore, it was also evident that the test data can again be found exactly in the data clouds of the training data.

The corresponding confusion matrices (Table 7.5 to Table 7.13; Chapter 7.5) show that for each microorganism an error-free classification of the test data of each stress condition was possible and all stress conditions were located in mostly isolated data clouds.

It can be observed that stressed microorganisms, in comparison to regularly treated microorganisms, show altered signals in the range of nucleic acids, polysaccharides, lipids and in the region of –CH2/–CH3 stretching vibrations. Additionally, in most cases a shift in the peak position was noticeable in the spectral region assigned to proteins (amide I and amide II vibrations) (Figure 7.9; Chapter 7.5). Particularly notable were features such as those in Figure 7.5 where incubation at 25 °C for *B. sub* (B) causes this point cloud to be far removed from all other influencing conditions. This is because, in this case, the above-mentioned peaks have an increased intensity compared to regularly treated bacteria. It was also noticeable that in the region of the amide I vibration there is a shift to smaller wavenumbers. Observations of this nature were also found during stress reactions of the other microorganisms. For example, the data from *B. therm* (C) stressed with 2-propanol and HCl cluster together as a result of a negative shift of the amide I band in both cases. Furthermore, a reduction of the bands in the fatty acid region was generally detected in *B. tii* and desiccation of *E. coli* K12 only results in marginal changes in the spectrum (Figure 7.9; Chapter 7.5). In addition, the heat drying of *E. coli* TOP10 results in a change in the ratio of nucleic acids, phospholipids and polysaccharides. *M. luteus* shows significant changes in the ratio of lipids, nucleic acids and proteins at incorrect incubation temperatures and under NaOH and 2-propanol influence. Additionally, the two *Pseudomonas* species behave largely similarly under stress but tend to an opposite shift, *Ps. fluor* 4358 to higher and *Ps. fluor* 50090 to lower wavenumbers, in the amide I band (Figure 7.9; Chapter 7.5).

For the range of 2800–3000 cm^{-1}, our observations were consistent with the findings of Saulou et al. and Loffhagen et al. who presented that spectra of viable microorganisms did not shift to lower wavenumbers thus the microorganisms did not alter their membrane fluidity, but continued to show the presence of unsaturated bonds in lipids [186,196]. Furthermore, our results confirm the findings that stressed microorganisms show changes in the region of amide bands as part of their stress response mechanisms, indicating the alteration of the proteins secondary

structure [186,190]. In addition, with the changes in the range of nucleic acids, polysaccharides and lipids resulting from the denaturation of nucleic acids, the production of exopolymer and effects on polysaccharides of the cell wall in the range of 900–1300 cm^{-1} could be confirmed [178,188,190,192].

In summary the spectral changes of sublethally stressed microorganisms, such as the change in the ranges 900–1500 cm^{-1} and 1500–1700 cm^{-1}, which indicate an altered concentration of nucleic acids, lipids, polysaccharides, as well as the shift of the amide bands, indicated by a change in the secondary structure of the proteins, are reproducible and extensively described in the before mentioned literature for living or stressed microorganisms. Thus, it can be stated that a rapid, robust and meaningful model for discrimination of food-related microorganisms down to the strain level, irrespective of sample age, lifetime stress conditions and sampling stress conditions, could be established.

7.4 Conclusions

Response of food-related bacteria to stress gives rise to changes in their spectral features in FT-IR. Specifically, a method using simple sample preparation, fast measurement by IR-microspectroscopy and chemometrics was carefully developed for rapid and non-destructive analysis of food-relevant bacteria independent of their time after incubation, cultivation conditions and sampling condition. Classification using canonical discriminant analysis showed that a robust and meaningful model was developed to discriminate nine different microorganisms at the genus, species, and strain levels with 96.6 % accuracy. Furthermore, it was demonstrated that sublethally stressed microorganisms, irrespective of lifetime or sampling condition, showed changes in the spectral range associated with nucleic acids, polysaccharides, lipids, –CH2/–CH3 stretching vibrations and especially in the range of proteins (amide I and amide II vibrations) compared to reference microorganisms grown under well-established guidelines. These spectral changes were discussed and could indicate, for example, the changes in the secondary structure of proteins and the production of exopolymer.

The results obtained not only confirm the potential of IR-microspectroscopy for rapid differentiation of microorganisms and elucidation of stress response of bacteria, but also show that the existing highly standardized databases should be expanded to include stress conditions and reconsidered in terms of sample preparation and

spectra quality. Continuing this approach, these models should be progressively supplemented by for example food samples in order to take into account the influence of food matrices to the models.

7.5 Supplementary Material

Table 7.4: Data splitting scheme for the trained and tested microorganisms. The time period after incubation is given in days for each data sets. Each data set consists of 50 spectra. Stress conditions are divided into lifetime conditions, in which the influence is already applied at inoculation and thus active over a life cycle, and sampling condition, in which the influence is a short major stress during sampling.

	Lifetime condition																				Sampling condition															
	25 °C				45 °C				2-propanol				NaOH				HCl				Heat dried				Regular				Desiccator				Cold sampling			
Data set	**1**	**2**	**3**	**4**	**1**	**2**	**3**	**4**	**1**	**2**	**3**	**4**	**1**	**2**	**3**	**4**	**1**	**2**	**3**	**4**	**1**	**2**	**3**	**4**	**1**	**2**	**3**	**4**	**1**	**2**	**3**	**4**	**1**	**2**	**3**	**4**
B. coag					24	1	2	7					3	6	7	8	3	9	15	17	8	9	15	15	8	12	6	8	9	10	13	14	8	12	3	9
B. sub	1	6	8	12	20	23	6	27	1	9	14	16	3	6	6	7	3	9	15	17	8	9	15	15	8	12	6	8	9	10	13	14	8	12	2	9
B. therm	3	6	1	20	6	12	39	40	11	14	14	16	3	6	6	7	10	13	16	17	14	16	9	15	1	6	7	8	15	21	9	14	14	7	9	10
B. tii	6	9	1	21					2	6	12	14	6	6	7	8	7	10	14	15	8	9	15	15	8	12	6	8	10	9	10	13	8	12	3	9
E. coli K12	3	6	8	21	20	23	39	40	2	9	14	16	3	6	7	8	6	13	16	17	14	16	9	15	1	6	7	12	15	21	9	14	14	20	9	14
M. luteus	8	12	20	21	23	6	12	39	1	9	14	16	3	6	6	7	3	9	15	17	9	11	9	15	24	1	2	7	10	1	9	14	9	15	9	13
Ps. fluor 4358	6	8	20	21					2	9	14	16	6	6	7	8	6	13	15	20	14	16	9	15	1	6	7	8	15	21	9	14	14	20	9	13
Ps. fluor 50090	6	1	20	21					1	9	14	16	3	6	6	7	6	9	15	17	14	16	9	15	1	6	7	8	15	21	9	14	14	7	9	13
E. coli TOP10	1	6	20	9	1	6	23	39	3	6	6	7	2	8	14	16	7	10	16	17	27	7	9	15	1	6	7	12	15	21	9	14	14	20	27	9

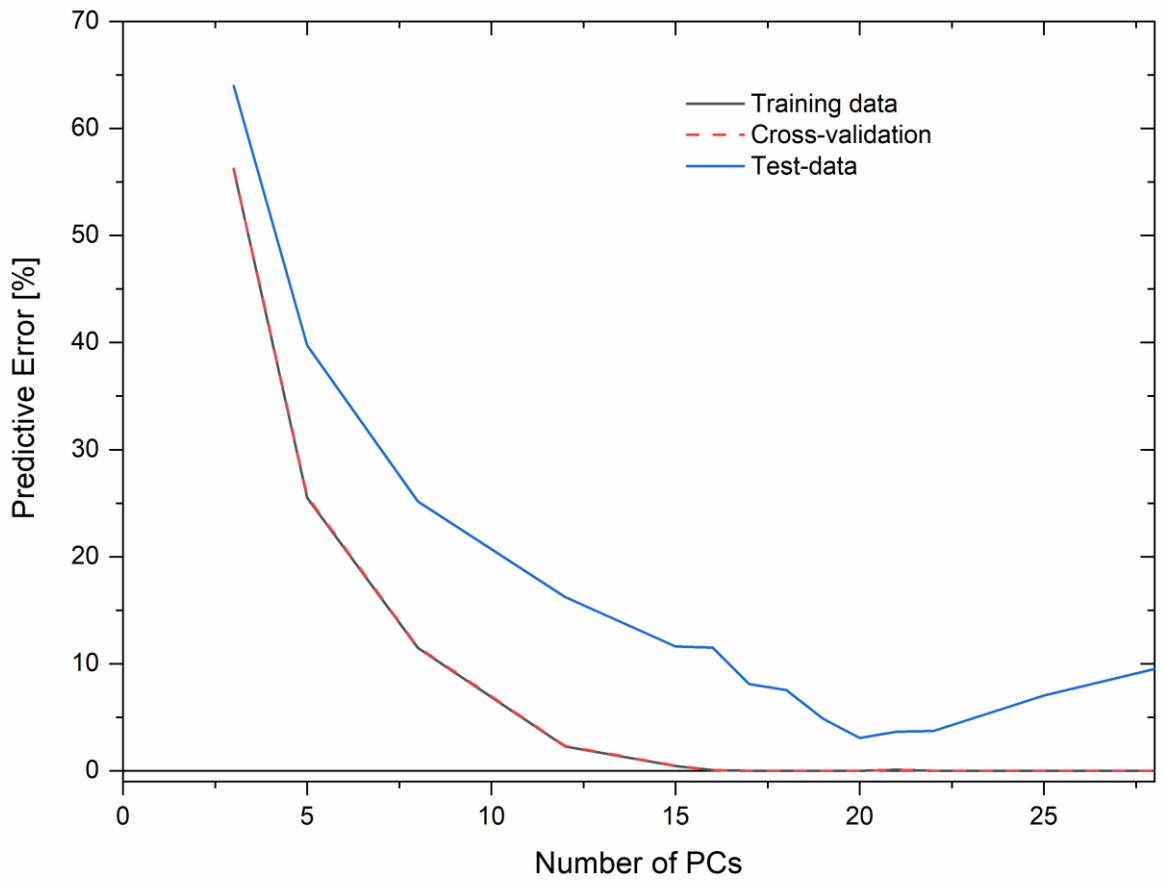

Figure 7.6: Check for overfitting for the general discrimination by plotting the error rate of the training data, the cross-validation and the test data against the number of PCs used for classification.

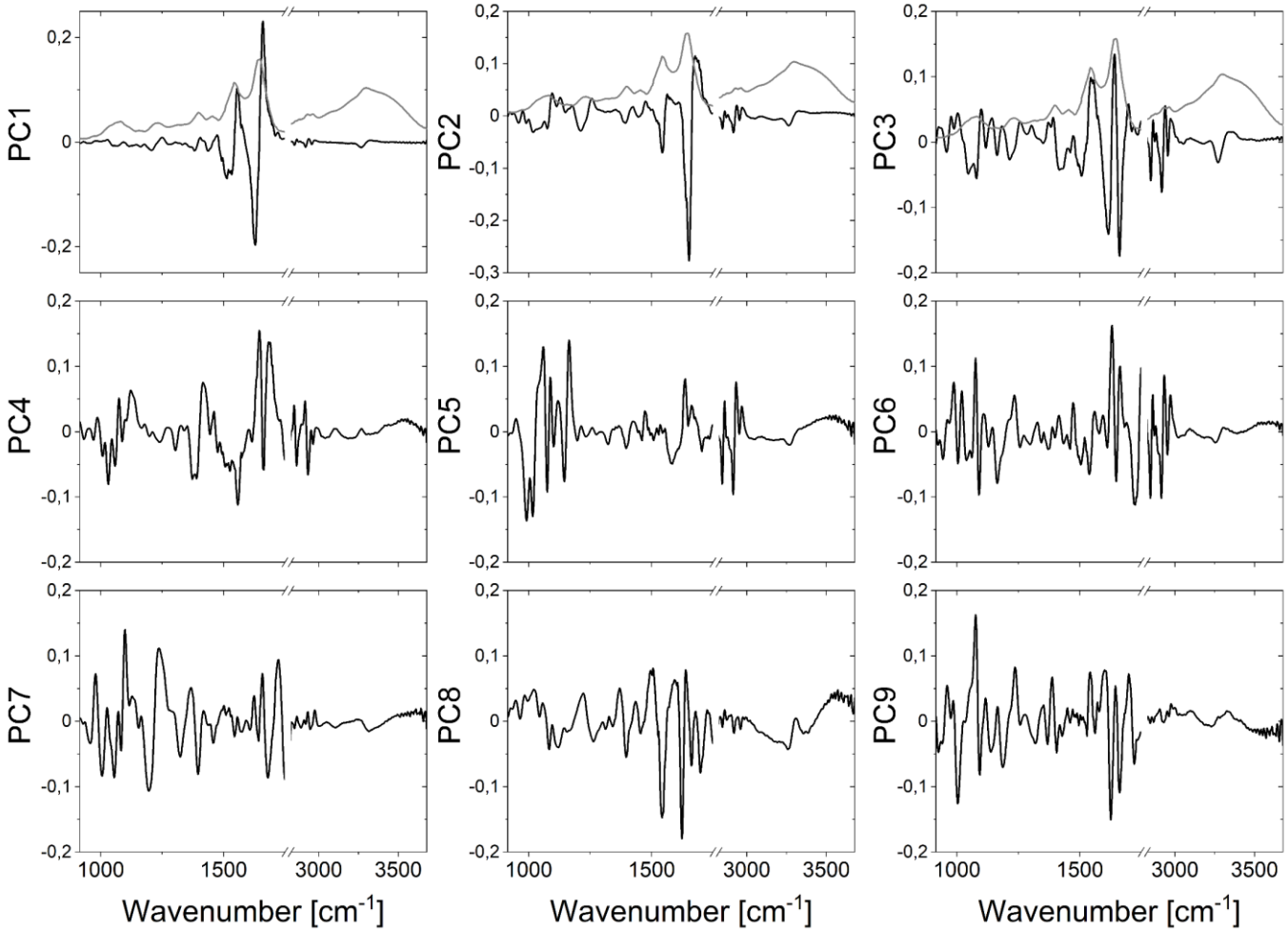

Figure 7.7: Loadings (PC1 – PC9) of the PCA of the training data set for the bacteria discrimination model. For a better spectral comparison in the graphs for PC1 – PC3 the average spectrum of B. coag is given in gray.

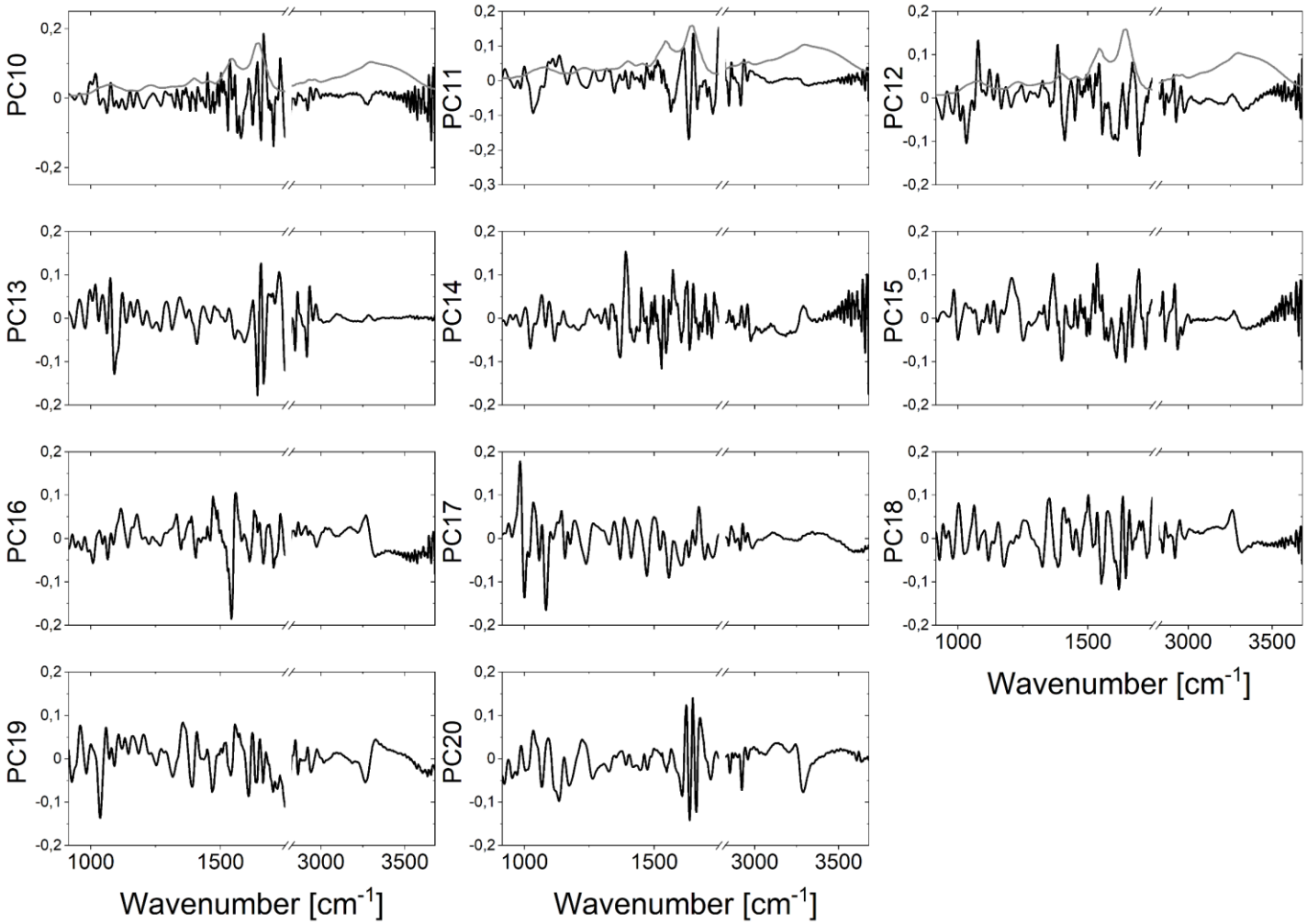

Figure 7.8: Loadings (PC10 – PC20) of the PCA of the training data set for the bacteria discrimination model. For a better spectral comparison in the graphs for PC10 – PC12 the average spectrum of B. coag is given in gray.

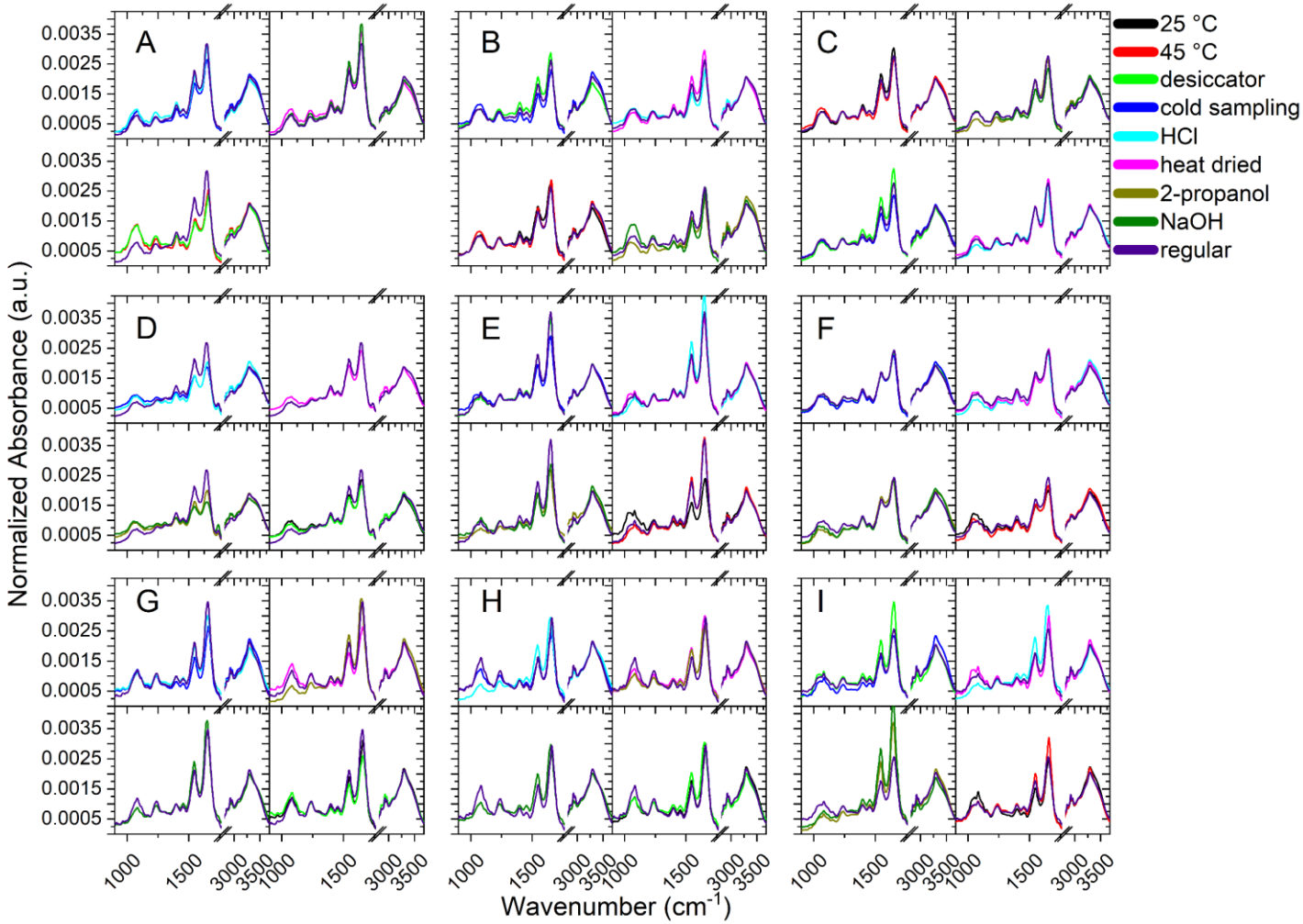

Figure 7.9: Raw IR spectra of each stress condition vs. regular treated of *B. coag* (A), *B. sub* (B), *B. therm* (C), *B. tii* (D), *E. coli K12* (E), *M. luteus* (F), *Ps. fluor 4358* (G), *Ps. fluor 50090 (H) and E. coli TOP10* (I).

Table 7.5: Confusion matrix for the independent test data set for the classification of all stress condition for *B. coag*. The values of the table reflect the correct classifications of observations.

B. coag	**Predicted class**							
	45 °C	**Desiccator**	**Cold sampling**	**HCl**	**Heat dried**	**2-Propanol**	**NaOH**	**Regular**
45 °C	50	0	0	0	0	0	0	0
Desiccator	0	50	0	0	0	0	0	0
Cold sampling	0	0	50	0	0	0	0	0
HCl	0	0	0	50	0	0	0	0
Heat dried	0	0	0	0	50	0	0	0
2-propanol	0	0	0	0	0	50	0	0
NaOH	0	0	0	0	0	0	50	0
Regular	0	0	0	0	0	0	0	50

Table 7.6: Confusion matrix for the independent test data set for the classification of all stress condition for *B. sub*. The values of the table reflect the correct classifications of observations.

B. sub	**Predicted class**								
	25 °C	**45 °C**	**Desiccator**	**Cold sampling**	**HCl**	**Heat dried**	**2-propanol**	**NaOH**	**Regular**
25 °C	50	0	0	0	0	0	0	0	0
45 °C	0	50	0	0	0	0	0	0	0
Desiccator	0	0	50	0	0	0	0	0	0
Cold sampling	0	0	0	50	0	0	0	0	0
HCl	0	0	0	0	50	0	0	0	0
Heat dried	0	0	0	0	0	50	0	0	0
2-propanol	0	0	0	0	0	0	50	0	0
NaOH	0	0	0	0	0	0	0	50	0
Regular	0	0	0	0	0	0	0	0	50

Table 7.7: Confusion matrix for the independent test data set for the classification of all stress condition for *B. therm*. The values of the table reflect the correct classifications of observations.

B. therm	**Predicted class**								
	25 °C	**45 °C**	**Desiccator**	**Cold sampling**	**HCl**	**Heat dried**	**2-propanol**	**NaOH**	**Regular**
25 °C	50	0	0	0	0	0	0	0	0
45 °C	0	50	0	0	0	0	0	0	0
Desiccator	0	0	50	0	0	0	0	0	0
Cold sampling	0	0	0	50	0	0	0	0	0
HCl	0	0	0	0	50	0	0	0	0
Heat dried	0	0	0	0	0	50	0	0	0
2-propanol	0	0	0	0	0	0	50	0	0
NaOH	0	0	0	0	0	0	0	50	0
Regular	0	0	0	0	0	0	0	0	50

Table 7.8: Confusion matrix for the independent test data set for the classification of all stress condition for *B. tii*. The values of the table reflect the correct classifications of observations.

B. tii	**Predicted class**							
	25 °C	**Desiccator**	**Cold sampling**	**HCl**	**Heat dried**	**2-propanol**	**NaOH**	**Regular**
25 °C	50	0	0	0	0	0	0	0
Desiccator	0	50	0	0	0	0	0	0
Cold sampling	0	0	50	0	0	0	0	0
HCl	0	0	0	50	0	0	0	0
Heat dried	0	0	0	0	50	0	0	0
2-propanol	0	0	0	0	0	50	0	0
NaOH	0	0	0	0	0	0	50	0
Regular	0	0	0	0	0	0	0	50

Table 7.9: Confusion matrix for the independent test data set for the classification of all stress condition for *E. coli* K12. The values of the table reflect the correct classifications of observations.

***E. coli* K12**	**Predicted class**								
	25 °C	**45 °C**	**Desiccator**	**Cold sampling**	**HCl**	**Heat dried**	**2-propanol**	**NaOH**	**Regular**
25 °C	50	0	0	0	0	0	0	0	0
45 °C	0	50	0	0	0	0	0	0	0
Desiccator	0	0	50	0	0	0	0	0	0
Cold sampling	0	0	0	50	0	0	0	0	0
HCl	0	0	0	0	50	0	0	0	0
Heat dried	0	0	0	0	0	50	0	0	0
2-propanol	0	0	0	0	0	0	50	0	0
NaOH	0	0	0	0	0	0	0	50	0
Regular	0	0	0	0	0	0	0	0	50

Table 7.10: Confusion matrix for the independent test data set for the classification of all stress condition for *M. luteus*. The values of the table reflect the correct classifications of observations.

M. luteus	**Predicted class**								
	25 °C	**45 °C**	**Desiccator**	**Cold sampling**	**HCl**	**Heat dried**	**2-propanol**	**NaOH**	**Regular**
25 °C	50	0	0	0	0	0	0	0	0
45 °C	0	50	0	0	0	0	0	0	0
Desiccator	0	0	50	0	0	0	0	0	0
Cold sampling	0	0	0	50	0	0	0	0	0
HCl	0	0	0	0	50	0	0	0	0
Heat dried	0	0	0	0	0	50	0	0	0
2-propanol	0	0	0	0	0	0	50	0	0
NaOH	0	0	0	0	0	0	0	50	0
Regular	0	0	0	0	0	0	0	0	50

Table 7.11: Confusion matrix for the independent test data set for the classification of all stress condition for *Ps. fluor* 4358. The values of the table reflect the correct classifications of observations.

***Ps. fluor* 4358**	**Predicted class**							
	25 °C	**Desiccator**	**Cold sampling**	**HCl**	**Heat dried**	**2-propanol**	**NaOH**	**Regular**
25 °C	50	0	0	0	0	0	0	0
Desiccator	0	50	0	0	0	0	0	0
Cold sampling	0	0	50	0	0	0	0	0
HCl	0	0	0	50	0	0	0	0
Heat dried	0	0	0	0	50	0	0	0
2-propanol	0	0	0	0	0	50	0	0
NaOH	0	0	0	0	0	0	50	0
Regular	0	0	0	0	0	0	0	50

Table 7.12: Confusion matrix for the independent test data set for the classification of all stress condition for *Ps. fluor* 50090. The values of the table reflect the correct classifications of observations.

***Ps. fluor* 50090**	**Predicted class**							
	25 °C	**Desiccator**	**Cold sampling**	**HCl**	**Heat dried**	**2-propanol**	**NaOH**	**Regular**
25 °C	50	0	0	0	0	0	0	0
Desiccator	0	50	0	0	0	0	0	0
Cold sampling	0	0	50	0	0	0	0	0
HCl	0	0	0	50	0	0	0	0
Heat dried	0	0	0	0	50	0	0	0
2-propanol	0	0	0	0	0	50	0	0
NaOH	0	0	0	0	0	0	50	0
Regular	0	0	0	0	0	0	0	50

Table 7.13: Confusion matrix for the independent test data set for the classification of all stress condition for *E. coli* TOP10. The values of the table reflect the correct classifications of observations.

***E. coli* TOP10**	**Predicted class**								
	25 °C	**45 °C**	**Desiccator**	**Cold sampling**	**HCl**	**Heat dried**	**2-propanol**	**NaOH**	**Regular**
25 °C	50	0	0	0	0	0	0	0	0
45 °C	0	50	0	0	0	0	0	0	0
Desiccator	0	0	50	0	0	0	0	0	0
Cold sampling	0	0	0	50	0	0	0	0	0
HCl	0	0	0	0	50	0	0	0	0
Heat dried	0	0	0	0	0	50	0	0	0
2-propanol	0	0	0	0	0	0	50	0	0
NaOH	0	0	0	0	0	0	0	50	0
Regular	0	0	0	0	0	0	0	0	50

Chapter 8

Concluding Remarks and Future Perspectives

Based on:

Klein, D., Breuch, R., von der Mark, S., Wickleder, C., Kaul, P., Detection of Spoilage Associated Bacteria using Raman-microspectroscopy Combined with Multivariate Statistical Analysis. Talanta 196 (2019), 325–328. https://doi.org/10.1016/j.talanta.2018.12.094.

Klein, D., Breuch, R., Reinmüller, J., Engelhard, C., Kaul, P., Rapid Detection and Discrimination of Food-related Bacteria using IR-microspectroscopy in Combination with Multivariate Statistical Analysis, Talanta 232 (2021), 122424. https://doi.org/10.1016/j.talanta.2021.122424.

Klein, D.; Breuch, R.; Reinmüller, J.; Engelhard, C.; Kaul, P., Investigation and Rapid Discrimination of Food-Related Bacteria under Stress Treatments Using IR Microspectroscopy. Foods 10 (2021), 1850. https://doi.org/10.3390/foods10081850.

Klein, D.; Breuch, R.; Reinmüller, J.; Engelhard, C.; Kaul, P., Discrimination of Stressed and Non-Stressed Food-Related Bacteria Using Raman-Microspectroscopy. Foods 11 (2022), 1506. https://doi.org/10.3390/foods11101506.

8.1 Summary and Conclusion

In this thesis, a fast and reliable sampling and analysis method by microspectroscopy for the determination and subsequent classification of spoilage bacteria is developed and optimized. Samples of spoilage microorganisms collected by rapid blotting using a disinfectable sampling stamp were analyzed by Raman- and IR-spectroscopy. Subsequently, the multivariate data were classified by means of careful preprocessing and well-considered chemometric model development. In order to verify the robustness and reliability of the developed methods and to test the models on real world samples and thus to exceed the strict standardization for measurements, preprocessing and laboratory conditions, extrinsic factors such as various extreme stress conditions to which the microorganisms were exposed were finally also taken into account in the classification.

In Chapter 4 and Chapter 5, a time-saving, cost-effective, and suitable sample preparation of microbiological samples with subsequent data evaluation and classification was developed. A fast and simple sampling procedure was developed using a disinfectable stainless steel cylinder and without the usual purification, dilution and drying steps. This method allows rapid surface blots from, for example, the surface of the culture medium.

The complex multivariate data were made manageable using reasonable chemometric data preprocessing and a PCA and were subsequently classified with a CDA. The results show that the presented techniques and methods with subsequent chemometric evaluation and only the use of the proteins, lipids, nucleic acids, and polysaccharides regions with Raman- (600–1200 cm^{-1}) and IR- (2815–3680 cm^{-1}) microspectroscopy are able to quickly and efficiently differentiate between spoilage-relevant microorganisms at genus, species and even strain level. Although all usual washing, centrifugation, and separation steps were omitted, the presented rapid preparation and measurement method was able to produce good quality spectra and delivered a robust method to differentiate between different microorganisms down to strain level.

In conclusion, the methods of Raman- and IR-microspectroscopy from rapid surface blots followed by chemometric analysis were successfully used for rapid and non-destructive analysis of meat spoilage. The presented pre-processing methods, successive principal component analysis, and canonical discriminant analysis showed that spoilage-related microorganisms could be separated and classified at

genus, species, and strain levels with 96.5 % (Raman) and 94.5 % (IR) accuracy, respectively. In addition, the chemometric models created are robust in terms of sampling, sample size, number of classes, and accuracy due to the balanced data sets.

Response to stress causes changes in the vibrational spectroscopic spectral properties of food-relevant microorganisms. Regardless of the cultivation conditions, sampling, and storage time, a method was developed for easy sample preparation, rapid measurement by Raman- (Chapter 6) and IR-microspectroscopy (Chapter 7), and chemometrics for rapid and nondestructive analysis of food-relevant bacteria.

Compared to reference microorganisms, sublethally stressed microorganisms reveal changes in lipids, nucleic acids, polysaccharides, and proteins regardless of lifetime exposure or sampling conditions. The observed changes result from changes in the secondary structure of proteins, exopolymer production, and denaturation of nucleic acids. Thus, it can be concluded that despite the various spectral changes of sublethally stressed microorganisms in the range of proteins, lipids, nucleic acids, and polysaccharides due to different stress factors (lifetime and sampling conditions) applied to nine different microorganisms, rapid, robust, and reliable methods and classification models for food-relevant microorganisms could be developed down to the strain level.

Classification using canonical discriminant analysis showed that a robust and informative model was developed to discriminate different microorganisms at the genus, species, and strain levels with 97.6 % (Raman) and 96.6 % (IR) accuracy, respectively. The results confirm the potential of Raman- and IR-microspectroscopy for bacterial discrimination and interpretation of microbial stress responses. In addition, they indicate that the strict sample preparation and standardization given in the literature should be reconsidered and that existing standardized databases should include stress conditions. Combining numerous stress factors with the traditional reference samples in one model also showed that the classification of unknown samples fits well into the landscape of existing classification models and thus represents a significant enrichment.

As the presented models are limited to a certain number of microorganisms further generalization is required. This includes the extension of the classes by additional

microorganisms, different species, strains, and the inclusion of non-spoilage and pathogenic bacteria.

For the practice oriented application of the approach, the extension of the models by wild type microorganisms as well as by samples directly from food or their contact surfaces is reasonable. This will improve the versatility of the models with regard to the influence of food matrix and reduce the dependence of long cultivation times.

Furthermore, the presented results should be compared with models derived from measurements with non-microscopic systems and thus larger spot sizes. This would enable larger areas to be scanned and evaluated in a shorter time. Additionally, the imaging methods could provide substantial benefits for the detection of microbial contamination, especially on assembly lines in the food sector, both monomodally and especially in the area of multimodal data evaluation and image fusion. It has to be examined whether the fusion of the modalities on hardware level seems to be reasonable besides the pure data or image data fusion from both modalities. The inconvenient registration of a sensitive biological sample that has to be manually transferred to the second modality and essentially has no microscopic markers could lead to a considerable loss of information or even to misinformation. However, hardware fusion would make it possible to acquire data from both modalities simultaneously from one measurement point. For the data collected in this way, pre-processing routines and chemometric models have to be generated again, which indicate that they appear to be very informative and robust.

References

[1] S. Jiang, F. Wang, Q. Li, H. Sun, H. Wang, Z. Yao, Environment and food safety: a novel integrative review, Environ. Sci. Pollut. Res. 28 (2021) 54511–54530. https://doi.org/10.1007/s11356-021-16069-6.

[2] I. Garcia-Herrero, D. Hoehn, M. Margallo, J. Laso, A. Bala, L. Batlle-Bayer, P. Fullana, I. Vazquez-Rowe, M.J. Gonzalez, M.J. Durá, C. Sarabia, R. Abajas, F.J. Amo-Setien, A. Quiñones, A. Irabien, R. Aldaco, On the estimation of potential food waste reduction to support sustainable production and consumption policies, Food Policy. 80 (2018) 24–38. https://doi.org/10.1016/j.foodpol.2018.08.007.

[3] Å. Stenmarck, C. Jensen, T. Quested, G. Moates, B. Cseh, S. Juul, A. Parry, A. Politano, B. Redlingshofer, S. Scherhaufer, K. Silvennoinen, H. Soethoudt, C. Zübert, K. Östergren, Estimates of european food waste levels, IVL Swedish Environmental Research Institute, Stockholm, 2016. https://doi.org/10.13140/RG.2.1.4658.4721.

[4] K. Candoğan, E.G. Altuntas, N. İğci, Authentication and quality assessment of meat products by Fourier-Transform infrared (FTIR) spectroscopy, Food Eng. Rev. 13 (2020) 66–91. https://doi.org/10.1007/s12393-020-09251-y.

[5] United Nations, World population prospects 2019: Highlights, United Nations, New York, 2019.

[6] T. Buettner, World population prospects – A long view, Econ. Stat. / Econ. Stat. (2020) 9–27. https://doi.org/10.24187/ecostat.2020.520d.2030.

[7] J. Mazor, Liberal Justice, Future People, and Natural Resource Conservation, Philos. Public Aff. 38 (2010) 380–408. http://www.jstor.org/stable/40926875.

[8] K.J. Ong, J. Johnston, I. Datar, V. Sewalt, D. Holmes, J.A. Shatkin, Food safety considerations and research priorities for the cultured meat and seafood industry, Compr. Rev. Food Sci. Food Saf. 20 (2021) 5421–5448. https://doi.org/10.1111/1541-4337.12853.

[9] L. Toma, M. Costa Font, B. Thompson, Impact of consumers' understanding of date labelling on food waste behaviour, Oper. Res. 20 (2020) 543–560. https://doi.org/10.1007/s12351-017-0352-3.

[10] M.G. Corradini, Shelf life of food products: From open labeling to real-time measurements, Annu. Rev. Food Sci. Technol. 9 (2018) 251–269. https://doi.org/10.1146/annurev-food-030117-012433.

[11] H. Forbes, T. Quested, C. O'Connor, Food waste index report 2021, Nairobi, 2021. https://www.unep.org/resources/report/unep-food-waste-index-report-2021.

[12] Bundesamt für Verbraucherschutz und Lebensmittelsicherheit, Mindesthaltbarkeitsdatum / Verbrauchsdatum / Haltbarkeitsdatum, (2023). https://www.bvl.bund.de/DE/Arbeitsbereiche/01_Lebensmittel/03_Verbraucher/17_FAQ/FAQ_MHD/FAQ_MHD_node.html (accessed March 3, 2023).

[13] European Parliament and Council, General principles and requirements of food law, establishing the European Food Safety Authority and laying down procedures in matters of food safety, 2002. http://eur-lex.europa.eu/LexUriServ/LexUriServ.do?uri=OJ:L:2002:031:0001:0024:EN:PDF.

[14] Wissenschaftliche Dienste Deutscher Bundestag, Mindesthaltbarkeitsdatum Nationaler Regelungsspielraum und fachwissenschaftliche Diskussion, 2019. https://www.bundestag.de/resource/blob/659870/1265fe4efbc90aa1ca13ac6dd1c7820b/WD-5-077-19-pdf-data.pdf.

[15] P.J. Taormina, M.D. Hardin, Food safety and quality-based shelf life of perishable foods, Springer International Publishing, Cham, 2021. https://doi.org/10.1007/978-3-030-54375-4.

[16] S. Van Boxstael, F. Devlieghere, D. Berkvens, A. Vermeulen, M. Uyttendaele, Understanding and attitude regarding the shelf life labels and dates on pre-packed food products by Belgian consumers, Food Control. 37 (2014) 85–92. https://doi.org/10.1016/j.foodcont.2013.08.043.

[17] R. Gurbanov, A.G. Gozen, F. Severcan, Rapid classification of heavy metal-exposed freshwater bacteria by infrared spectroscopy coupled with chemometrics using supervised method, Spectrochim. Acta Part A Mol. Biomol. Spectrosc. 189 (2018) 282–290. https://doi.org/10.1016/j.saa.2017.08.038.

[18] X. Lu, H.M. Al-Qadiri, M. Lin, B.A. Rasco, Application of mid-infrared and Raman spectroscopy to the study of bacteria, Food Bioprocess Technol. 4 (2011) 919–935. https://doi.org/10.1007/s11947-011-0516-8.

[19] V. Velusamy, K. Arshak, O. Korostynska, K. Oliwa, C. Adley, An overview of foodborne pathogen detection: In the perspective of biosensors, Biotechnol. Adv. 28 (2010) 232–254. https://doi.org/10.1016/j.biotechadv.2009.12.004.

[20] S. Hameed, L. Xie, Y. Ying, Conventional and emerging detection techniques for pathogenic bacteria in food science: A review, Trends Food Sci. Technol. 81 (2018) 61–73. https://doi.org/10.1016/j.tifs.2018.05.020.

[21] L. Teng, X. Wang, X. Wang, H. Gou, L. Ren, T. Wang, Y. Wang, Y. Ji, W.E. Huang, J. Xu, Label-free, rapid and quantitative phenotyping of stress response in E. coli via ramanome, Sci. Rep. 6 (2016) 34359. https://doi.org/10.1038/srep34359.

[22] A. Van Bemmel, K. Parizeau, Is it food or is it waste? The materiality and relational agency of food waste across the value chain, J. Cult. Econ. 13 (2020) 207–220. https://doi.org/10.1080/17530350.2019.1684339.

[23] European Commission, Directorate-General for Health and Food Safety, Food waste and date marking: summary, 2015. https://doi.org/10.2875/25093.

[24] World Health Organisation, Food safety, fact sheet number 399, Fact Sheet Number 399. (2022) 1–6. http://www.who.int/mediacentre/factsheets/fs399/en/ (accessed March 3, 2023).

[25] PubMed National Library of Medicine, Number of Publications, (2022). https://pubmed.ncbi.nlm.nih.gov/?term=(food safety or bacteria) AND (Raman or IR)&timeline=expanded.

[26] S. Pahlow, S. Meisel, D. Cialla-May, K. Weber, P. Rösch, J. Popp, Isolation and identification of bacteria by means of Raman spectroscopy, Adv. Drug Deliv. Rev. 89 (2015) 105–120. https://doi.org/10.1016/j.addr.2015.04.006.

[27] J.-K. Hong, S. Bin Kim, E.S. Lyou, T.K. Lee, Microbial phenomics linking the phenotype to function: The potential of Raman spectroscopy, J. Microbiol. 59 (2021) 249–258. https://doi.org/10.1007/s12275-021-0590-1.

[28] K.J. Boor, Bacterial stress responses: What doesn't kill them can make them stronger, PLoS Biol. 4 (2006) e23. https://doi.org/10.1371/journal.pbio.0040023.

[29] H. Kim, K. Wu, C. Lee, Stress-responsive periplasmic chaperones in bacteria, Front. Mol. Biosci. 8 (2021) 1–14. https://doi.org/10.3389/fmolb.2021.678697.

[30] J.D. Oliver, The viable but nonculturable state in bacteria., J. Microbiol. 43 Spec No (2005) 93–100. http://www.ncbi.nlm.nih.gov/pubmed/15765062.

[31] B.H. Kim, G.M. Gadd, Bacterial Physiology and Metabolism, Cambridge University Press, Cambridge, UK, 2008.

[32] J.M. Willey, L.M. Sherwood, C.J. Woolverton, Prescott's Microbiology, 9th ed., McGraw-Hill, New York, NY, 2014. https://www.scientificamerican.com/article/dinosaurs-in-the-halls.

[33] D. Naumann, Infrared spectroscopy in microbiology, in: Encycl. Anal. Chem., John Wiley & Sons, Ltd, Chichester, UK, 2006: pp. 1–29. https://doi.org/10.1002/9780470027318.a0117.

[34] J.H.J. Huis in't Veld, Microbial and biochemical spoilage of foods: an overview, Int. J. Food Microbiol. 33 (1996) 1–18. https://doi.org/10.1016/0168-1605(96)01139-7.

[35] J. Kreyenschmidt, R. Ibald, Modeling shelf life using microbial indicators, Shelf Life Assess. Food. (2012) 127–168. https://doi.org/10.1201/b11871.

[36] G.J.E. Nychas, E.H. Drosinos, Meat and Poultry – Spoilage of Meat, in: Encycl. Food Microbiol., 2nd Editio, Academic Press, London, 2000: pp. 1253–1284.

[37] R. Gospavic, J. Kreyenschmidt, S. Bruckner, V. Popov, N. Haque, Mathematical modelling for predicting the growth of Pseudomonas spp. in poultry under variable temperature conditions, Int. J. Food Microbiol. 127 (2008) 290–297. https://doi.org/10.1016/j.ijfoodmicro.2008.07.022.

[38] S. Rossaint, J. Kreyenschmidt, Intelligent label – a new way to support food waste reduction, Proc. Inst. Civ. Eng. - Waste Resour. Manag. 168 (2015) 63–71. https://doi.org/10.1680/warm.13.00035.

[39] U. Herbert, Assessment of different packaging atmospheres for the poultry meat industry based on an overall quality index, Rheinische Friedrich-Wilhelms-Universität Bonn, 2014.

[40] X. Ye, K. Iino, S. Zhang, Monitoring of bacterial contamination on chicken meat surface using a novel narrowband spectral index derived from hyperspectral imagery data, Meat Sci. 122 (2016) 25–31. https://doi.org/10.1016/j.meatsci.2016.07.015.

[41] J. Popp, Identification of micro-organisms by Raman spectroscopy, SPIE Newsroom. (2007) 3–4. https://doi.org/10.1117/2.1200708.0856.

[42] H. Yang, J. Irudayaraj, Rapid detection of foodborne microorganisms on food surface using Fourier transform Raman spectroscopy, J. Mol. Struct. 646 (2003) 35–43. https://doi.org/10.1016/S0022-2860(02)00575-6.

[43] S. Sieuwerts, F.A.M. de Bok, E. Mols, W.M. de Vos, J.E.T. van Hylckama Vlieg, A simple and fast method for determining colony forming units, Lett. Appl. Microbiol. 47 (2008) 275–278. https://doi.org/10.1111/j.1472-765X.2008.02417.x.

[44] C. Liu, C. Yeung, P. Chen, M. Yeh, S. Hou, Salmonella detection using 16S ribosomal DNA/RNA probe-gold nanoparticles and lateral flow immunoassay, Food Chem. 141 (2013) 2526–2532. https://doi.org/10.1016/j.foodchem.2013.05.089.

[45] T. Junillon, A. Vimont, D. Mosticone, B. Mallen, F. Baril, C. Rozand, J. Flandrois, Simplified detection of food-borne pathogens: An in situ high affinity capture and staining concept, J. Microbiol. Methods. 91 (2012) 501–505. https://doi.org/10.1016/j.mimet.2012.09.015.

[46] R. Karoui, C. Blecker, Fluorescence Spectroscopy Measurement for Quality Assessment of Food Systems—a Review, Food Bioprocess Technol. 4 (2011) 364–386. https://doi.org/10.1007/s11947-010-0370-0.

[47] D. Helm, H. Labischinski, G. Schallehn, D. Naumann, Classification and identification of bacteria by Fourier-transform infrared spectroscopy, J. Gen. Microbiol. 137 (1991) 69–79. https://doi.org/10.1099/00221287-137-1-69.

[48] Â. Novais, A.R. Freitas, C. Rodrigues, L. Peixe, Fourier transform infrared spectroscopy: unlocking fundamentals and prospects for bacterial strain typing, Eur. J. Clin. Microbiol. Infect. Dis. 38 (2019) 427–448. https://doi.org/10.1007/s10096-018-3431-3.

[49] R. Davis, L. Mauer, Fourier transform infrared (FT-IR) spectroscopy: a rapid tool for detection and analysis of foodborne pathogenic bacteria, Curr. Res. Technol. Educ. Top. Appl. Microbiol. Microb. Biotechnol. A. Méndez-Vilas. 2 (2010) 1582–1594. http://www.formatex.info/microbiology2/1582-1594.pdf.

[50] F. Adzitey, N. Huda, G.R.R. Ali, Molecular techniques for detecting and typing of bacteria, advantages and application to foodborne pathogens isolated from ducks, 3 Biotech. 3 (2013) 97–107. https://doi.org/10.1007/s13205-012-0074-4.

[51] B. Lorenz, C. Wichmann, S. Stöckel, P. Rösch, J. Popp, Cultivation-free Raman spectroscopic investigations of bacteria, Trends Microbiol. 25 (2017) 413–424. https://doi.org/10.1016/j.tim.2017.01.002.

[52] D. Helm, H. Labischinski, D. Naumann, Elaboration of a procedure for identification of bacteria using Fourier-Transform IR spectral libraries: a stepwise correlation approach, J. Microbiol. Methods. 14 (1991) 127–142. https://doi.org/10.1016/0167-7012(91)90042-O.

[53] R. Davis, G. Paoli, L.J. Mauer, Evaluation of Fourier transform infrared (FT-IR) spectroscopy and chemometrics as a rapid approach for sub-typing Escherichia coli O157:H7 isolates, Food Microbiol. 31 (2012) 181–190. https://doi.org/10.1016/j.fm.2012.02.010.

[54] D. Naumann, S. Keller, D. Helm, C. Schultz, B. Schrader, FT-IR spectroscopy and FT-Raman spectroscopy are powerful analytical tools for the non-invasive characterization of intact microbial cells, J. Mol. Struct. 347 (1995) 399–405. https://doi.org/10.1016/0022-2860(95)08562-A.

[55] C. Wang, R. Chen, J. Xu, L. Jin, Single-cell Raman spectroscopy identifies Escherichia coli persisters and reveals their enhanced metabolic activities, Front. Microbiol. 13 (2022). https://doi.org/10.3389/fmicb.2022.936726.

[56] K.C. Schuster, E. Urlaub, J.R. Gapes, Single-cell analysis of bacteria by Raman microscopy: spectral information on the chemical composition of cells and on the heterogeneity in a culture, J. Microbiol. Methods. 42 (2000) 29–38. https://doi.org/10.1016/S0167-7012(00)00169-X.

[57] M. Li, J. Xu, M. Romero-Gonzalez, S.A. Banwart, W.E. Huang, Single cell Raman spectroscopy for cell sorting and imaging, Curr. Opin. Biotechnol. 23 (2012) 56–63. https://doi.org/10.1016/j.copbio.2011.11.019.

[58] B. Moen, A.O. Janbu, S. Langsrud, Ø. Langsrud, J.L. Hobman, C. Constantinidou, A. Kohler, K. Rudi, Global responses of Escherichia coli to adverse conditions determined by microarrays and FT-IR spectroscopy, Can. J. Microbiol. 55 (2009) 714–728. https://doi.org/10.1139/W09-016.

[59] R. Weiss, M. Palatinszky, M. Wagner, R. Niessner, M. Elsner, M. Seidel, N.P. Ivleva, Surface-enhanced Raman spectroscopy of microorganisms: Limitations and applicability on the single-cell level, Analyst. 144 (2019) 943–953. https://doi.org/10.1039/c8an02177e.

[60] M. Kemmler, E. Rodner, P. Rösch, J. Popp, J. Denzler, Automatic identification of novel bacteria using Raman spectroscopy and Gaussian processes, Anal. Chim. Acta. 794 (2013) 29–37. https://doi.org/10.1016/j.aca.2013.07.051.

[61] P. Larkin, Infrared and Raman Spectroscopy, Elsevier, Amsterdam, 2011. https://doi.org/10.1016/C2010-0-68479-3.

[62] D.A. Skoog, F.J. Holler, S.R. Crouch, Principles of Instrumental Analysis, 6th Editio, Thomson Higher Education, Belmont, CA, 2007. https://doi.org/10.1017/CBO9781107415324.004.

[63] H. Liu, Y. Chen, C. Shi, X. Yang, D. Han, FT-IR and Raman spectroscopy data fusion with chemometrics for simultaneous determination of chemical quality indices of edible oils during thermal oxidation, Lwt. 119 (2020) 108906. https://doi.org/10.1016/j.lwt.2019.108906.

[64] W.E. Huang, M. Li, R.M. Jarvis, R. Goodacre, S.A. Banwart, Shining light on the microbial world the application of Raman microspectroscopy., 1st ed., Elsevier Inc., 2010. https://doi.org/10.1016/S0065-2164(10)70005-8.

[65] L.G. Thygesen, M.M. Løkke, E. Micklander, S.B. Engelsen, Vibrational microspectroscopy of food. Raman vs. FT-IR, Trends Food Sci. Technol. 14 (2003) 50–57. https://doi.org/10.1016/S0924-2244(02)00243-1.

[66] S. Lohumi, M.S. Kim, J. Qin, B.K. Cho, Raman imaging from microscopy to macroscopy: Quality and safety control of biological materials, TrAC - Trends Anal. Chem. 93 (2017) 183–198. https://doi.org/10.1016/j.trac.2017.06.002.

[67] M. Otto, Chemometrics: Statistics and computer application in analytical chemistry, 3rd ed., Wiley-VCH Verlag GmbH & Co. KGaA, Weinheim, Germany, 2017. http://www.tandfonline.com/doi/abs/10.1198/tech.2001.s596.

[68] T. Bocklitz, A. Walter, K. Hartmann, P. Rösch, J. Popp, How to pre-process Raman spectra for reliable and stable models?, Anal. Chim. Acta. 704 (2011) 47–56. https://doi.org/10.1016/j.aca.2011.06.043.

[69] N.K. Afseth, V.H. Segtnan, J.P. Wold, Raman spectra of biological samples: A study of preprocessing methods, Appl. Spectrosc. 60 (2006) 1358–1367. https://doi.org/10.1366/000370206779321454.

[70] K. Varmuza, P. Filzmoser, Introduction to multivariate statistical analysis in chemometrics, CRC Press, Taylor & Francis Group, Boca Raton, Fl, USA, 2008.

[71] L. Cayton, Algorithms for manifold learning, (2005). https://www.semanticscholar.org/paper/Algorithms-for-manifold-learning-Cayton/100dcf6aa83ac559c83518c8a41676b1a3a55fc0.

[72] P. Rösch, Raman-spektroskopische Untersuchungen an Pflanzen und Mikroorganismen, Julius-Maximilians-Universität Würzburg, 2002.

[73] P. Mishra, D.N. Rutledge, J.-M. Roger, K. Wali, H.A. Khan, Chemometric pre-processing can negatively affect the performance of near-infrared spectroscopy models for fruit quality prediction, Talanta. 229 (2021) 122303. https://doi.org/10.1016/j.talanta.2021.122303.

[74] J.R. Ferraro, K. Nakamoto, C.W. Brown, Introductory Raman spectroscopy, in: Introd. Raman Spectrosc., 2nd ed., Elsevier, London, UK, 2003: p. iii. https://doi.org/10.1016/B978-0-12-254105-6.50020-2.

[75] P. Vandenabeele, Practical Raman spectroscopy – An introduction, Wiley, 2013. https://doi.org/10.1002/9781119961284.

[76] E. Smith, G. Dent, Modern Raman spectroscopy - A practical approach, John Wiley & Sons, Ltd, Chichester, UK, 2004. https://doi.org/10.1002/0470011831.

[77] P. Rösch, M. Harz, M. Schmitt, K.D. Peschke, O. Ronneberger, H. Burkhardt, H.W. Motzkus, M. Lankers, S. Hofer, H. Thiele, J. Popp, Chemotaxonomic identification of single bacteria by micro-Raman spectroscopy: Application to clean-room-relevant biological contaminations, Appl. Environ. Microbiol. 71 (2005) 1626–1637. https://doi.org/10.1128/AEM.71.3.1626-1637.2005.

[78] U. Schmid, Entwicklung chemometrischer Methoden für die Klassifikation von Bakterien mittels Mikro-Raman-Spektroskopie, Diss. Fak. Für Leb. Der Tech. Univ. Carolo-Wilhelmina Zu Braunschweig. (2009).

[79] GM electronic, GM Electron. (2022). https://www.gmelectronic.com/bipolar-transistor-2n2905a-to39 (accessed November 13, 2022).

[80] Robert Koch Institute, Report: Final presentation and evaluation of epidemiological findings in the EHEC O104:H4 outbreak, Germany 2011., Berlin, 2011.

[81] Statistisches Bundesamt, Diagnosedaten der Krankenhäuser Deutschland, 2022. (2022). http://www.gbe-bund.de/oowa921-install/servlet/oowa/aw92/dboowasys921.xwdevkit/xwd_init?gbe.isgbetol/xs_start_neu/&p_aid=i&p_aid=95370735&nummer=550&p_sprache=D&p_indsp=99999999&p_aid=88983924#SOURCES (accessed February 22, 2022).

[82] Bundesamt für Verbraucherschutz und Lebensmittelsicherheit, D. Statistisches Bundesamt, Berichte zur Lebensmittelsicherheit 2013, Springer International Publishing, Cham, 2015. https://doi.org/10.1007/978-3-319-14658-4.

[83] J. Gustavsson, C. Cederberg, U. Sonesson, R. van Otterdijk, A. Meybeck, Global food losses and food waste: extent, causes and prevention., in: Save Food!, Interpack 2011, Food and Agriculture Organization of the United Nations, Düsseldorf, 2011. http://www.fao.org/docrep/014/mb060e/mb060e00.pdf.

[84] D. V. Lim, Microbiology, 2nd Editio, McGraw-Hill, Boston, 1998.

[85] J. Baumgart, B. Becker, Mikrobiologische Untersuchung von Lebensmitteln, in: 5. Auflage, Behr´s Verlag, Hamburg, Germany, 2004: p. 467.

[86] World Health Organisation, Bacillus thuringiensis israelensis (Bti) in drinking-water Background document for development of WHO Guidelines for Drinking-water Quality, WHO Guidel. Drink. Qual. (2009) 1–8. http://www.who.int/water_sanitation_health/gdwqrevision/RevisedFourthEditionBacillusthuringiensis_Bti_July272009_2.pdf.

[87] S. Pahlow, S. Stöckel, S. Pollok, D. Cialla-May, P. Rösch, K. Weber, J. Popp, Rapid Identification of Pseudomonas spp. via Raman Spectroscopy Using Pyoverdine as Capture Probe, Anal. Chem. 88 (2016) 1570–1577. https://doi.org/10.1021/acs.analchem.5b02829.

[88] D. Leibniz Institut, Leibniz Institute DSMZ-German Collection of Microorganisms and Cell Cultures, Catalogue of Microorganisms, (2023). https://www.dsmz.de/catalogues/catalogue-microorganisms.html (accessed March 3, 2023).

[89] R.A. Fisher, The use of multiple measurements in taxonomic problems, Ann. Eugen. 7 (1936) 179–188. https://doi.org/10.1111/j.1469-1809.1936.tb02137.x.

[90] K. Backhaus, B. Erichson, W. Plinke, R. Weiber, Multivariate Analysemethoden, in: Multivar. Anal., Springer Berlin Heidelberg, Berlin, Heidelberg, 2011: pp. 188–247. https://doi.org/10.1007/978-3-642-16491-0.

[91] R. Netzer, M.H. Stafsnes, T. Andreassen, A. Goksøyr, P. Bruheim, T. Brautaset, Biosynthetic pathway for γ-cyclic sarcinaxanthin in Micrococcus luteus : Heterologous expression and evidence for diverse and multiple catalytic functions of C 50 carotenoid cyclases, J. Bacteriol. 192 (2010) 5688–5699. https://doi.org/10.1128/JB.00724-10.

[92] J. Xie, Z. Qiu, The effect of imbalanced data sets on LDA: A theoretical and empirical analysis, Pattern Recognit. 40 (2007) 557–562. https://doi.org/10.1016/j.patcog.2006.01.009.

[93] W. Burgos-Paz, S.E. Ramos-Onsins, M. Pérez-Enciso, L. Ferretti, Correcting for unequal sampling in principal component analysis of genetic data, in: Correcting Unequal Sampl. Princ. Compon. Anal. Genet. Data, 10th World Congress of Genetics Applied to Livestock Production, 2014: pp. 1–3. https://www.asas.org/docs/default-source/wcgalp-proceedings-oral/210_paper_8713_manuscript_220_0.pdf?sfvrsn=2.

[94] V.J. Ajaykumar, P.K. Mandal, Modern concept and detection of spoilage in meat and meat products, in: Meat Qual. Anal., Elsevier, 2020: pp. 335–349. https://doi.org/10.1016/B978-0-12-819233-7.00018-5.

[95] L.S. Kantor, K. Lipton, A. Manchester, V. Oliveira, Estimating and addressing America´s food losses, Food Rev. Natl. Food Rev. 20 (1997) 2–12. https://doi.org/10.22004/ag.econ.234453.

[96] N.L.W. Wilson, B.J. Rickard, R. Saputo, S.-T. Ho, Food waste: The role of date labels, package size, and product category, Food Qual. Prefer. 55 (2017) 35–44. https://doi.org/10.1016/j.foodqual.2016.08.004.

[97] M. Nemati, A. Hamidi, S. Maleki Dizaj, V. Javaherzadeh, F. Lotfipour, An overview on novel microbial determination methods in pharmaceutical and food quality control, Adv. Pharm. Bull. 6 (2016) 301–308. https://doi.org/10.15171/apb.2016.042.

[98] H.P. Dwivedi, L.-A. Jaykus, Detection of pathogens in foods: the current state-of-the-art and future directions, Crit. Rev. Microbiol. 37 (2011) 40–63. https://doi.org/10.3109/1040841X.2010.506430.

[99] S. Huayhongthong, P. Khuntayaporn, K. Thirapanmethee, P. Wanapaisan, M.T. Chomnawang, Raman spectroscopic analysis of food-borne microorganisms, LWT. 114 (2019) 108419. https://doi.org/10.1016/j.lwt.2019.108419.

[100] K. Schanes, K. Dobernig, B. Gözet, Food waste matters - A systematic review of household food waste practices and their policy implications, J. Clean. Prod. 182 (2018) 978–991. https://doi.org/10.1016/j.jclepro.2018.02.030.

[101] S. Johler, R. Stephan, D. Althaus, M. Ehling-Schulz, T. Grunert, High-resolution subtyping of Staphylococcus aureus strains by means of Fourier-transform infrared spectroscopy, Syst. Appl. Microbiol. 39 (2016) 189–194. https://doi.org/10.1016/j.syapm.2016.03.003.

[102] D. Martak, B. Valot, M. Sauget, P. Cholley, M. Thouverez, X. Bertrand, D. Hocquet, Fourier-Transform InfraRed Spectroscopy Can Quickly Type Gram-Negative Bacilli Responsible for Hospital Outbreaks, Front. Microbiol. 10 (2019). https://doi.org/10.3389/fmicb.2019.01440.

[103] S. Meisel, S. Stöckel, P. Rösch, J. Popp, Identification of meat-associated pathogens via Raman microspectroscopy, Food Microbiol. 38 (2014) 36–43. https://doi.org/10.1016/j.fm.2013.08.007.

[104] C.-S.S. Ho, N. Jean, C.A. Hogan, L. Blackmon, S.S. Jeffrey, M. Holodniy, N. Banaei, A.A.E.E. Saleh, S. Ermon, J. Dionne, Rapid identification of pathogenic bacteria using Raman spectroscopy and deep learning, Nat. Commun. 10 (2019) 1–28. https://doi.org/10.1038/s41467-019-12898-9.

[105] R. Breuch, D. Klein, E. Siefke, M. Hebel, U. Herbert, C. Wickleder, P. Kaul, Differentiation of meat-related microorganisms using paper-based surface-enhanced Raman spectroscopy combined with multivariate statistical analysis, Talanta. 219 (2020) 1–7. https://doi.org/10.1016/j.talanta.2020.121315.

[106] M.K. Grewal, P. Jaiswal, S.N. Jha, Detection of poultry meat specific bacteria using FTIR spectroscopy and chemometrics, J. Food Sci. Technol. 52 (2015) 3859–3869. https://doi.org/10.1007/s13197-014-1457-9.

[107] B. Feng, H. Shi, F. Xu, F. Hu, J. He, H. Yang, C. Ding, W. Chen, S. Yu, FTIR-assisted MALDI-TOF MS for the identification and typing of bacteria, Anal. Chim. Acta. 1111 (2020) 75–82. https://doi.org/10.1016/j.aca.2020.03.037.

[108] O. Ryabchykov, J. Popp, T. Bocklitz, Fusion of MALDI spectrometric imaging and Raman spectroscopic data for the analysis of biological samples, Front. Chem. 6 (2018) 1–10. https://doi.org/10.3389/fchem.2018.00257.

[109] K. Weidemaier, E. Carruthers, A. Curry, M. Kuroda, E. Fallows, J. Thomas, D. Sherman, M. Muldoon, Real-time pathogen monitoring during enrichment: a novel nanotechnology-based approach to food safety testing, Int. J. Food Microbiol. 198 (2015) 19–27. https://doi.org/10.1016/j.ijfoodmicro.2014.12.018.

[110] K. Kochan, D. Perez-Guaita, J. Pissang, J.-H. Jiang, A.Y. Peleg, D. McNaughton, P. Heraud, B.R. Wood, In vivo atomic force microscopy–infrared spectroscopy of bacteria, J. R. Soc. Interface. 15 (2018) 20180115. https://doi.org/10.1098/rsif.2018.0115.

[111] M. Tang, G.D. McEwen, Y. Wu, C.D. Miller, A. Zhou, Characterization and analysis of mycobacteria and Gram-negative bacteria and co-culture mixtures by Raman microspectroscopy, FTIR, and atomic force microscopy, Anal. Bioanal. Chem. 405 (2013) 1577–1591. https://doi.org/10.1007/s00216-012-6556-8.

[112] D. Read, W.E. Huang, A.S. Whiteley, Single cell microbial ecophysiology with Raman-FISH, in: T. McGenity, K. Timmis, B. Nogales (Eds.), Hydrocarb. Lipid Microbiol. Protoc., Springer-Verlag, Heidelberg, 2015: pp. 65–76. https://doi.org/10.1007/8623_2015_153.

[113] A.G. Dinkelacker, S. Vogt, P. Oberhettinger, N. Mauder, J. Rau, M. Kostrzewa, J.W.A.A. Rossen, I.B. Autenrieth, S. Peter, J. Liese, Typing and species identification of clinical Klebsiella isolates by Fourier Transform Infrared Spectroscopy and Matrix-Assisted Laser Desorption Ionization–Time of Flight Mass Spectrometry, J. Clin. Microbiol. 56 (2018) 1–13. https://doi.org/10.1128/JCM.00843-18.

[114] T.G. Mayerhöfer, S. Pahlow, U. Hübner, J. Popp, CaF 2 : An ideal substrate material for Infrared Spectroscopy?, Anal. Chem. 92 (2020) 9024–9031. https://doi.org/10.1021/acs.analchem.0c01158.

[115] O. Ryabchykov, S. Guo, T. Bocklitz, Analyzing Raman spectroscopic data, Phys. Sci. Rev. 4 (2019) 1–10. https://doi.org/10.1515/psr-2017-0043.

[116] O. Preisner, J.A. Lopes, R. Guiomar, J. Machado, J.C. Menezes, Fourier transform infrared (FT-IR) spectroscopy in bacteriology: towards a reference method for bacteria discrimination, Anal. Bioanal. Chem. 387 (2007) 1739–1748. https://doi.org/10.1007/s00216-006-0851-1.

[117] C.G. Mallidis, P. Frantzeskakis, G. Balatsouras, C. Katsaboxakis, Thermal treatment of aseptically processed tomato paste, Int. J. Food Sci. Technol. 25 (1990) 442–448. https://doi.org/10.1111/j.1365-2621.1990.tb01101.x.

[118] R. Lucas, M.J. Grande, H. Abriouel, M. Maqueda, N. Ben Omar, E. Valdivia, M. Martínez-Cañamero, A. Gálvez, Application of the broad-spectrum bacteriocin enterocin AS-48 to inhibit Bacillus coagulans in canned fruit and vegetable foods, Food Chem. Toxicol. 44 (2006) 1774–1781. https://doi.org/10.1016/j.fct.2006.05.019.

[119] C. Apetroaie-Constantin, R. Mikkola, M.A. Andersson, V. Teplova, I. Suominen, T. Johansson, M. Salkinoja-Salonen, Bacillus subtilis and B. mojavensis strains connected to food poisoning produce the heat stable toxin amylosin, J. Appl. Microbiol. 106 (2009) 1976–1985. https://doi.org/10.1111/j.1365-2672.2009.04167.x.

[120] I. Vilar, M.C. Garcia Fontan, B. Prieto, M.E. Tornadijo, J. Carballo, A survey on the microbiological changes during the manufacture of dry-cured lacon, a Spanish traditional meat product, J. Appl. Microbiol. 89 (2000) 1018–1026. https://doi.org/10.1046/j.1365-2672.2000.01210.x.

[121] H. Rosenquist, L. Smidt, S.R. Andersen, G.B. Jensen, A. Wilcks, Occurrence and significance of Bacillus cereus and Bacillus thuringiensis in ready-to-eat food, FEMS Microbiol. Lett. 250 (2005) 129–136. https://doi.org/10.1016/j.femsle.2005.06.054.

[122] U. Herbert, Assessment of different packaging atmospheres for the poultry meat industry based on an overall quality index, Rheinischen Friedrich-Wilhelms-Universität Bonn, 2014. http://hss.ulb.uni-bonn.de/2014/3774/3774.htm.

[123] D. Klein, R. Breuch, S. von der Mark, C. Wickleder, P. Kaul, Detection of spoilage associated bacteria using Raman-microspectroscopy combined with multivariate statistical analysis, Talanta. 196 (2019) 325–328. https://doi.org/10.1016/j.talanta.2018.12.094.

[124] F. Yang, K. Doksum, K.-W. Tsui, Principal Component Analysis (PCA) for high-dimensional data. PCA is dead. Long live PCA, in: Proc. Work. Perspect. High Dimens. Data Anal. II, Providence, Rhode Island, 2014: pp. 1–10. https://doi.org/10.1090/conm/622/12430.

[125] S. Garip, A.C. Gozen, F. Severcan, Use of Fourier transform infrared spectroscopy for rapid comparative analysis of Bacillus and Micrococcus isolates, Food Chem. 113 (2009) 1301–1307. https://doi.org/10.1016/j.foodchem.2008.08.063.

[126] F. Garczarek, K. Gerwert, Functional waters in intraprotein proton transfer monitored by FTIR difference spectroscopy, Nature. 439 (2006) 109–112. https://doi.org/10.1038/nature04231.

[127] D.H. Moore, Combining linear and quadratic discriminants, Comput. Biomed. Res. 6 (1973) 422–429. https://doi.org/10.1016/0010-4809(73)90075-X.

[128] M.C. Fulcomer, P.H. Schönemann, G. Molnar, Classification by linear and quadratic discriminant scores, Behav. Res. Methods Instrum. 6 (1974) 443–445. https://doi.org/10.3758/BF03200398.

[129] W. Wu, Y. Mallet, B. Walczak, W. Penninckx, D.L. Massart, S. Heuerding, F. Erni, Comparison of regularized discriminant analysis linear discriminant analysis and quadratic discriminant analysis applied to NIR data, Anal. Chim. Acta. 329 (1996) 257–265. https://doi.org/10.1016/0003-2670(96)00142-0.

[130] C.A. Rebuffo-Scheer, J. Dietrich, M. Wenning, S. Scherer, Identification of five Listeria species based on infrared spectra (FTIR) using macrosamples is superior to a microsample approach, Anal. Bioanal. Chem. 390 (2008) 1629–1635. https://doi.org/10.1007/s00216-008-1834-1.

[131] A.O. Janbu, T. Møretrø, D. Bertrand, A. Kohler, FT-IR microspectroscopy: A promising method for the rapid identification of Listeria species, FEMS Microbiol. Lett. 278 (2008) 164–170. https://doi.org/10.1111/j.1574-6968.2007.00995.x.

[132] N.A. Ngo-Thi, C. Kirschner, D. Naumann, Characterization and identification of microorganisms by FT-IR microspectrometry, J. Mol. Struct. 661–662 (2003) 371–380. https://doi.org/10.1016/j.molstruc.2003.08.012.

[133] M. Wenning, N.R. Büchl, S. Scherer, Species and strain identification of lactic acid bacteria using FTIR spectroscopy and artificial neural networks, J. Biophotonics. 3 (2010) 493–505. https://doi.org/10.1002/jbio.201000015.

[134] J. Campos, C. Sousa, J. Mourão, J. Lopes, P. Antunes, L. Peixe, Discrimination of non-typhoid Salmonella serogroups and serotypes by Fourier Transform Infrared Spectroscopy: A comprehensive analysis, Int. J. Food Microbiol. 285 (2018) 34–41. https://doi.org/10.1016/j.ijfoodmicro.2018.07.005.

[135] T. Grunert, M. Wenning, M.S. Barbagelata, M. Fricker, D.O. Sordelli, F.R. Buzzola, M. Ehling-Schulz, Rapid and reliable identification of Staphylococcus aureus capsular serotypes by means of artificial neural network-assisted fourier transform infrared spectroscopy, J. Clin. Microbiol. 51 (2013) 2261–2266. https://doi.org/10.1128/JCM.00581-13.

[136] European Commission, Internal market, industry, entrepreneurship and SMEs - Food and drink industry, (2022). https://single-market-economy.ec.europa.eu/sectors/food-and-drink-industry_en (accessed March 3, 2023).

[137] A. Alvarez-Ordóñez, D.J.M.J.M. Mouwen, M. López, M. Prieto, Fourier transform infrared spectroscopy as a tool to characterize molecular composition and stress response in foodborne pathogenic bacteria, J. Microbiol. Methods. 84 (2011) 369–378. https://doi.org/10.1016/j.mimet.2011.01.009.

[138] D.J. Troy, K.S. Ojha, J.P. Kerry, B.K. Tiwari, Sustainable and consumer-friendly emerging technologies for application within the meat industry: An overview, Meat Sci. 120 (2016) 2–9. https://doi.org/10.1016/j.meatsci.2016.04.002.

[139] K. Maquelin, C. Kirschner, L.-P. Choo-Smith, N. van den Braak, H.P. Endtz, D. Naumann, G.. Puppels, Identification of medically relevant microorganisms by vibrational spectroscopy, J. Microbiol. Methods. 51 (2002) 255–271. https://doi.org/10.1016/S0167-7012(02)00127-6.

[140] M.M. Hlaing, M. Dunn, P.R. Stoddart, S.L. McArthur, Raman spectroscopic identification of single bacterial cells at different stages of their lifecycle, Vib. Spectrosc. 86 (2016) 81–89. https://doi.org/10.1016/j.vibspec.2016.06.008.

[141] T. Yamamoto, J.N. Taylor, S. Koseki, K. Koyama, Classification of food spoilage bacterial species and their sodium chloride, sodium acetate and glycine tolerance using chemometrics analysis and Raman spectroscopy, J. Microbiol. Methods. 190 (2021) 106326. https://doi.org/10.1016/j.mimet.2021.106326.

[142] P.B. Price, T. Sowers, Temperature dependence of metabolic rates for microbial growth, maintenance, and survival, Proc. Natl. Acad. Sci. 101 (2004) 4631–4636. https://doi.org/10.1073/pnas.0400522101.

[143] C. Wichmann, M. Chhallani, T. Bocklitz, P. Rösch, J. Popp, Simulation of transportation and storage and their influence on Raman spectra of bacteria, Anal. Chem. 91 (2019) 13688–13694. https://doi.org/10.1021/acs.analchem.9b02932.

[144] A.A. Argyri, R.M. Jarvis, D. Wedge, Y. Xu, E.Z. Panagou, R. Goodacre, G.J.E.J.E. Nychas, A comparison of Raman and FT-IR spectroscopy for the prediction of meat spoilage, Food Control. 29 (2013) 461–470. https://doi.org/10.1016/j.foodcont.2012.05.040.

[145] U. Münchberg, S. Kloß, D. Kusić, S. Meisel, R. Heinke, S. Stöckel, P. Rösch, J. Popp, IR and Raman spectroscopy for pathogen detection, in: Mod. Tech. Pathog. Detect., Wiley-VCH Verlag GmbH & Co. KGaA, Weinheim, Germany, 2015: pp. 253–294. https://doi.org/10.1002/9783527687978.ch6.

[146] K. Wang, D.-W. Sun, Imaging Spectroscopic Technique: Raman Chemical Imaging, in: Mod. Tech. Food Authentication, 2nd ed., Elsevier, 2018: pp. 287–319. https://doi.org/10.1016/B978-0-12-814264-6.00009-8.

[147] H. Schulz, Spectroscopic Technique: Raman Spectroscopy, in: Mod. Tech. Food Authentication, 2nd ed., Elsevier, 2018: pp. 139–191. https://doi.org/10.1016/B978-0-12-814264-6.00005-0.

[148] J.P. Harrison, D. Berry, Vibrational spectroscopy for imaging single microbial cells in complex biological samples, Front. Microbiol. 8 (2017) 1–7. https://doi.org/10.3389/fmicb.2017.00675.

[149] J.M. Florence, C.C. Allshouse, F.W. Glaze, C.H. Hahner, Absorption of near-infrared energy by certain glasses, J. Res. Natl. Bur. Stand. (1934). 45 (1950) 121. https://doi.org/10.6028/jres.045.011.

[150] R.M. Jarvis, R. Goodacre, Discrimination of bacteria using Surface-Enhanced Raman Spectroscopy, Anal. Chem. 76 (2004) 40–47. https://doi.org/10.1021/ac034689c.

[151] M. Harz, P. Rösch, K.-D. Peschke, O. Ronneberger, H. Burkhardt, J. Popp, Micro-Raman spectroscopic identification of bacterial cells of the genus Staphylococcus and dependence on their cultivation conditions, Analyst. 130 (2005) 1543. https://doi.org/10.1039/b507715j.

[152] S. Sil, R. Mukherjee, N.S. Kumar, A. S., J. Kingston, U.K. Singh, Detection and classification of bacteria using Raman spectroscopy combined with multivariate analysis, Def. Life Sci. J. 2 (2017) 435. https://doi.org/10.14429/dlsj.2.12275.

[153] A. Walter, M. Reinicke, T. Bocklitz, W. Schumacher, P. Rösch, E. Kothe, J. Popp, Raman spectroscopic detection of physiology changes in plasmid-bearing Escherichia coli with and without antibiotic treatment, Anal. Bioanal. Chem. 400 (2011) 2763–2773. https://doi.org/10.1007/s00216-011-4819-4.

[154] T. Verma, H. Annappa, S. Singh, S. Umapathy, D. Nandi, Profiling antibiotic resistance in Escherichia coli strains displaying differential antibiotic susceptibilities using Raman spectroscopy, J. Biophotonics. 14 (2021) 1–17. https://doi.org/10.1002/jbio.202000231.

[155] A.I.M. Athamneh, R.A. Alajlouni, R.S. Wallace, M.N. Seleem, R.S. Senger, Phenotypic profiling of antibiotic response signatures in Escherichia coli using Raman spectroscopy, Antimicrob. Agents Chemother. 58 (2014) 1302–1314. https://doi.org/10.1128/AAC.02098-13.

[156] C. García-Timermans, P. Rubbens, F.-M. Kerckhof, B. Buysschaert, D. Khalenkow, W. Waegeman, A.G. Skirtach, N. Boon, Label-free Raman characterization of bacteria calls for standardized procedures, J. Microbiol. Methods. 151 (2018) 69–75. https://doi.org/10.1016/j.mimet.2018.05.027.

[157] C. Wichmann, T. Bocklitz, P. Rösch, J. Popp, Bacterial phenotype dependency from CO2 measured by Raman spectroscopy, Spectrochim. Acta Part A Mol. Biomol. Spectrosc. 248 (2021) 119170. https://doi.org/10.1016/j.saa.2020.119170.

[158] T.N.K. Zu, A.I.M. Athamneh, R.S. Wallace, E. Collakova, R.S. Senger, Near-real-time analysis of the phenotypic responses of Escherichia coli to 1-butanol exposure using Raman spectroscopy, J. Bacteriol. 196 (2014) 3983–3991. https://doi.org/10.1128/JB.01590-14.

[159] T.N.K. Zu, A.I.M. Athamneh, R.S. Senger, Characterizing the phenotypic responses of Escherichia coli to multiple 4-carbon alcohols with raman spectroscopy, Fermentation. 2 (2016). https://doi.org/10.3390/fermentation2010003.

[160] R. Mukherjee, T. Verma, D. Nandi, S. Umapathy, Understanding the effects of culture conditions in bacterial growth: A biochemical perspective using Raman microscopy, J. Biophotonics. 13 (2020) 1–11. https://doi.org/10.1002/jbio.201900233.

[161] A. Němcová, D. Gonová, O. Samek, M. Sipiczki, E. Breierová, I. Márová, The use of Raman spectroscopy to monitor metabolic changes in stressed Metschnikowia sp. yeasts, Microorganisms. 9 (2021) 277. https://doi.org/10.3390/microorganisms9020277.

[162] R. Li, D. Dhankhar, J. Chen, A. Krishnamoorthi, T.C. Cesario, P.M. Rentzepis, Identification of live and dead bacteria: A Raman spectroscopic study, IEEE Access. 7 (2019) 23549–23559. https://doi.org/10.1109/ACCESS.2019.2899006.

[163] Y. Ryu, M. Hong, S. Bin Kim, T.K. Lee, W. Park, Raman spectroscopy reveals alteration of spore compositions under different nutritional conditions in Lysinibacillus boronitolerans YS11, J. Microbiol. 59 (2021) 491–499. https://doi.org/10.1007/s12275-021-0679-6.

[164] I. Tanniche, E. Collakova, C. Denbow, R.S. Senger, Characterizing metabolic stress-induced phenotypes of Synechocystis PCC6803 with Raman spectroscopy, PeerJ. 8 (2020) e8535. https://doi.org/10.7717/peerj.8535.

[165] D. Klein, R. Breuch, J. Reinmüller, C. Engelhard, P. Kaul, Rapid detection and discrimination of food-related bacteria using IR-microspectroscopy in combination with multivariate statistical analysis, Talanta. 232 (2021) 122424. https://doi.org/10.1016/j.talanta.2021.122424.

[166] M.F. Escoriza, J.M. Van Briesen, S. Stewart, J. Maier, Raman spectroscopic discrimination of cell response to chemical and physical inactivation, Appl. Spectrosc. 61 (2007) 812–823. https://doi.org/10.1366/000370207781540132.

[167] R. Withnall, B.Z. Chowdhry, J. Silver, H.G.M. Edwards, L.F.C. De Oliveira, Raman spectra of carotenoids in natural products, Spectrochim. Acta - Part A Mol. Biomol. Spectrosc. 59 (2003) 2207–2212. https://doi.org/10.1016/S1386-1425(03)00064-7.

[168] K.C. Schuster, I. Reese, E. Urlaub, J.R. Gapes, B. Lendl, Multidimensional information on the chemical composition of single bacterial cells by confocal Raman microspectroscopy, Anal. Chem. 72 (2000) 5529–5534. https://doi.org/10.1021/ac000718x.

[169] D. Malyshev, R. Öberg, T. Dahlberg, K. Wiklund, L. Landström, P.O. Andersson, M. Andersson, Laser induced degradation of bacterial spores during micro-Raman spectroscopy, Spectrochim. Acta - Part A Mol. Biomol. Spectrosc. 265 (2022). https://doi.org/10.1016/j.saa.2021.120381.

[170] L. Kong, P. Zhang, G. Wang, J. Yu, P. Setlow, Y.Q. Li, Characterization of bacterial spore germination using phase-contrast and fluorescence microscopy, Raman spectroscopy and optical tweezers, Nat. Protoc. 6 (2011) 625–639. https://doi.org/10.1038/nprot.2011.307.

[171] P. Zhang, P. Setlow, Y. Li, Characterization of single heat-activated Bacillus spores using laser tweezers Raman spectroscopy, Opt. Express. 17 (2009) 16480. https://doi.org/10.1364/OE.17.016480.

[172] L. Kong, P. Setlow, Y. Li, Analysis of the Raman spectra of Ca2+-dipicolinic acid alone and in the bacterial spore core in both aqueous and dehydrated environments, Analyst. 137 (2012) 3683. https://doi.org/10.1039/c2an35468c.

[173] K. Maquelin, L.-P. Choo-Smith, T. van Vreeswijk, H.P. Endtz, B. Smith, R. Bennett, H.A. Bruining, G.J. Puppels, Raman spectroscopic method for identification of clinically relevant microorganisms growing on solid culture medium, Anal. Chem. 72 (2000) 12–19. https://doi.org/10.1021/ac991011h.

[174] J. De Gelder, K. De Gussem, P. Vandenabeele, L. Moens, Reference database of Raman spectra of biological molecules, J. Raman Spectrosc. 38 (2007) 1133–1147. https://doi.org/10.1002/jrs.1734.

[175] C. Fan, Z. Hu, A. Mustapha, M. Lin, Rapid detection of food- and waterborne bacteria using surface-enhanced Raman spectroscopy coupled with silver nanosubstrates, Appl. Microbiol. Biotechnol. 92 (2011) 1053–1061. https://doi.org/10.1007/s00253-011-3634-3.

[176] C. Wichmann, T. Bocklitz, P. Rösch, J. Popp, Bacterial phenotype dependency from CO2 measured by Raman spectroscopy, Spectrochim. Acta Part A Mol. Biomol. Spectrosc. 248 (2021) 119170. https://doi.org/10.1016/j.saa.2020.119170.

[177] H.J. Butler, L. Ashton, B. Bird, G. Cinque, K. Curtis, J. Dorney, K. Esmonde-White, N.J. Fullwood, B. Gardner, P.L. Martin-Hirsch, M.J. Walsh, M.R. McAinsh, N. Stone, F.L. Martin, Using Raman spectroscopy to characterize biological materials, Nat. Protoc. 11 (2016) 664–687. https://doi.org/10.1038/nprot.2016.036.

[178] M.M. Hlaing, B.R. Wood, D. McNaughton, J.I. Rood, E.M. Fox, M.A. Augustin, Vibrational spectroscopy combined with transcriptomic analysis for investigation of bacterial responses towards acid stress, Appl. Microbiol. Biotechnol. 102 (2018) 333–343. https://doi.org/10.1007/s00253-017-8561-5.

[179] S.A. Strola, J.-C. Baritaux, E. Schultz, A.C. Simon, C. Allier, I. Espagnon, D. Jary, J.-M. Dinten, Single bacteria identification by Raman spectroscopy, J. Biomed. Opt. 19 (2014) 111610. https://doi.org/10.1117/1.JBO.19.11.111610.

[180] J. Marles-Wright, R.J. Lewis, Stress responses of bacteria, Curr. Opin. Struct. Biol. 17 (2007) 755–760. https://doi.org/10.1016/j.sbi.2007.08.004.

[181] F. Bozoglu, H. Alpas, G. Kaletunc, Injury recovery of foodborne pathogens in high hydrostatic pressure treated milk during storage, FEMS Immunol. Med. Microbiol. 40 (2004) 243–247. https://doi.org/10.1016/S0928-8244(04)00002-1.

[182] D. Ami, A. Natalello, T. Schultz, P. Gatti-Lafranconi, M. Lotti, S.M. Doglia, A. de Marco, Effects of recombinant protein misfolding and aggregation on bacterial membranes, Biochim. Biophys. Acta - Proteins Proteomics. 1794 (2009) 263–269. https://doi.org/10.1016/j.bbapap.2008.10.015.

[183] C.M. Scherber, J.L. Schottel, A. Aksan, Membrane phase behavior of Escherichia coli during desiccation, rehydration, and growth recovery, Biochim. Biophys. Acta - Biomembr. 1788 (2009) 2427–2435. https://doi.org/10.1016/j.bbamem.2009.08.011.

[184] L. Beney, Y. Mille, P. Gervais, Death of Escherichia coli during rapid and severe dehydration is related to lipid phase transition, Appl. Microbiol. Biotechnol. 65 (2004) 457–464. https://doi.org/10.1007/s00253-004-1574-x.

[185] M. Lin, M. Al-Holy, H. Al-Qadiri, D.-H. Kang, A.G. Cavinato, Y. Huang, B.A. Rasco, Discrimination of Intact and Injured Listeria monocytogenes by Fourier Transform Infrared Spectroscopy and Principal Component Analysis, J. Agric. Food Chem. 52 (2004) 5769–5772. https://doi.org/10.1021/jf049354q.

[186] C. Saulou, F. Jamme, L. Girbal, C. Maranges, I. Fourquaux, M. Cocaign-Bousquet, P. Dumas, M. Mercier-Bonin, Synchrotron FTIR microspectroscopy of Escherichia coli at single-cell scale under silver-induced stress conditions, Anal. Bioanal. Chem. 405 (2013) 2685–2697. https://doi.org/10.1007/s00216-013-6725-4.

[187] Y. Liu, L. He, A. Mustapha, H. Li, Z.Q. Hu, M. Lin, Antibacterial activities of zinc oxide nanoparticles against Escherichia coli O157:H7, J. Appl. Microbiol. 107 (2009) 1193–1201. https://doi.org/10.1111/j.1365-2672.2009.04303.x.

[188] E.S. Kepenek, M. Severcan, A.G. Gozen, F. Severcan, Discrimination of heavy metal acclimated environmental strains by chemometric analysis of FTIR spectra, Ecotoxicol. Environ. Saf. 202 (2020) 110953. https://doi.org/10.1016/j.ecoenv.2020.110953.

[189] E.S. Kepenek, A.G. Gozen, F. Severcan, Molecular characterization of acutely and gradually heavy metal acclimated aquatic bacteria by FTIR spectroscopy, J. Biophotonics. 12 (2019) 1–10. https://doi.org/10.1002/jbio.201800301.

[190] H.M. Al-Qadiri, M. Lin, M.A. Al-Holy, A.G. Cavinato, B.A. Rasco, Detection of sublethal thermal injury in Salmonella enterica serotype Typhimurium and Listeria monocytogenes using Fourier Transform Infrared (FT-IR) Spectroscopy (4000 to 600 cm −1), J. Food Sci. 73 (2008) M54–M61. https://doi.org/10.1111/j.1750-3841.2007.00640.x.

[191] K. V. Kilimann, W. Doster, R.F. Vogel, C. Hartmann, M.G. Gänzle, Protection by sucrose against heat-induced lethal and sublethal injury of Lactococcus lactis: An FT-IR study, Biochim. Biophys. Acta - Proteins Proteomics. 1764 (2006) 1188–1197. https://doi.org/10.1016/j.bbapap.2006.04.016.

[192] X. Lu, Q. Liu, D. Wu, H.M. Al-Qadiri, N.I. Al-Alami, D.-H. Kang, J.-H. Shin, J. Tang, J.M.F. Jabal, E.D. Aston, B.A. Rasco, Using of infrared spectroscopy to study the survival and injury of Escherichia coli O157:H7, Campylobacter jejuni and Pseudomonas aeruginosa under cold stress in low nutrient media, Food Microbiol. 28 (2011) 537–546. https://doi.org/10.1016/j.fm.2010.11.002.

[193] K. Papadimitriou, E. Boutou, G. Zoumpopoulou, P.A. Tarantilis, M. Polissiou, C.E. Vorgias, E. Tsakalidou, RNA Arbitrarily Primed PCR and Fourier Transform Infrared Spectroscopy Reveal Plasticity in the Acid Tolerance Response of Streptococcus macedonicus, Appl. Environ. Microbiol. 74 (2008) 6068–6076. https://doi.org/10.1128/AEM.00315-08.

[194] T. Stanborough, N. Fegan, S.M. Powell, M. Tamplin, P.S. Chandry, Insight into the Genome of Brochothrix thermosphacta, a Problematic Meat Spoilage Bacterium, Appl. Environ. Microbiol. 83 (2017) 1–20. https://doi.org/10.1128/AEM.02786-16.

[195] S. Sabbatini, C. Conti, G. Orilisi, E. Giorgini, Infrared spectroscopy as a new tool for studying single living cells: Is there a niche?, Biomed. Spectrosc. Imaging. 6 (2017) 85–99. https://doi.org/10.3233/BSI-170171.

[196] N. Loffhagen, C. Härtig, W. Geyer, M. Voyevoda, H. Harms, Competition betweencis, trans and Cyclopropane Fatty Acid Formation and its Impact on Membrane Fluidity, Eng. Life Sci. 7 (2007) 67–74. https://doi.org/10.1002/elsc.200620168.

List of Abbreviations

B

B. coag……*Bacillus coagulans*

B. sub……..……..*Bacillus subtilis*

B. therm. ……..*Brochothrix thermosphacta*

B. tii…….……*Bacillus thuringiensis israelensis*

C

CCD…….……charge-coupled device

CDA……..……canonical discriminant analysis

coad…….……coadditions

CV……..……canonical variables

D

DNA……deoxyribonucleic acid

DSM……...German Collection of Microorganisms

DSMZ…….German Collection of Microorganisms and Cell Cultures

E

E. coli……*Escherichia coli*

EHEC……..……enterohemorrhagic *E. coli*

et al. ……et alii

F

FT……..Fourier-transform

I

IR……infrared

L

LDA……...linear discriminant analysis

M

M. luteus……*Micrococcus luteus*

MCT……Mercury/Cadmium/Telluride

MLST……..……multilocus sequence typing

MLVA……multilocus variable-number tandem repeat analysis

P

PC……..……principal component

PCA……..……principal component analysis

PFGE……pulsed-field gel electrophoresis

PLSR…….……partial least squares regression analysis

Ps. fluor. ……..……Pseudomonas fluorescens

Q

QDA……..…..……quadratic discriminant analysis

R

RNA……..……ribonucleic acid

S

SIMCA……..…soft independent modelling of class analogies

spp. ……species

Supplemental Notice:

Abbreviations commonly used in this scientific discipline and units of measurement defined in the International System of Units are not listed.

List of Figures

List of Tables

Acknowledgements

First, I would like to thank my supervisor Peter Kaul, who created all the possibilities and the general conditions for me to realize this work. I thank him for his suggestions and new perspectives and especially for the great freedom of action I had during my work.

I would also like to thank Mr. Engelhard and Ms. Wickleder. In addition to taking over the supervision of my work at short notice, they have always supported me with constructive feedback and targeted discussions.

Special thanks to my colleague René Breuch who always had an open ear for the problems and supported me enormously with our countless long discussions.

In addition, I would like to thank Savanna Sewell and Markus Witzler for relentlessly and patiently correcting my English.